

# Stellar Dynamics and Galaxies

Jacob Pilawa

Fall 2021

## Contents

|  |           |
|--|-----------|
| <b>1 August 25, 2021: Introduction and Course Overview</b>   | <b>5</b>  |
| 1.1 The Milky Way . . . . .  | 6         |
| <b>2 August 27, 2021: Global Properties and Galaxy Correlations</b>                                      | <b>7</b>  |
| 2.1 Morphology, Continued . . . . .  | 7         |
| 2.2 Units and Quantities . . . . .   | 9         |
| 2.3 Sloan Digital Sky Survey . . . . .   | 11        |
| 2.4 K Corrections . . . . .  | 13        |
| 2.5 Trends of Stellar Mass with Color . . . . .  | 15        |
| <b>3 September 1, 2021: Global Properties and Galaxy Correlations</b>                                    | <b>15</b> |
| 3.1 AB Magnitudes and Vega Magnitudes . . . . .  | 15        |
| 3.2 Synthetic galaxy spectra as a function of age . . . . .  | 16        |
| 3.3 K-corrections . . . . .  | 16        |
| 3.4 Stellar Masses (Bell & de Jong 2001) . . . . .   | 17        |
| 3.5 SEDs for Different Metallicities . . . . .   | 17        |
| 3.6 Color Sequences . . . . .  | 19        |
| 3.7 Galaxy Correlations in the SDSS . . . . .  | 19        |
| 3.8 Stellar metallicity - mass relation (Gallazzi et al., 2005) . . . . .                                | 22        |
| <b>4 September 3, 2021: Global properties, galaxy correlations, and statistics</b>                       | <b>23</b> |
| 4.1 Measuring gas-phase metallicity . . . . .  | 23        |
| 4.2 Brief Review of Last Time: Color Sequences, . . . . .  | 23        |
| 4.3 Stellar mass-halo mass relation . . . . .  | 25        |
| 4.4 Galaxy Sizes . . . . .   | 26        |
| 4.4.1 Sersic (1968) Profiles . . . . .   | 26        |
| 4.5 Stellar mass-size relation (Shen et al., 2003) . . . . .   | 27        |
| 4.6 Measuring galaxy sizes and Sersic indices . . . . .  | 27        |
| 4.7 Galaxy sizes over cosmic time . . . . .  | 27        |
| 4.8 Relation with Environment . . . . .  | 28        |
| 4.9 Disentangling environment, mass, morphological type, and Sersic parameter (van der Wel 2008. . . . . | 29        |
| 4.10 Staistical properties of the galaxy population . . . . .  | 29        |
| 4.11 The luminosity function of galaxies . . . . .   | 29        |
| 4.12 Peculiar Motions . . . . .  | 29        |

|   |           |
|---|-----------|
| <b>5 September 8, 2021: Finish galaxy statistics; stellar populations; stellar evolution review</b> | <b>31</b> |
| 5.1 Luminosity Function for Different Hubble Types . . . . .  | 31        |
| 5.1.1 Challenges . . . . .  | 31        |
| 5.1.2 Vmax Correction, Revisited . . . . .  | 31        |
| 5.2 Luminosity Functions as a function of color (Blanton 2001) . . . . .                            | 31        |
| 5.3 Luminosity Function as a function of environment (Christlein 2000) . . . . .                    | 31        |
| 5.4 Luminosity and Mass Functions (Yang et al. 2009) . . . . .                                      | 31        |
| 5.5 Physical Origin of the Luminosity Function . . . . .  | 31        |
| 5.6 Evolution of the Mass Function (with redshift) [Muzzin et al 2013] . . . . .                    | 31        |
| 5.7 Evolution of the UV Luminosity Function (Bouwens et al 2000) . . . . .                          | 32        |
| 5.8 Star formation history of the Universe . . . . .  | 32        |
| 5.9 Quiz! . . . . .   | 32        |
| <b>6 September 10, 2021: Stellar Evolution and Stellar Populations</b>                              | <b>32</b> |
| 6.1 Background . . . . .  | 32        |
| 6.2 A quick thing about Problem 3e: Photon and Energy Counting Detectors . . . . .                  | 32        |
| 6.3 Stellar Evolution . . . . .   | 33        |
| 6.3.1 HR Diagrams: Main Sequence . . . . .  | 33        |
| 6.3.2 Difference in Chemical Composition . . . . .  | 34        |
| 6.3.3 Relation between luminosity and mass . . . . .  | 34        |
| 6.3.4 Post MS Evolution . . . . .   | 35        |
| 6.3.5 Production of Carbon and Oxygen . . . . .   | 37        |
| 6.3.6 Stellar Evolution Tracks . . . . .  | 38        |
| 6.3.7 Massive Stars . . . . .   | 38        |
| 6.3.8 Binding energy per nucleon . . . . .  | 38        |
| 6.3.9 Evolution of a solar mass star . . . . .  | 38        |
| 6.3.10 Stellar remnants . . . . .   | 38        |
| <b>7 September 15, 2021: Stellar Populations</b>  | <b>39</b> |
| 7.1 Ingredients . . . . .   | 39        |
| 7.2 Initial Mass Function . . . . .   | 39        |
| 7.3 Evolving a simple stellar population . . . . .  | 40        |
| 7.4 Evolution of Color and Mass-to-Light Ratio . . . . .  | 40        |
| 7.5 Dust Attenuation Law . . . . .  | 41        |
| 7.6 Dust Attenuation Curve . . . . .  | 42        |
| 7.7 Calzetti Law . . . . .  | 43        |
| <b>8 September 17, 2021: Stellar Populations continued</b>  | <b>44</b> |
| 8.1 An error from last time... . . . . .  | 44        |
| 8.2 Dust Emission Models (Draine and Li, 2007) . . . . .  | 45        |
| 8.3 Negative k-correction . . . . .   | 45        |
| 8.4 Simple Stellar Populations . . . . .  | 46        |
| 8.5 Star formation history of a simulated galaxy . . . . .  | 46        |
| 8.6 Star formation and enrichment history . . . . .   | 47        |
| 8.7 Fractional contribution to the total flux . . . . .   | 48        |
| 8.8 Fractional contribution to the total flux for a star forming galaxy . . . . .                   | 49        |
| 8.9 Light-weighted age as a function of wavelength . . . . .  | 50        |
| 8.10 Nebular Emission . . . . .   | 50        |
| 8.11 Complex Stellar Population . . . . .   | 50        |
| 8.12 Fitting broadband photometry . . . . .   | 51        |
| 8.13 Fitting Spectra without parametrizing the SFH . . . . .  | 51        |
| 8.14 Uncertainties in the stellar population modeling . . . . .                                     | 51        |

|  |           |
|--|-----------|
| 8.15 Thermally pulsing AGB phase . . . . .   | 51        |
| 8.16 Challenges of SPS Modeling . . . . .  | 51        |
| <b>9 September 22, 2021: Gas and Star Formation</b>                                | <b>52</b> |
| 9.1 IMF Completion . . . . .   | 52        |
| 9.2 Star formation in the nearby Universe . . . . .                                | 53        |
| 9.3 Mass function of dense cores in GMCs (Alves+2007) . . . . .                    | 54        |
| 9.4 Jeans Mass and Cloud Fragmentation . . . . .                                   | 54        |
| 9.5 Star formation rate indicators (recipes) . . . . .                             | 56        |
| 9.6 UV Emission . . . . .  | 56        |
| 9.6.1 Correction UV Emission using Beta Slope (Meurer+1999) . . . . .              | 57        |
| 9.7 Recombination Lines . . . . .  | 58        |
| 9.8 FIR Emission . . . . .   | 59        |
| 9.9 X-ray emission (Menou et al 2012) . . . . .                                    | 60        |
| 9.10 Radio Emission . . . . .  | 61        |
| 9.11 Measuring gas surface densities . . . . .                                     | 61        |
| 9.12 Kennicutt-Schmidt Law (1998) . . . . .  | 61        |
| <b>10 September 24, 2021: Gas and star formation, chemical evolution</b>           | <b>62</b> |
| 10.1 Group Exercise . . . . .  | 62        |
| 10.2 Gas components of a galaxy . . . . .  | 63        |
| 10.3 CO to H <sub>2</sub> Conversions . . . . .                                    | 64        |
| 10.4 Kennicutt-Schmidt Law . . . . .   | 64        |
| 10.5 KS Law Explanations . . . . .   | 64        |
| 10.6 The star formation law in atomic and molecular gas . . . . .                  | 65        |
| 10.7 Molecular Fraction vs. Gas Surface Density . . . . .                          | 66        |
| 10.8 Summary of Today . . . . .  | 67        |
| <b>11 September 29, 2021: The Circumgalactic Medium</b>                            | <b>67</b> |
| 11.1 History of CGM . . . . .  | 68        |
| 11.2 The Missing Baryons & Where Are They . . . . .                                | 68        |
| 11.3 General GCM Properties . . . . .  | 68        |
| 11.4 Top 10 Observationally Derived Properties of the CGM (Jessica Werk) . . . . . | 68        |
| 11.5 Curve of Growth . . . . .   | 68        |
| <b>12 October 6, 2021: Chemical Evolution</b>                                      | <b>69</b> |
| 12.1 Chemical Evolution Outline . . . . .  | 69        |
| 12.2 Terminology and Things . . . . .  | 69        |
| 12.3 Solar Abundance Pattern . . . . .   | 70        |
| 12.4 Sources of Heavy Elements . . . . .   | 70        |
| 12.5 Neutron Capture Elements . . . . .  | 70        |
| 12.6 R vs. S Process Elements . . . . .  | 71        |
| 12.7 Metallicities of galaxies . . . . .   | 71        |
| 12.8 Gas-phase metallicities, direct T method . . . . .                            | 72        |
| 12.9 Quasar Absorption Line Studies . . . . .                                      | 74        |
| <b>13 October 8, 2021: Chemical Evolution Continued</b>                            | <b>75</b> |
| 13.1 Damped Lyman Alpha Systems . . . . .  | 75        |
| 13.2 Chemical Evolution Models, ingredients . . . . .                              | 75        |
| 13.3 Closed Box Model Chemical Evolution . . . . .                                 | 75        |
| 13.4 The G-Dwarf Problem: THIS IS PRE-LIM PRIME . . . . .                          | 77        |
| 13.5 Mass-metallicity relation . . . . .   | 78        |

|   |           |
|---|-----------|
| 13.6 Leaky Box model . . . . .  | 78        |
| 13.7 Gas Accretion over Time . . . . .  | 79        |
| 13.8 Observational Constraints on Infall . . . . .                                  | 81        |
| 13.9 Lyman Alpha Blobs . . . . .  | 81        |
| 13.10 Milky Way Clouds? . . . . .   | 82        |
| <b>14 October 13, 2021: Chemical Evolution and DM Halos</b>                         | <b>82</b> |
| 14.1 CC SN Stellar Yields Depend on the Stellar Mass . . . . .                      | 82        |
| 14.2 CC SN Stellar Yields Depend on the Stellar Metallicity . . . . .               | 83        |
| 14.3 Type Ia Supernovae Delay Time Distribution . . . . .                           | 83        |
| 14.4 R-process Elements . . . . .   | 84        |
| 14.5 PRELIMMABLE: Core-Collapse vs. Type Ia Supernovae Enrichment . . . . .         | 84        |
| 14.6 Examples - Effect of IMF on Alpha-Fe and Fe-H Diagram . . . . .                | 85        |
| 14.7 Examples - Effect of Star Formation on Alpha-Fe and Fe-H Diagram . . . . .     | 86        |
| 14.8 Examples - Effect of Inflow and Outflow on Alpha-Fe and Fe-H Diagram . . . . . | 86        |
| 14.9 The Dark Matter Rap . . . . .  | 87        |
| 14.10 Cold, Warm DM Power Spectrum . . . . .  | 87        |
| 14.11 Rotation Curves . . . . .   | 87        |
| 14.12 Probes for Dark Matter Halos and Halo Shapes . . . . .                        | 88        |
| 14.13 Dark Matter Halo: A universal density profile . . . . .                       | 88        |
| 14.14 Halos which form earlier are more concentrated . . . . .                      | 89        |
| 14.15 Mergers of Dark Matter Halos . . . . .  | 90        |
| 14.16 Halo growth; mass accretion histories . . . . .                               | 90        |
| 14.17 Halo growth; concentration parameter histories . . . . .                      | 91        |
| 14.18 Dark Matter Halo Mergers: A Universal Fitting Form . . . . .                  | 91        |
| 14.19 Problems with Cold Dark Matter . . . . .                                      | 93        |
| 14.20 Missing Satellites Problem . . . . .  | 93        |
| 14.21 Core vs. Cusp Problem . . . . .   | 95        |
| 14.22 Summary of DM Halos . . . . .   | 96        |

# 1 August 25, 2021: Introduction and Course Overview

The major themes and sections of the class are:

- General properties of the galaxy population
  - Classification
  - Observations
  - Physical properties
  - Correlations
  - Statistical properties.
- Key ingredients
  - Stellar populations
  - Star formation
  - Gas and dust (ISM/CGM/IGM)
  - Chemical evolution and baryon cycle
  - Dark matter halos
- Elliptical and Disk Galaxies
  - Structures
  - Dynamics
  - Scaling relations
  - Maybe dwarf galaxies
- Nuclear activity and black holes
  - Different AGN
  - Relations between BHs and host galaxies
  - Black hole accretion histories
- Galaxy interactions and environment
  - Galaxy Interactions
  - Clusters
  - Environment
  - Large Scale Structure
  - Galaxy clustering
- First galaxies and galaxy evolution
  - Observing over cosmic time
  - First galaxies
  - Cosmic star formation history
  - Assemblt history
  - Evolution models
  - Formation models and simulations

We now turn our attention to the **Milky Way**.

## 1.1 The Milky Way

- Disk
  - Components
    - \*  $M_\star \sim 6 \times 10^{10} M_\odot$
    - \* Cold gas  $m \sim 5 \times 10^9 M_\odot$ 
      - about 20% of this is  $H_2$ . Cold and dense, associated with star formation.
      - other 80% is HI and often thought of as reservoirs for future star formation.
    - \* Hot gas  $\geq 10^6$  K.
  - Disk is kinematically cold ( $\sim 10 \text{ km s}^{-1}$ ) and rotating
  - The youngest stars in the disk are about  $10^6$  years old
  - There's a radial metallicity gradient such that metals increase toward the center
  - MW has spiral arms!
  - The disk can be further divided into the thin and thick disk:
- Thin Disk
  - $M_\star \sim 5 \times 10^{10} M_\odot$
  - Radial scale height  $h_r \sim 0.3 \text{ kpc}$ , with a drop off in surface brightness
  - Vertical scale height  $h_z \sim 0.3 \text{ kpc}$
  - Radius  $r \sim 35 \text{ kpc}$
  - Mixed stellar ages
- Thick Disk
- Dark Matter Halo
  - $M_{DM} \sim 10^{12} M_\odot$ , known within a factor 2 – 3 or so
  - Virial radius of roughly 150 kpc
- Rotation Curve
  - Sun is moving at roughly  $V = 220 \text{ km s}^{-1}$ . This speed is set by the enclosed mass which can be found by equating gravity to the Sun's centripetal acceleration:

$$\frac{mv^2(r)}{R} = \frac{GmM(r)}{R^2} \rightarrow \boxed{v_{circ}(r) = \sqrt{\frac{GM}{R}}}; \boxed{M_{enc} \propto r} \quad (1)$$

We care about classifying galaxies for a variety of reasons. There are a few classification schemes. Here's **Hubble's**:

There have been others developed since then, such as the deVaucouleur system or the T-type system.  
Recently, we have started a **newer, fresher** classification based on rotation!  
There are some difficulties in determining morphology, though:

- It depends on orientation.
- It depends on wavelength.
- Subjective.
- etc.

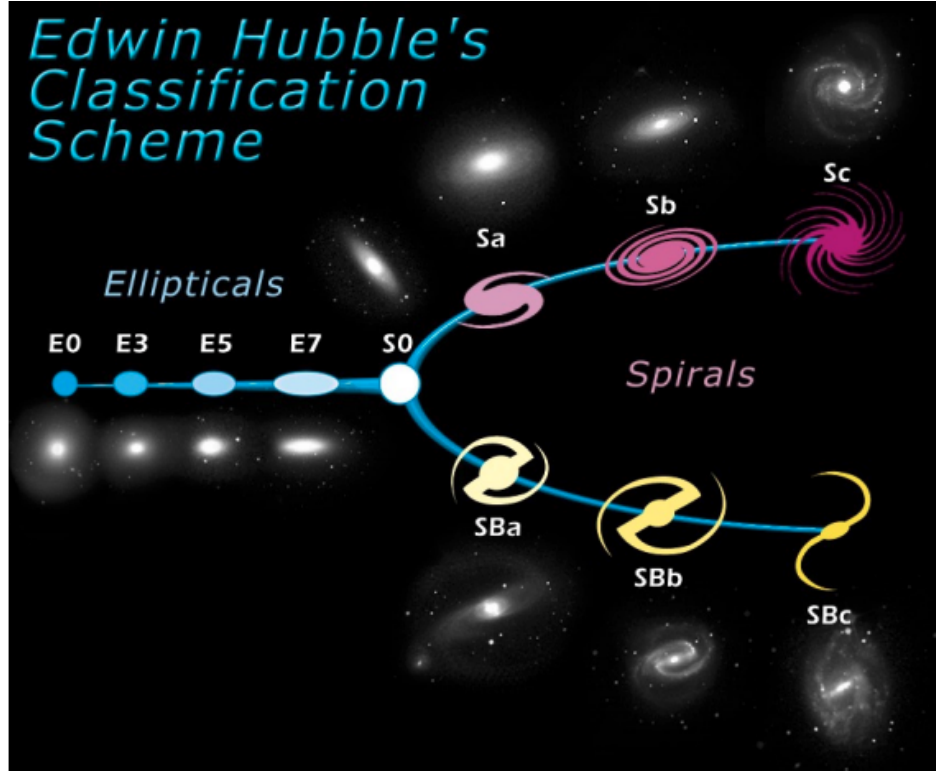


Figure 1: Hubble Classification Scheme

## 2 August 27, 2021: Global Properties and Galaxy Correlations

### 2.1 Morphology, Continued

Let's start by looking a little deeper at the morphological classifications from last time. First, let's look at spectra along the Hubble sequence, HI content, stellar mass, stellar surface density, oxygen abundance, and environment. The results are presented in Figures 4 through 7.

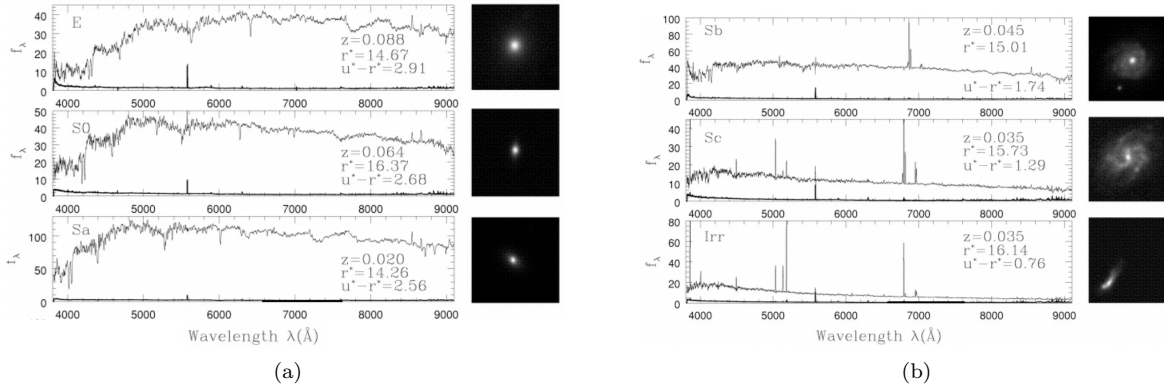


Figure 4: Spectra along the Hubble sequence. Early type galaxies are much redder and have deeper absorption features. Later-type galaxies have spectra that are dominated by emission from hot stars.

Table 2.5. Galaxy morphological types.

| Hubble | E  | E-SO            | SO              | SO-Sa           | Sa | Sa-b | Sb | Sb-c | Sc  | Sc-Irr | Irr |
|--------|----|-----------------|-----------------|-----------------|----|------|----|------|-----|--------|-----|
| deV    | E  | SO <sup>-</sup> | SO <sup>0</sup> | SO <sup>+</sup> | Sa | Sab  | Sb | Sbc  | Scd | Sdm    | Im  |
| T      | -5 | -3              | -2              | 0               | 1  | 2    | 3  | 4    | 6   | 8      | 10  |

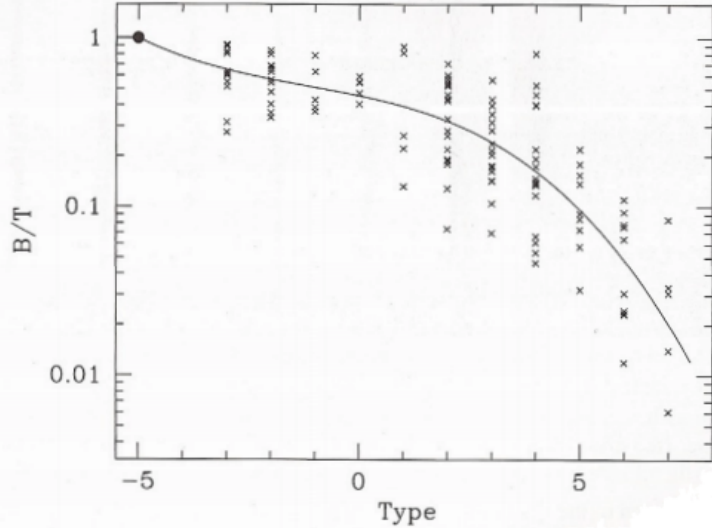


Figure 2: Other classification schemes.

Cappellari et al. (2011)

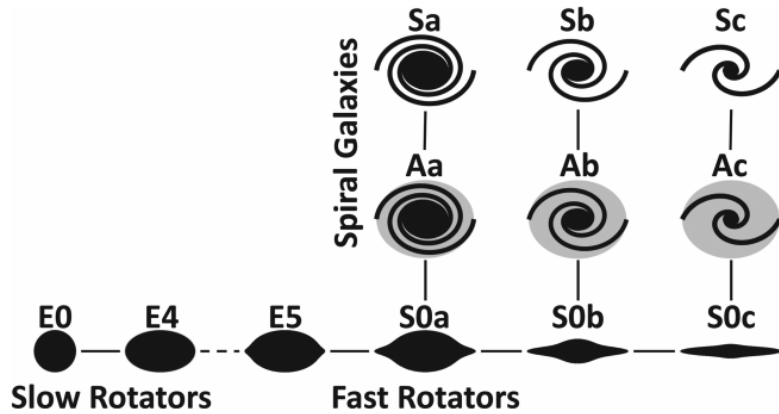


Figure 3: Fast and slow rotation scheme.

Here are the general trends. Star formation rate, gas fractions, and rotational support increase for later-type galaxies. Mass, metallicity, environment, and mass surface density increase for earlier-type galaxies.

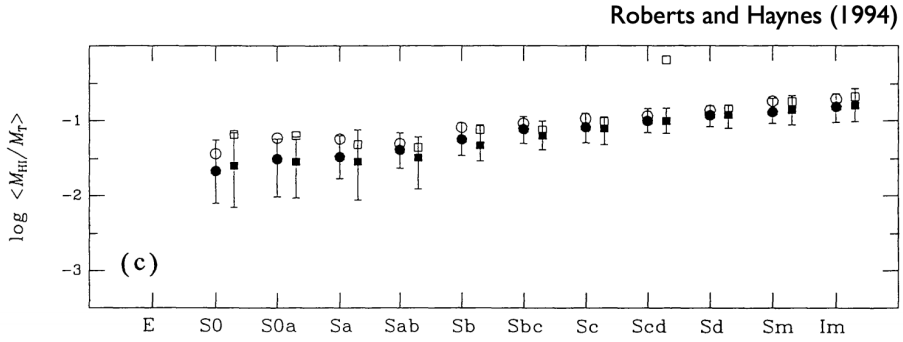


Figure 5: HI content as a function of morphology.

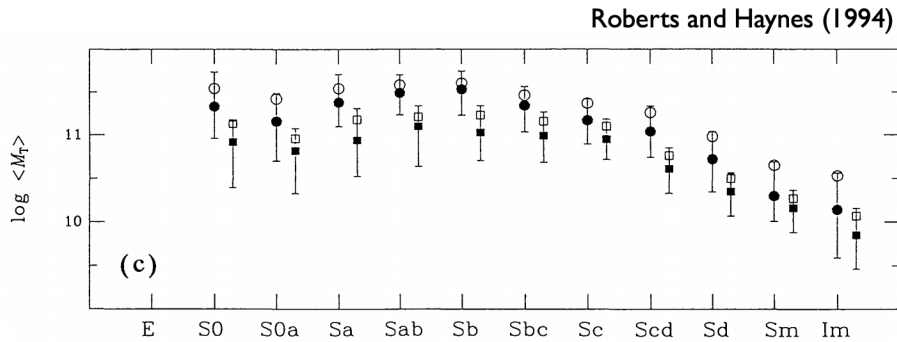


Figure 6: Total stellar mass as a function of morphology.

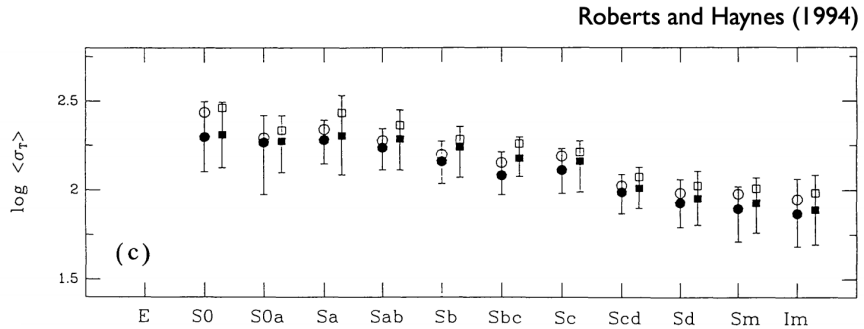


Figure 7: Stellar surface density as a function of morphology.

## 2.2 Units and Quantities

Let's do a quick review of units and other quantities we will use through the semester. Recall **specific intensity**:

$$[I_\nu] = \frac{\text{ergs}}{\text{s cm}^2 \text{sr Hz}} \quad (2)$$

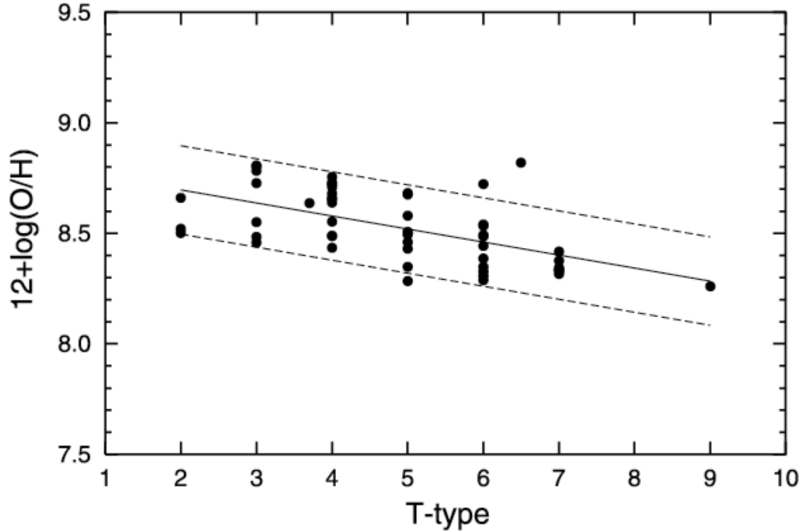


Figure 8: Oxygen abundance as a function of morphology. Note that the +12 is just to make things positive!

We also have the quantity of **flux density**:

$$[F_\lambda] = \frac{\text{ergs}}{\text{s cm}^2 \text{\AA}} \quad (3)$$

In general, remember that  $F_\lambda \neq F_\nu$ . Instead,  $F_\lambda d\lambda = F_\nu d\nu$ , and thus:

$$F_\nu = \frac{c}{\nu^2} F_\lambda \quad (4)$$

We also discussed magnitudes which are a terrible unit. But alas, we must use them. The apparent magnitude is defined as:

$$m_x = -2.5 \log_{10} \left( \frac{F_x}{F_{x,0}} \right) \quad (5)$$

where the subscript  $x$  represents a filter and  $F_{x,0}$  is the flux of a reference in filter  $x$ . Historically, stellar astronomers have used Vega as the reference point. Galactic astronomers have used AB magnitudes (I have no idea what the reference is, here). In this **AB Magnitude system**, we have:

$$m_x = -2.5 \log_{10} (F_x) - 48.57 \quad (6)$$

**Absolute magnitudes** are defined as:

$$\underbrace{m_x - M_x}_{\text{distance modulus } \mu} = 5 \log_{10} \left( \frac{d}{d_0} \right), \text{ where } d_0 \equiv 10 \text{ pc} \quad (7)$$

We also need to be familiar with redshift, both due to expansion and relativistic velocities. We define the redshift  $z$ :

$$1 + z = \frac{\lambda_{obs}}{\lambda_{em}} \quad (8)$$

In the case of particles moving at relativistic speeds, we have:

$$1 + z = \sqrt{\frac{1 + v/c}{1 - v/c}} \quad (9)$$

In the non-relativistic case, we have the **Hubble's Law**:

$$v \approx cz \quad (10)$$

Lastly, we defined the **luminosity distance** as:

$$d_L^2 \equiv \frac{L}{4\pi F} \quad (11)$$

### 2.3 Sloan Digital Sky Survey

The Sloan Digital Sky Survey (SDSS) revolutionized astronomy. Not only did it take spectra and photometry of millions of galaxies, but it also redefined the photometric system from the Johnson-Cousins system to the familiar *ugriz* system. First, let's discuss an important aspect of filters: **filter response functions**. This is basically like a sensitivity/efficiency, and these curves look like this:

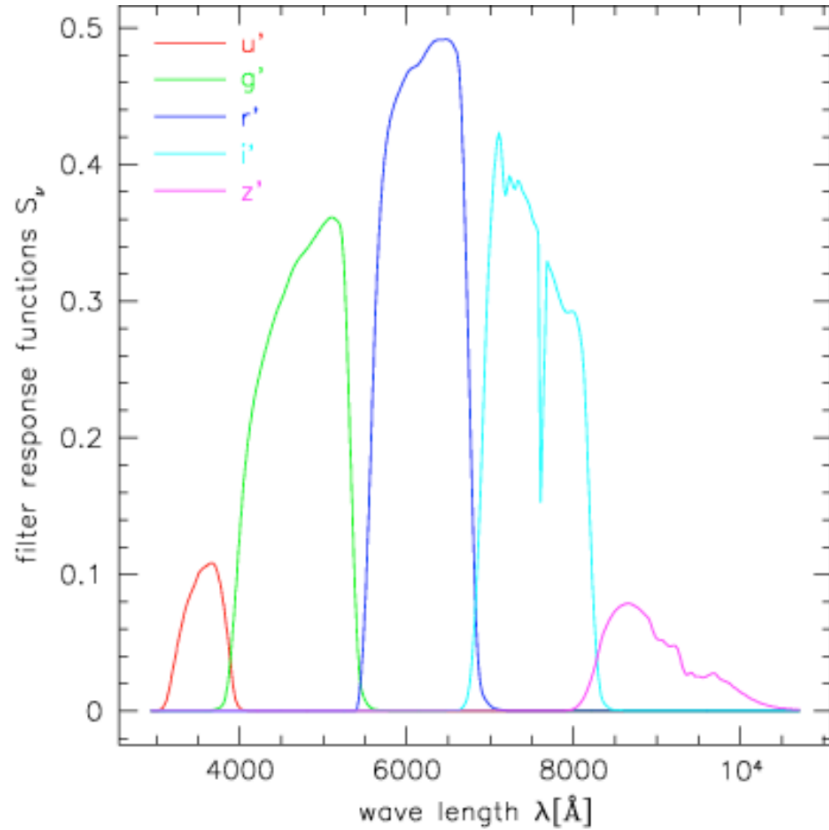


Figure 9: SDSS transmission curves.

Note that:

$$F_x = \frac{\int_0^\infty S_\nu F_\nu d\nu}{\int_0^\infty S_\nu d\nu} \quad (12)$$

SDSS had 5 band photometry for millions of objects, which means we need to look at spectral energy distributions (SEDs). These are basically low resolution spectra, but we can still learn a ton from these plots! We can match SEDs to synthetic galaxy spectra to measure photometric redshift or learn about broad properties of the galaxies.

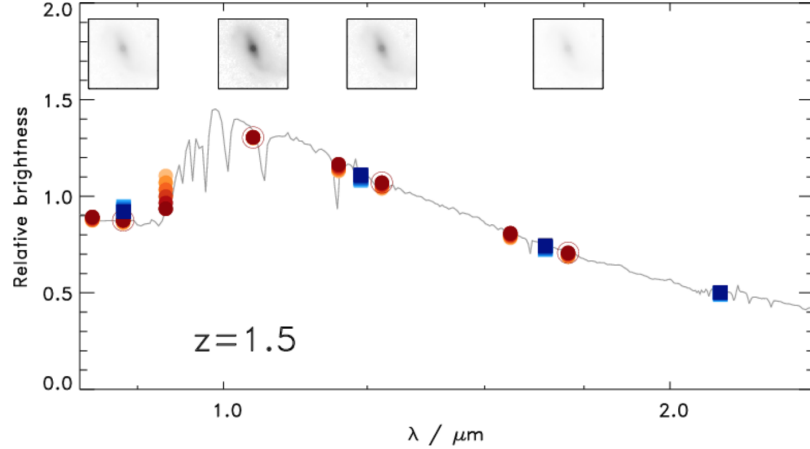


Figure 10: Example SED with fit for photometric redshift.

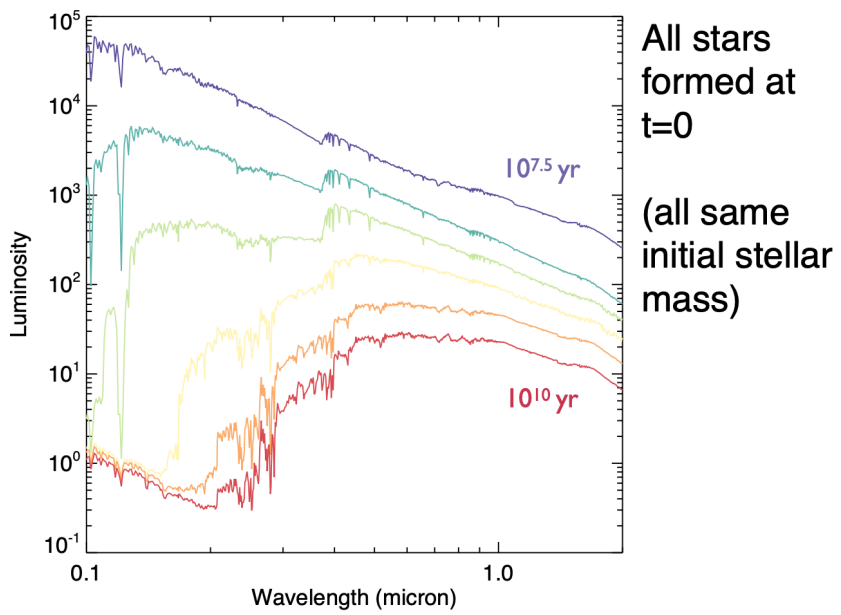


Figure 11: Synthetic galaxy spectra as a function of age.

One thing to note is that redder galaxies are less luminous for the same stellar mass, as we can see in the synthetic spectra. This result in redder galaxies having higher mass to light ratios!

## 2.4 K Corrections

Here's a figure to demonstrate K-corrections.

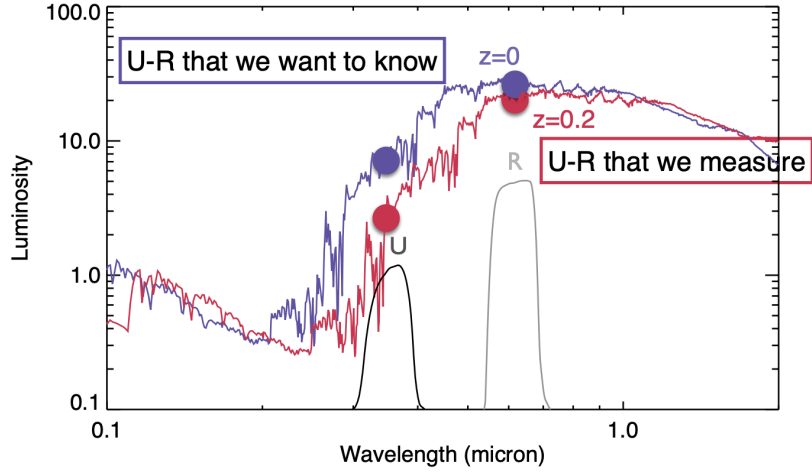


Figure 12: The SED changes as a function of redshift. We ultimately want the rest-frame  $u - r$  value, but we need to correct the observed spectrum in some way since  $u - r$  itself is a function of redshift. This is the concept of a  $K$  correction.

We model  $K$  corrections in this way:

$$m = M + \mu + K \quad (13)$$

$$\text{observed} = \text{intrinsic} + \text{distance} + \text{expansion} \quad (14)$$

## 2.5 Trends of Stellar Mass with Color

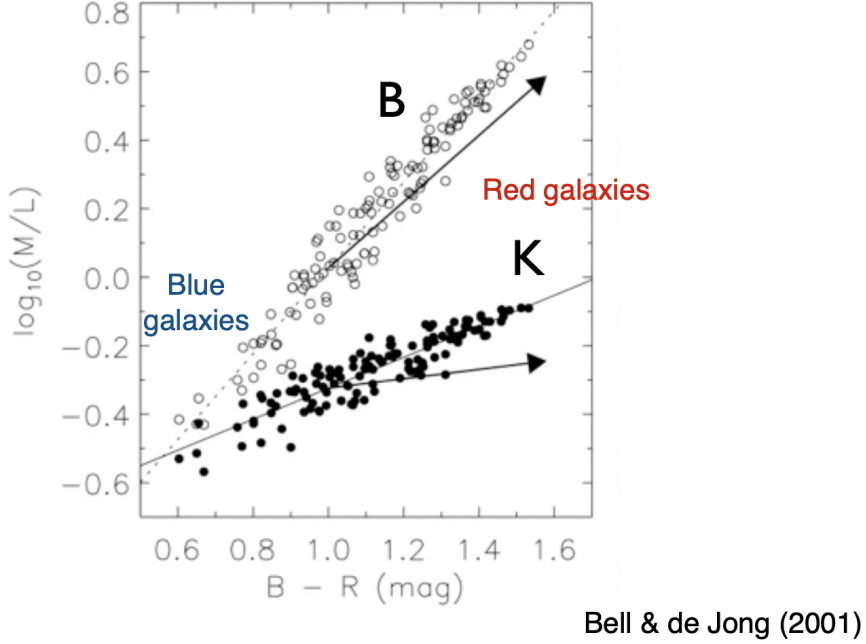


Figure 13: Trends of stellar mass to light ratio with color.

TABLE 1  
STELLAR  $M/L$  RATIO AS A FUNCTION OF COLOR FOR THE FORMATION EPOCH MODEL WITH BURSTS, ADOPTING A SCALED SALPETER IMF

| Color       | $a_B$  | $b_B$ | $a_V$  | $b_V$ | $a_R$  | $b_R$ | $a_I$  | $b_I$ | $a_J$  | $b_J$ | $a_H$  | $b_H$ | $a_K$  | $b_K$ |
|-------------|--------|-------|--------|-------|--------|-------|--------|-------|--------|-------|--------|-------|--------|-------|
| $B-V$ ..... | -0.994 | 1.804 | -0.734 | 1.404 | -0.660 | 1.222 | -0.627 | 1.075 | -0.621 | 0.794 | -0.663 | 0.704 | -0.692 | 0.652 |
| $B-R$ ..... | -1.224 | 1.251 | -0.916 | 0.976 | -0.820 | 0.851 | -0.768 | 0.748 | -0.724 | 0.552 | -0.754 | 0.489 | -0.776 | 0.452 |
| $V-I$ ..... | -1.919 | 2.214 | -1.476 | 1.747 | -1.314 | 1.528 | -1.204 | 1.347 | -1.040 | 0.987 | -1.030 | 0.870 | -1.027 | 0.800 |
| $V-J$ ..... | -1.903 | 1.138 | -1.477 | 0.905 | -1.319 | 0.794 | -1.209 | 0.700 | -1.029 | 0.505 | -1.014 | 0.442 | -1.005 | 0.402 |
| $V-H$ ..... | -2.181 | 0.978 | -1.700 | 0.779 | -1.515 | 0.684 | -1.383 | 0.603 | -1.151 | 0.434 | -1.120 | 0.379 | -1.100 | 0.345 |
| $V-K$ ..... | -2.156 | 0.895 | -1.683 | 0.714 | -1.501 | 0.627 | -1.370 | 0.553 | -1.139 | 0.396 | -1.108 | 0.346 | -1.087 | 0.314 |

NOTE— $\log_{10} (M/L) = a_\lambda + b_\lambda \text{Color}$ . Note that the stellar  $M/L$  values can be estimated for any combination of the above colors by a simple linear combination of the above fits. Note also that if all (even very high surface brightness) disks are submaximal, the above zero points should be modified by subtracting a constant from the above relations.

$$\log_{10} (M/L) = a_\lambda + b_\lambda \text{Color}$$

Figure 14: Table which was a first attempt at quantifying this relationship. Much better ways of doing this now!

## 3 September 1, 2021: Global Properties and Galaxy Correlations

### 3.1 AB Magnitudes and Vega Magnitudes

The AB magnitude system is the **absolute** system.

$$m_{AB} = -2.5 \log_{10} \left( \frac{f_\nu}{3631 \text{ Jy}} \right) = -2.5 \log_{10} (f_\nu) - 48.57 \quad (15)$$

We have a differ net system called the **STmag**, which is similar but in wavelength; not in frequency. The conversion between the two is non-trivial. The corrections in the optical are small, but these increase at larger and smaller wavelengths.

### 3.2 Synthetic galaxy spectra as a function of age

This discussion primarily revolves around Figure 11, the figure of the synthetic spectra as a function of age. Make sure to be able to re-create this type of plot!

Imagine taking a stellar population synthesis model at the same time, with some mass. Young populations are brighter per unit mass, and they are bluer. Redder galaxies have higher mass to light ratios.

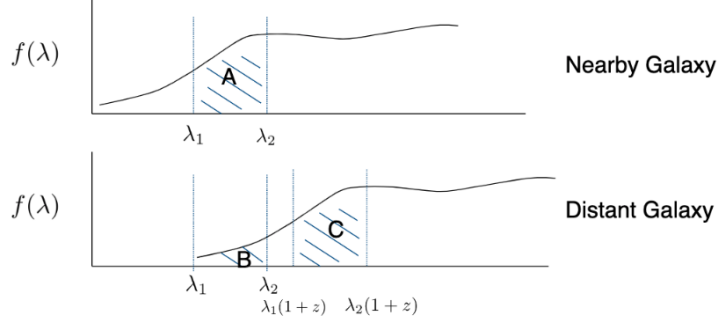
Let's now move onto K-corrections...

### 3.3 K-corrections

The idea: Normally we observe through filters, meaning over some specific  $d\lambda$ . For a typical galaxy spectra at  $z = 0$ :

$$L = \int_{\lambda_1}^{\lambda_2} f(\lambda) d\lambda \quad (16)$$

Due to redshift effects, the light emitted gets shifted by a factor of  $(1+z)$ . Looking at galaxies at higher  $z$ , we receive emission from shorter wavelengths at a slower rate. Knowing the spectra shape, we can correct for this via K-correction. The **assumption: we know something about the intrinsic spectrum**. Here's a figure explaining what we mean:



We measure B, but want to measure C to compare to A.

$$K(z) = \frac{\int_0^\infty T(\lambda/(1+z))f(\lambda/(1+z))d\lambda}{(1+z)\int_0^\infty T(\lambda)f(\lambda)d\lambda}$$

Made by Greg Taylor

Figure 15: K-corrections, by Greg Taylor.

Here's a derivation:

The flux we observe per unit wavelength,  $F_\lambda$  (the emitted luminosity is:  $L_{\lambda/(1+z)}$ ):

$$F_\lambda = \frac{1}{1+z} \frac{L_{\lambda/(1+z)}}{4\pi D_L^2} = \frac{1}{1+z} \frac{L_{\lambda/(1+z)}}{L_\lambda} \frac{L_\lambda}{4\pi D_L^2} \quad (17)$$

Equivalently:  $F_\nu \propto (1 + z)$ . After some work, we can see that:

$$m = M + \mu + K, \text{ where } K \equiv -2.5 \log_{10} (F_\lambda) \quad (18)$$

Generally,  $K$  corrections are positive. There are unusual cases where the  $K$  correction is negative, but that's uncommon.

### 3.4 Stellar Masses (Bell & de Jong 2001)

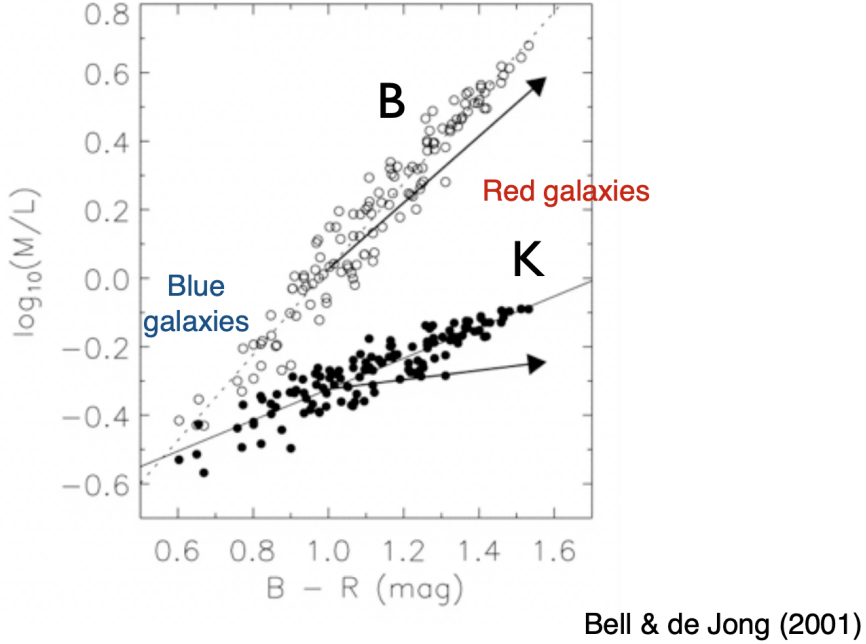


Figure 16: Re-visited on September 1!

We're discussing the figure here. The x-axis is the  $B - R$  color, and the y-axis is the inferred mass-to-light ratio. Each dot is an individual galaxy. The two groups are  $B$  and  $K$  band mass to light ratios, with the key takeaway is that **there is no one-to-one mapping between mass and luminosity**. Instead, luminosity and color can give you a mass.

It's best to observe  $K$  band for measuring mass to light ratios so that the spectrum isn't dominated by **single O stars**. The ideal case is a filter for which the mass-to-light does not depend on the color.  $K$  is close, but it's not ideal!

However, bluer colors are better at disentangling the age of a stellar population.

### 3.5 SEDs for Different Metallicities

Here's an interesting figure:

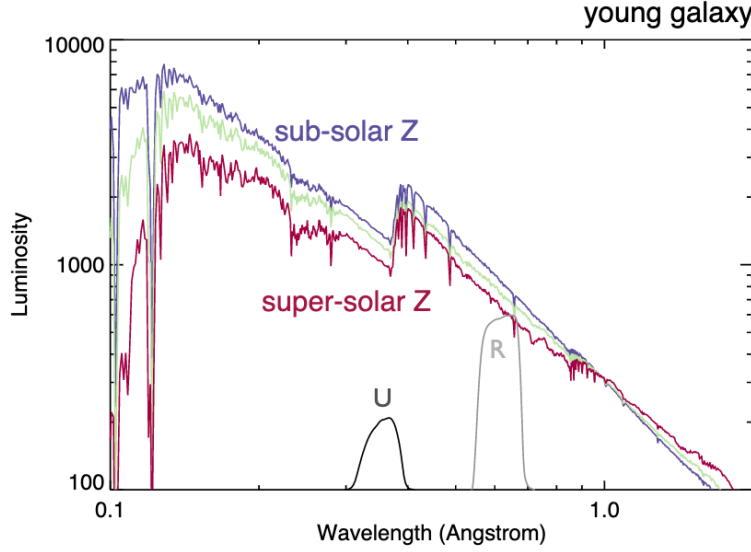


Figure 17: SEDs for different metallicities for a young galaxy. What are the takeaways?

For a fixed mass and galaxy type, lower-metallicities are brighter, particularly in the blue! As you go to the red end of the spectrum, the SEDs blend together better.

This is due to **opacity**. Fewer metallicites have a lower opacity, and so more light gets out. For higher metallicities, we have a higher opacity and thus less light gets out.

Also know that the age has a huge impact on the spectra, but metallicity has much less of an effect. This also means that metallicity is harder to measure than age. They're also **degenerate** with each other.

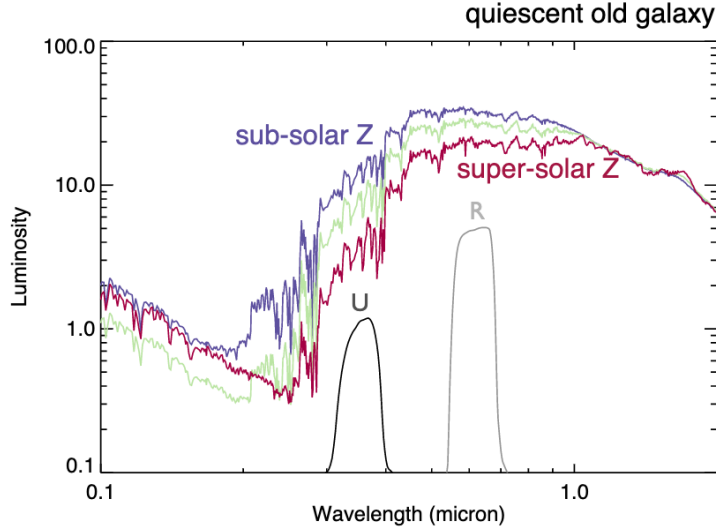


Figure 18: SEDs for different metallicities for an old galaxy. What are the takeaways?

What's different for the older, quiescent galaxy? At the blue end of the spectrum, solar metallicity populations are actually **weakest**! Detailed stellar physics of post-main sequence stars dictate this effect.

### 3.6 Color Sequences

Let's look at color vs. stellar mass of galaxies. The color of the galaxy  $m_u - m_r$  can be thought of as the slope of the SED. Interpreted differently, this is:

$$u - r = -2.5 \log_{10}(F_u) + 2.5 \log_{10}(F_r) \rightarrow u - r = -2.5 \log_{10} \left( \frac{F_u}{F_R} \right) \quad (19)$$

Here's a cool plot:

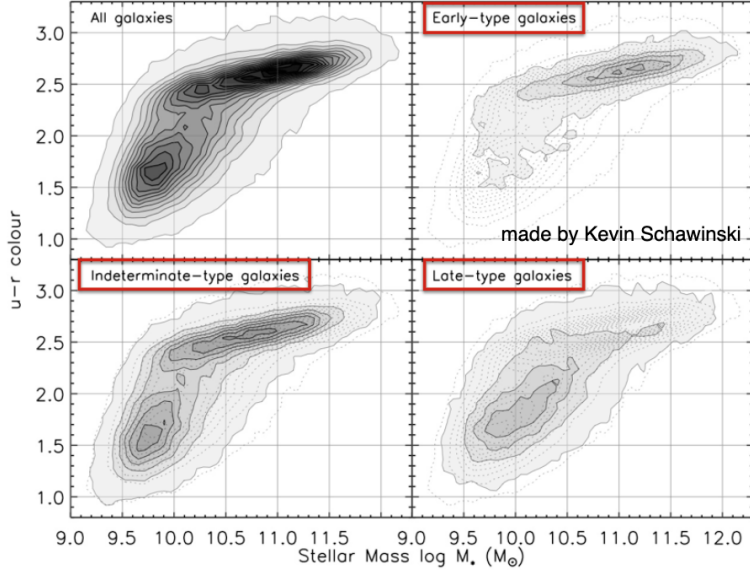


Figure 19: Color sequences. Note that there are two pileups: redder and more massive; blue and less massive.

If you measure a galaxy color, we can measure the mass to light ratio. **This is a key reason to measure color.** If we also measure the spectrum (or the SED with multi-band photometry), we can get the galaxy flux, redshift, and make a K-correction. Note we can also measure the mass-to-light (or mass) from the SED, too!

What are some other trends in this plot? The early-type galaxies hardly change in color but increase 2 dex in mass. This

### 3.7 Galaxy Correlations in the SDSS

Let's talk about the D-4000 decrement from Kauffmann et al., 2003:

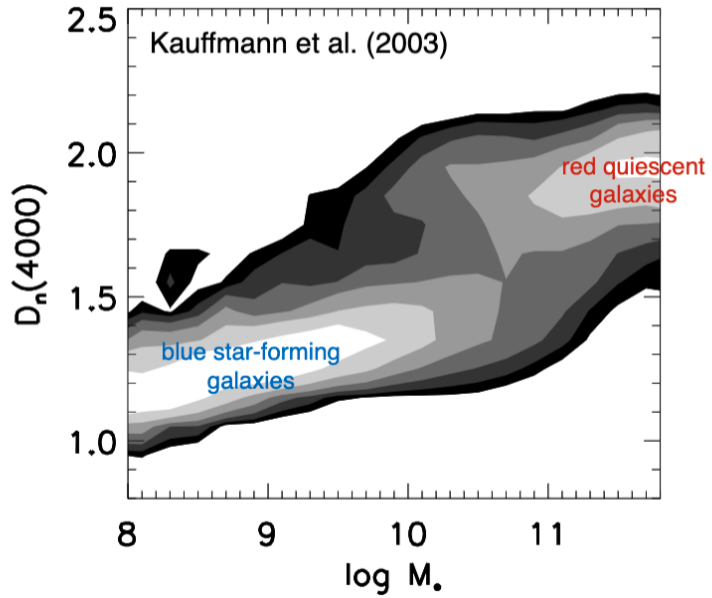


Figure 20: We can see that the D4000 feature very nicely separates the red, quiescent galaxies from the blue, star-forming galaxies.

So what is D4000? It's a flux ratio (color) between 4000Å and 4100Å as well as the flux between 3856Å to 3950Å. There are lots of age sensitive features here, which make it ideal. Note that these ranges are not exact.

$$D_n(4000\text{\AA}) = \frac{F(4000\text{\AA} - 4100\text{\AA})}{F(3856\text{\AA} - 3950\text{\AA})} \quad (20)$$

This looks like this:

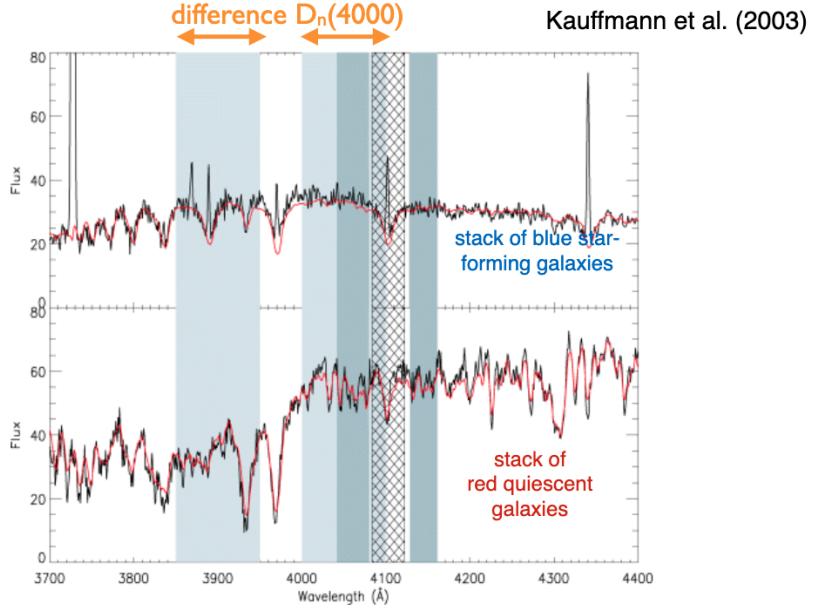


Figure 21: Star forming galaxies have a very small break, but the red galaxies have a very large break near  $4000\text{\AA}$ .

Here is the 4000 Angstrom break as a function of both age and metallicity:

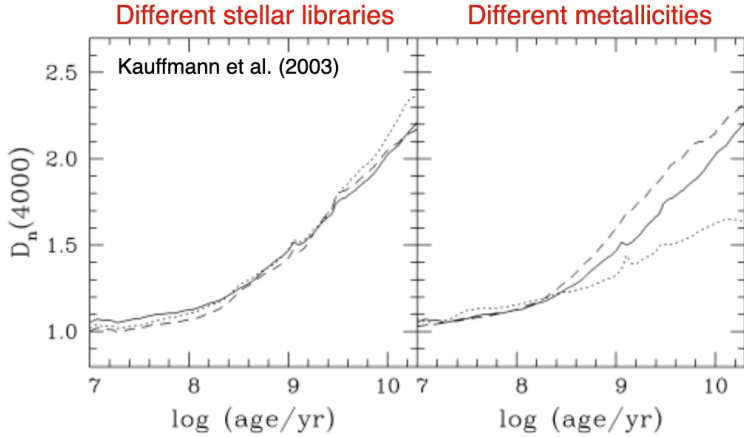


Figure 22: The 4000 Angstrom break.

So, the takeaway is that the  $4000\text{\AA}$  break is a much better measurement of age compared to broadband photometry, but much more expensive. There's also a pretty strong signal to noise requirements needed for  $D_{4000}$  measurements.

$D_{4000}$  measurements are tough with k-corrections in the mix as well since we need to know the intrinsic shape of the spectrum, which is much harder for high redshift galaxies.

### 3.8 Stellar metallicity - mass relation (Gallazzi et al., 2005)

At higher masses, stars are more metal-rich. As you go to lower masses, we have lower metallicity. Under the hood, star formation is generating metals. Massive galaxies have more star formation, and thus more metals, to zeroth order.

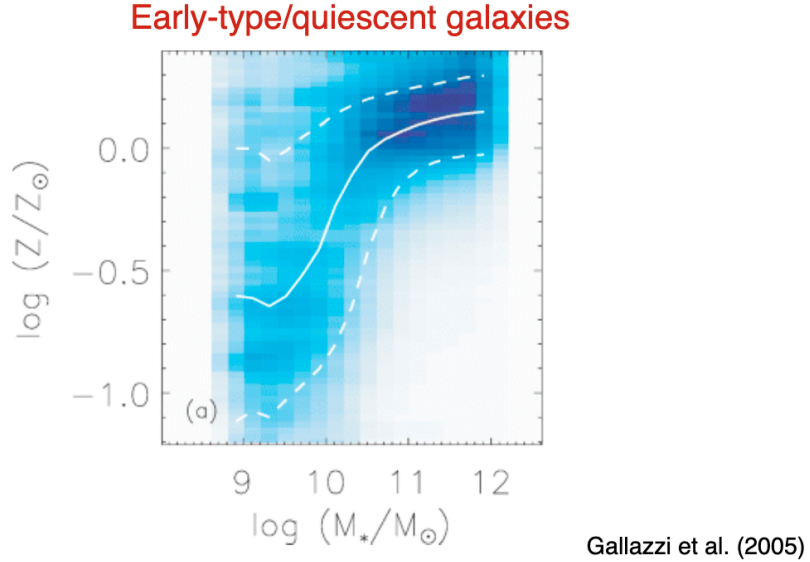


Figure 23: Stellar metallicity-mass relation for early-type galaxies.

For **late type galaxies**, this is more complicated but gives a similar trend.

## Late-type / star-forming galaxies

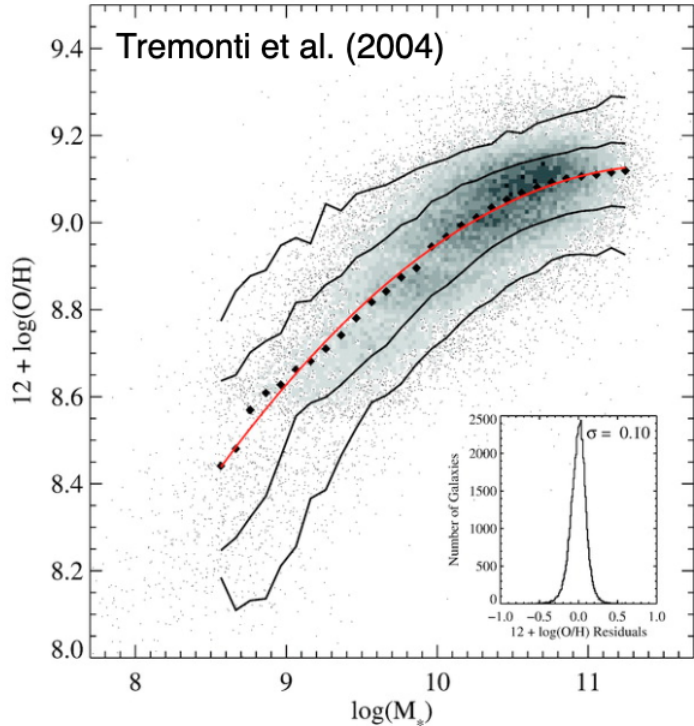


Figure 24: Stellar metallicity-mass relation for late-type galaxies.

How do you make a measurement like this? Ionized HII regions emit oxygen lines in late-type galaxies. This doesn't happen in early type galaxies!

We will continue next time with the late-type slope in the color-mass plot!

## 4 September 3, 2021: Global properties, galaxy correlations, and statistics

### 4.1 Measuring gas-phase metallicity

What is going on with the fiber versus total spectra in the SDSS data? SDSS is a fiber fed system, with each fiber being really tiny. As a result, only the central regions are getting spectra!

We are thus assuming that in the central region, oxygen emission comes only from star formation. It turns out that AGN also create emission line patterns which complicate things!

In our problem set, we are asked for gas-phase metallicity for our galaxies, so what do we do? For our homework, use total fluxes and not fiber fluxes!

### 4.2 Brief Review of Last Time: Color Sequences,

Remember the  $u - r$  color slope is primarily driven by the metallicity (mass-metallicity relation) for early type galaxies.

Late-type galaxies are driven by star-formation properties. The way we can see this most clearly is the star formation rate-stellar mass relation (Samir et al, 2007):

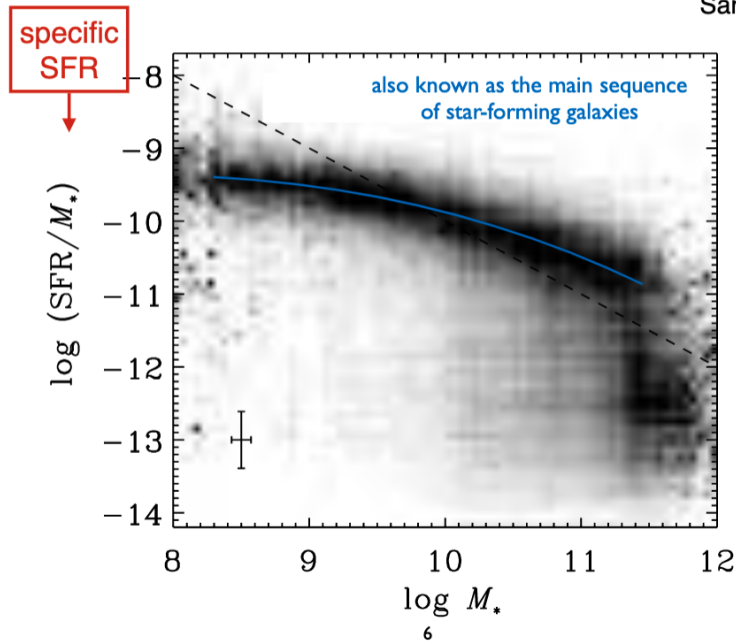


Figure 25: sSFR-stellar mass relation.

This isn't the most obvious thing to plot, however. It'd be more obvious to plot star formation rate versus the stellar mass (star-forming main sequence). The shape changes when we plot the specific star formation rate. So what does this tell us/what is the interpretation?

As we go to higher masses, the **star formation rate per unit mass is lower because it's less efficient**. One way to think about this (since the previous statement is pretty empty): low mass galaxies have younger populations which have formed more recently (and thus have no converted mass into stars yet because the potential is shallower). Another explanation is that larger galaxies have had time to spread mass out over the whole halo (where gas density is too low to form stars).

### 4.3 Stellar mass-halo mass relation

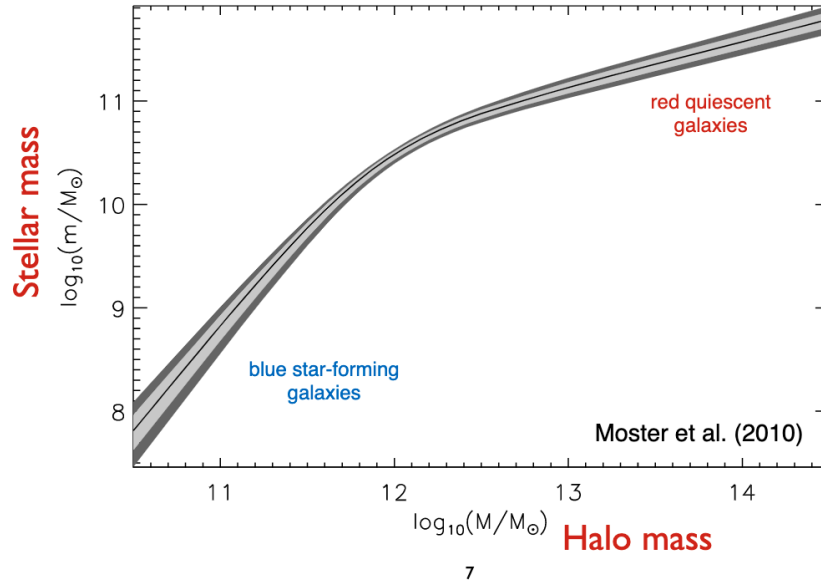


Figure 26: Stellar mass-halo mass relation (Moster 2010).

One of the ideas in galaxy formation is that the dark matter halo drives galaxy formation moreso than anything else. The halo mass should thus determine the evolution of the galaxy as a whole. It sets the potential, temperatures of gas (kinematic temperature), accretion rate (mass inflow rate), etc. **The problem is that measuring halo masses is really difficult!**

We can assign galaxies to halos with **abundance matching**, shown in Figure 26, giving rise to the stellar-mass halo-mass relation (SMHM, SMH relation). The most massive stellar and dark galaxies are red, quiescent galaxies. At the low end, there are blue star-forming galaxies.

This leads to one of the most important plots in the course:

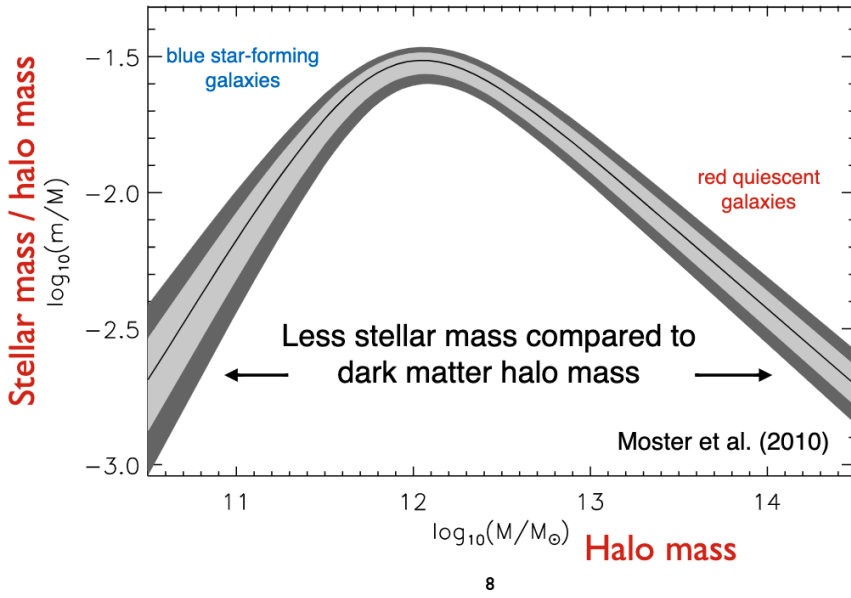


Figure 27: Stellar mass-halo mass ratio vs. halo mass. This is saying that, as you go to really low or high mass haloes, there is less stellar mass! **Per unit halo mass, really massive and really low-mass galaxies are inefficient at star formation.** The peak is where star formation is the most efficient!

## 4.4 Galaxy Sizes

### 4.4.1 Sersic (1968) Profiles

The generalized version is:

$$I(R) = I_0 e^{-\beta_n (R/R_e)^{1/n}} = I_e e^{-\beta_n ((R/R_e)^{1/n} - 1)} \quad (21)$$

Here,  $I_0$  is the central intensity,  $\beta_n$  is a scale factor,  $n$  is the Sersic index,  $R_e = R_{1/2}$  is the effective radius or the half-light radius.

You often see this written in terms of surface brightness, which is just the magnitude form.

There are two specific cases of the Sersic profile. For early type galaxies, we have deVaucouleur's Law:

$$I(R) = I_e e^{-7.7[(R/R_e)^{1/4} - 1]} \quad (22)$$

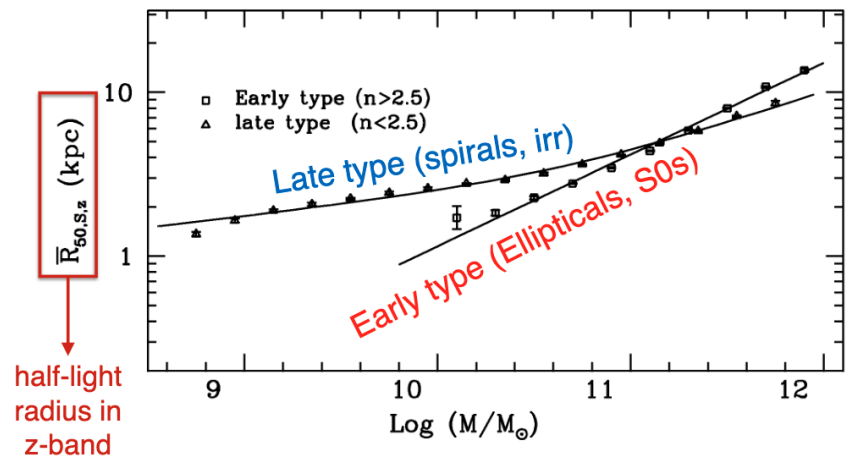
This is a Sersic with  $n = 4$  and  $\beta_n = -7.7$ . If we plot  $\mu$  versus  $r^{1/4}$ , this is a straight line:

Late-type galaxies are even more difficult to fit. For late-type galaxies, we have:

$$I(r) = I_0 e^{-r/h} \quad (23)$$

where  $I_0$  is the central surface brightness,  $h$  is the scale length (1e folding of light). In this case, plotting  $\mu$  versus  $r$  alone gives the straight line.

## 4.5 Stellar mass-size relation (Shen et al., 2003)



Shen et al. (2003)

Figure 28: Stellar mass-size relation.

## 4.6 Measuring galaxy sizes and Sersic indices

Large sersic indices are peaky toward the middle (ETGs), smaller values (late-type) are toward the outskirts.

## 4.7 Galaxy sizes over cosmic time

Good to know that sizes are not constant over time, and we will come back to this.

## 4.8 Relation with Environment

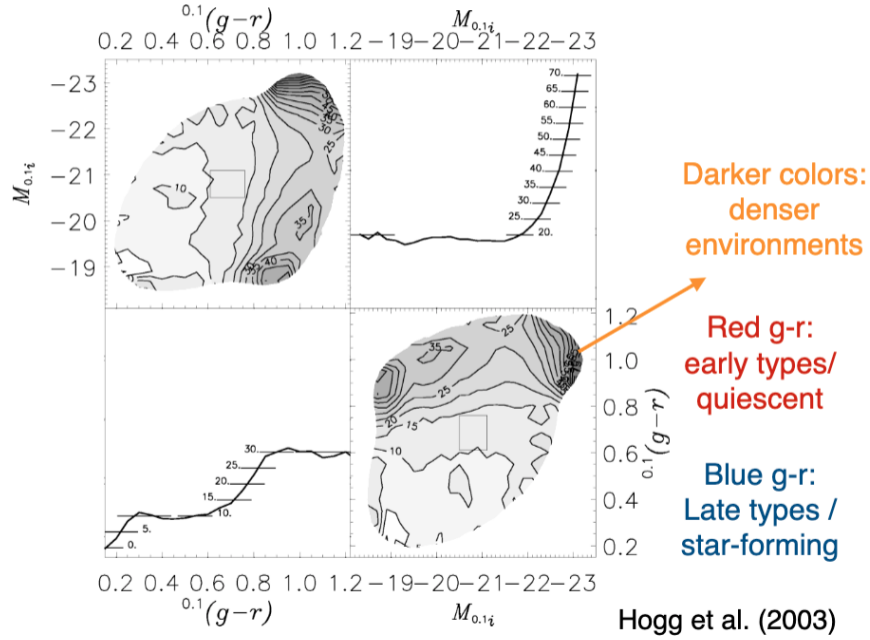


Figure 29: Relation with environment. Bottom right: Contours are density, with darker colors being denser environments (number per volume). In higher density environments, you find early type galaxies.

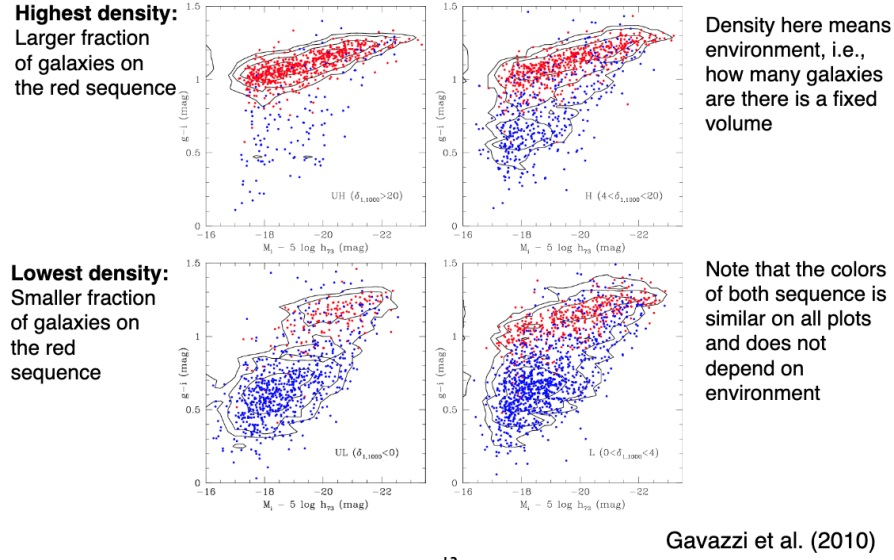


Figure 30: Color-magnitude diagrams in different environments (Gavazzi et al. (2010)).

## 4.9 Disentangling environment, mass, morphological type, and Sersic parameter (van der Wel 2008).

Left hand column x-axis is number per volume.

## 4.10 Staistical properties of the galaxy population

Look at the M87 field. We can start to plot the number of galaxies as a function of luminosity bin since they are all at the same (rough) distance. Our theories can make predictions on this!

## 4.11 The luminosity function of galaxies

First posited by Schechter (1975), we have the Schechter luminosity function. For better or worse, there are no physical bases for this even though it works really well!

$$\Phi(L) dL = \Phi_* \left( \frac{L}{L_*} \right)^\alpha e^{-L/L_*} d \left( \frac{L}{L_*} \right) \quad (24)$$

$L_*$  is the inflection point in the luminosity function,  $\alpha$  is the “faint-end slope”,  $\Phi_*$  is a normalization. Note that the units of  $\Phi$  are number/volume. Sometimes this is further divided into magnitude bins.

When  $L \ll L_*$ , we have power law behavior with  $\alpha$  dominating. For  $L \gg L_*$ , we have exponential decline dominating. In the local universe, the Milky Way is approximately an  $L_*$  galaxy. In physical units, we have:

$$L_{\text{B-band}}^{\text{MW}} \sim 10^{10} L_\odot \quad (25)$$

## 4.12 Peculiar Motions

To get a luminosity, we first need a distance! Occasionally, you see a **huge** scatter in the relationship because of peculiar velocities of things like the Virgo cluster.

This introduces the concept of **Malmquist bias**. You can see brighter objects farther away:

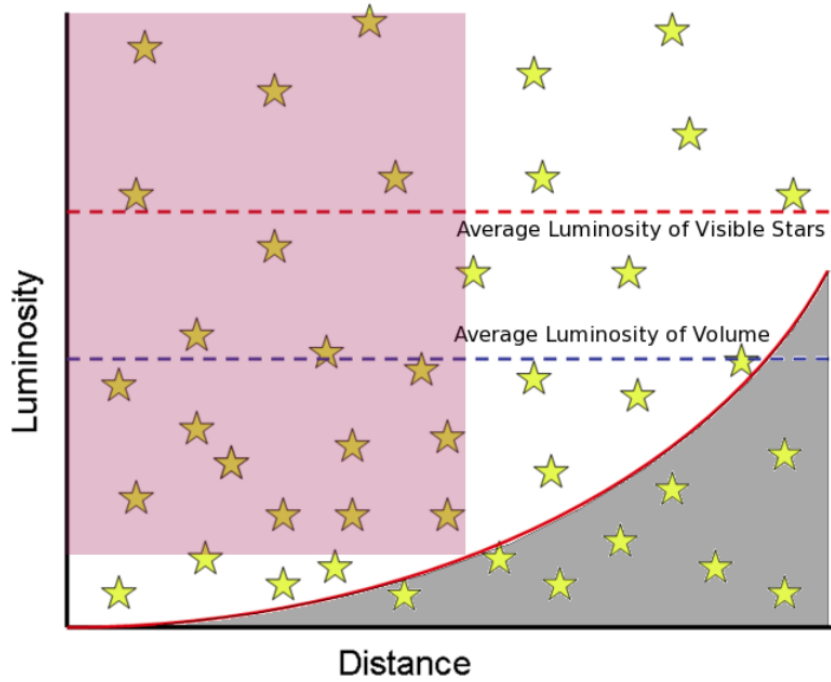


Figure 31: Malmquist bias.

Perhaps most obvious fix is a luminosity cutoff, but this has disadvantages in that you impose a distance cutoff and also you're throwing out data. The better solution is a  $1/V_{max}$  correction:

### $1/V_{max}$ corrections for Malmquist bias

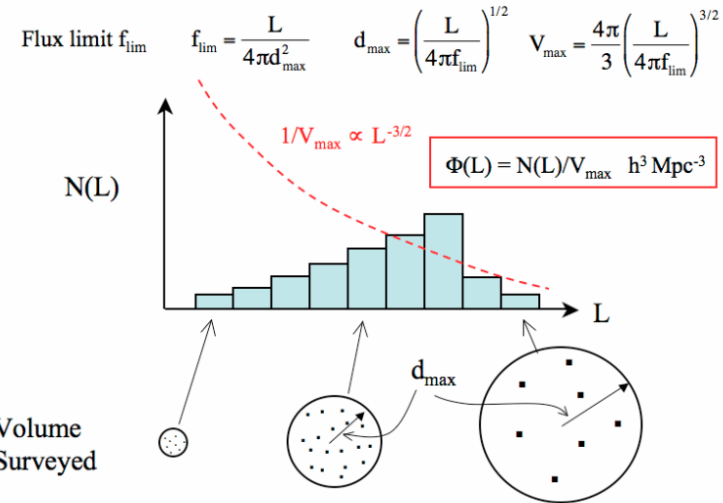


Figure 32: Malmquist bias solution as a  $1/V_{max}$  correction.

## 5 September 8, 2021: Finish galaxy statistics; stellar populations; stellar evolution review

### 5.1 Luminosity Function for Different Hubble Types

Why does the Schechter function work? See Binggeli (1998). The composite of individual galaxy functions form a Schechter function, but each individual function does not! Is this accurate? Maybe not...are these complete at the faint end? To first order, yes. But nothing is first order.

#### 5.1.1 Challenges

- Need to know distances; redshifts for low-z galaxies reflect distance and peculiar motion
- Low surface brightness galaxies are hard to detect.
- Malquist bias: brighter galaxies can be traced to larger distances than fainter galaxies. We can correct by only considering range of luminosity and distance; or you can apply volume corrections for each luminosity.

#### 5.1.2 Vmax Correction, Revisited

### 5.2 Luminosity Functions as a function of color (Blanton 2001)

Red galaxies dominate the bright end of the luminosity function – the biggest are the brightest! The blue galaxies dominate the faint end. This is not totally a surprise! Remember the stellar mass versus color diagram!

### 5.3 Luminosity Function as a function of environment (Christlein 2000)

There are more galaxies in denser environments. Also, the faint end slope gets steeper in low density environments. There are many more low mass galaxies in dense environments.

### 5.4 Luminosity and Mass Functions (Yang et al. 2009)

Redder galaxies have higher mass-to-light ratios  $\Upsilon$ , and thus the red function moves to the right compared to the blue function when going from luminosity to mass. Working in mass function space is **much better** than in luminosity space, but you need way more data to get masses.

### 5.5 Physical Origin of the Luminosity Function

Ratio of these two lines give us the plot from last time of the halo mass versus stellar mass per halo mass plot (with peak efficiency near the MW).

### 5.6 Evolution of the Mass Function (with redshift) [Muzzin et al 2013]

The normalization shifts, for sure, but you also start to see other patterns emerge. At high redshift ( $z \sim 2$ ), the functions are more or less on top of each other. We can see changes in galaxy populations!

**The mass function can be used to trace the build up of stellar mass in both star-forming and quiescent galaxies over cosmic time.**

## 5.7 Evolution of the UV Luminosity Function (Bouwens et al 2000)

UV Luminosity functions (UVLF) can be used to trace the evolution of the SFR density over cosmic time. At high redshift, we have low number densities of galaxies because galaxies have not formed yet! We can also look at the confidence intervals for the Schechter fit parameters, and we see the evolution!

## 5.8 Star formation history of the Universe

Inferred by integrating the UV luminosity function. This is basically the star formation rate per unit volume as a function of redshift. Going back in time, cosmic SFR peaks around  $z \sim 2 - 3$ , and declines steeply to high redshift. The peak epoch was around 2 – 3 billion years after the Big Bang.

To make these measurements, we get a UVLF at a redshift, fit a Schechter function, integrate to some limit (giving total UV luminosity at that redshift), use a stellar population model which gives a number of stars and masses, and then get star formation rate.

The blue line above is the integrated UV luminosity. The red shows what happens when we dust correct. No dust was really present at a redshift of  $z > 6$ . Dustiest galaxies are near  $z \sim 2 - 3$ . Early galaxies were low metallicity and thus couldn't enrich with dust until SFR kicked in (with other chemical evolution).

## 5.9 Quiz!

- The specific star formation rate is slightly lower though for more massive star-forming galaxies on the star forming main sequence, and thus these galaxies are slightly more evolved and redder. Also think about the color-mass relation – smaller mass has lower  $u - r$  and thus is bluer.

# 6 September 10, 2021: Stellar Evolution and Stellar Populations

## 6.1 Background

- Stellar spectra and spectral types
- Stellar evolution
- Stellar initial mass function
- Dust attenuation and emission
- Star formation histories
- Stellar population synthesis modeling

## 6.2 A quick thing about Problem 3e: Photon and Energy Counting Detectors

Here's the issue. We wrote down an equation:

$$\int_0^\infty S_\lambda F_\lambda d\lambda \quad (26)$$

This equation is ambiguous. It's not specific enough. This  $F_\lambda$  and  $S_\lambda$  have different units, actually. There are actually units attached to  $S_\lambda$  that are ignored, typically. The units don't make sense because  $S_\lambda$  is kind of like a "fraction of photons," and thus we have to convert to number of photons instead of the energy of photons.

Apparently, here is the solution – don't derive from first principles, but think dimensionally. Take  $F_\lambda$  and go from energy to number. We do this by:

$$F_\lambda \rightarrow \frac{F_\lambda}{E} = \frac{\lambda F_\lambda}{hc} \quad (27)$$

This is a **photon counting detector**, not an **energy counting detector**. In that case, it's more complicated, and we have  $\lambda^2 F_\lambda S_\lambda d\lambda$ .

## 6.3 Stellar Evolution

### 6.3.1 HR Diagrams: Main Sequence

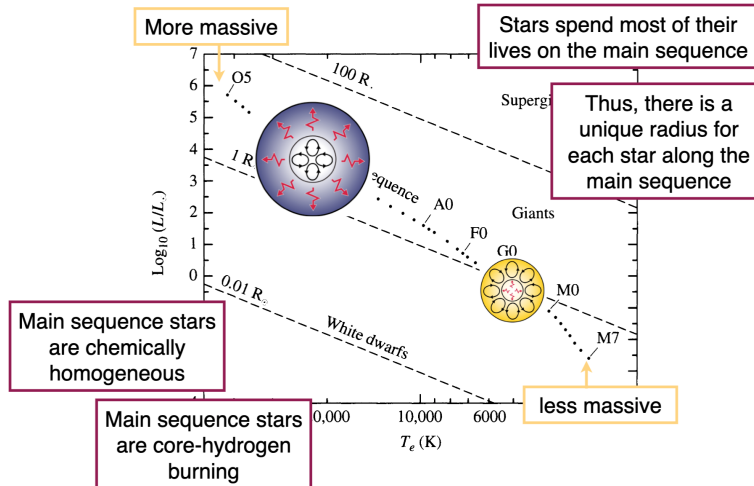


Figure 33: HR Diagram.

- Stars spend most of their life on the main sequence, defined as core hydrogen burning.
- Thus, there is a unique radius for each star along the main sequence. We infer a radius with the Stefan-Boltzmann law (derived from blackbodies, good for stars). We measure a luminosity  $L = 4\pi Fd^2$  and temperature from spectra or colors:

$$L = 4\pi R^2 \sigma T^4 \quad (28)$$

- More massive stars in the top left; less massive in the bottom right.
- Main sequence stars are chemically homogeneous
  - Main sequence stars are in hydrostatic equilibrium.
- Low mass stars and high mass stars differ in energy transport. Low mass has convection exterior; high mass stars have convection in the core. Determined by adiabatic temperature gradients. If the temperature gradient is super adiabatic, you have convection.

### 6.3.2 Difference in Chemical Composition

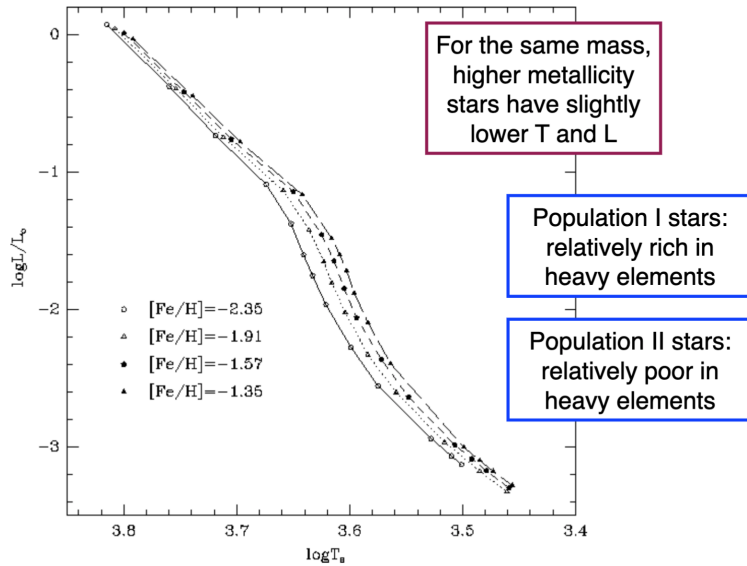


Figure 34: Differences in chemical composition.

$\text{Fe}/\text{H}$  is the amount of iron-content of a star relative to the sun. The more negative, the more metal poor.

- For the same mass, high metallicity is cooler and less luminous.
  - Pop I: Relatively rich in heavy elements
  - Pop II: Relatively poor in heavy elements
  - Pop III: Metal free stars.

### 6.3.3 Relation between luminosity and mass

Over the entire main sequence, it's almost  $L \sim M^{3.5}$ .

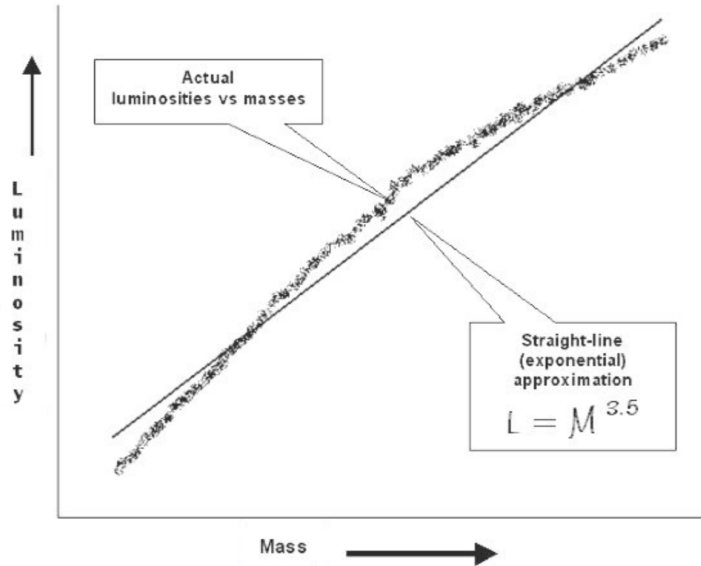


Figure 35: Proportionality.

#### 6.3.4 Post MS Evolution

Stars spend about 90% of their time on the MS. After the core is exhausted of hydrogen, we enter the **sub-giant branch**. The core contracts and heats. Hydrogen burning shell gets formed around the Helium core. Energy release from H-envelope leads to expansion of intermediate layers, and thus a drop in temperature  $T$ .

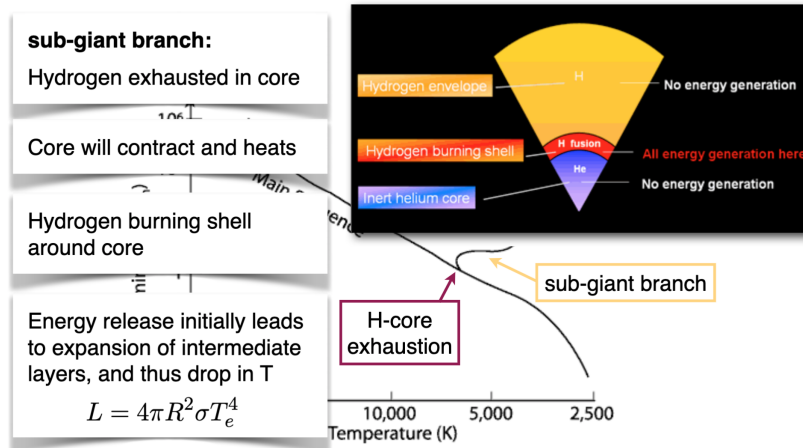


Figure 36: Sub-giant branch.

Then, we have vertical evolution on the HR diagram called the **red giant branch**. There is an ascent phase during which the core is contracting and hydrogen is burning in shells ferociously. The luminosity increases rapidly. You have mass loss because it's non-stable phase of evolution, shedding some of the outer envelopes (not much compared to the total mass of the star). The core continues to contract as material is dumped on the core.

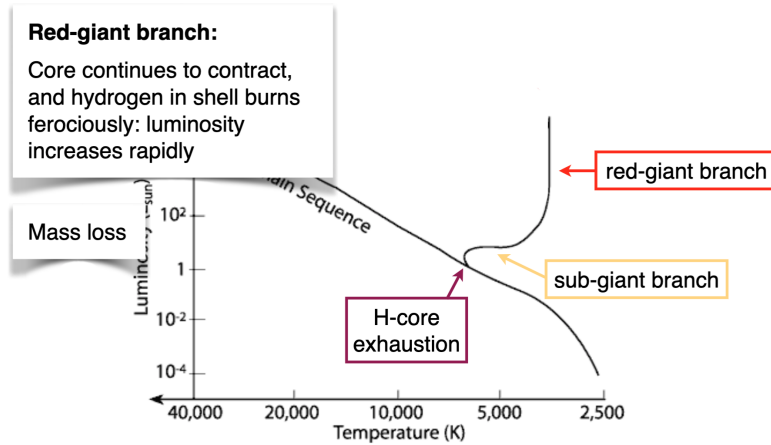


Figure 37: Red-giant branch.

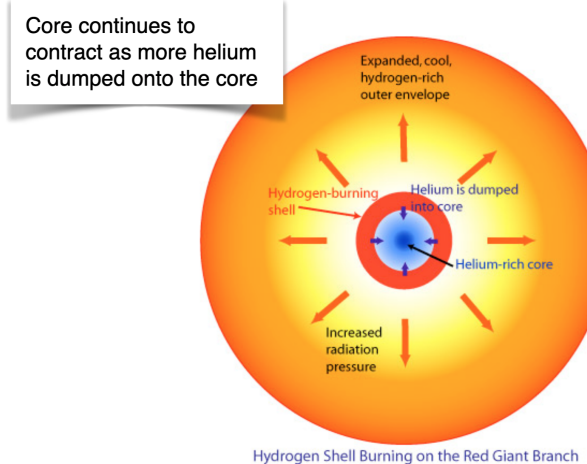


Figure 38: Red-giant branch 2.

We then hit the **helium flash**. This is when the core temperature gets to about  $T \sim 10^8$  K. This is so high that helium starts to burn. The core is no longer in free-fall contraction. Boom, we have a burst of energy! The core expands, gravity weakens, and energy production rate goes down. The evolution is to higher temperature and lower luminosity. This is the **horizontal branch**.

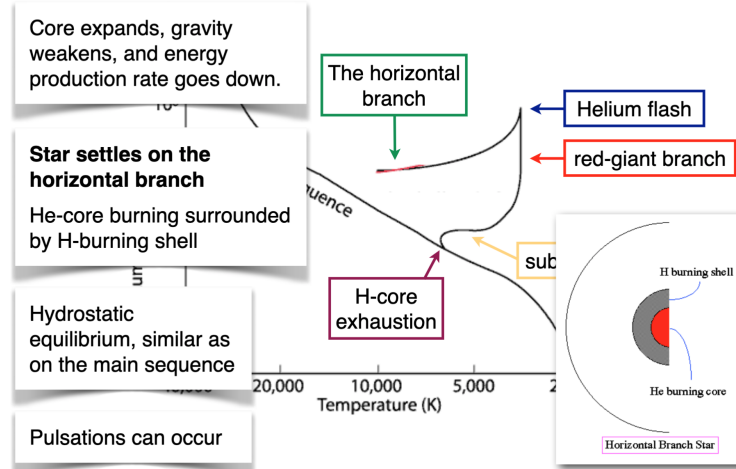
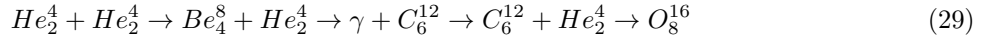


Figure 39: Horizontal branch.

**The horizontal branch** is characterized by core helium burning with a surrounding H-burning shell. Tons of details go here, and we don't really fully understand it. This is in hydrostatic equilibrium, however (getting us in the ballpark, sparing the details). This is when pulsations can occur! RR Lyrae are horizontal branch stars. Think of a pot of water with a top on and the pot-top is shaking, allowing for these pulsations.

### 6.3.5 Production of Carbon and Oxygen

We know how H turns into He. We fuse He with the triple alpha process (helium nucleus is an alpha particle). We basically have:



This is what is happening in horizontal branch stars! As you hit the end of the horizontal branch (i.e., not hot enough to fuse helium to carbon and oxygen). Carbon-oxygen core is not burning; the helium burning stars in a shell and the core mass increases. The star mass increases and we are now on the **asymptotic giant branch**. There is a lot of mass loss here. This is also the **double shell** burning phase, by the way.

### 6.3.6 Stellar Evolution Tracks

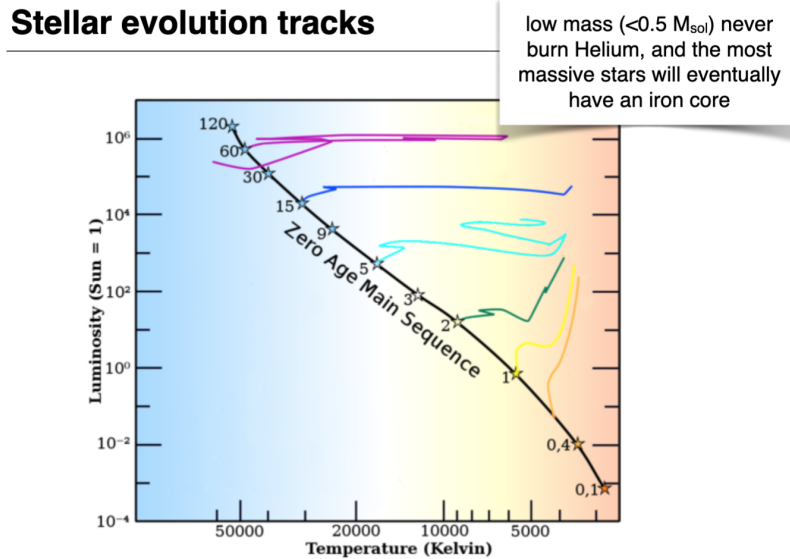


Figure 40: Stellar evolution tracks.

Evolution of a star at fixed initial mass is a “track.” The evolution of high mass stars is crazy! Low mass go mostly vertical, high mass stars bounce around horizontally.

### 6.3.7 Massive Stars

This is a crazy onion with tons of shells. They burn unbelievably fast, on the order of a few million years. The reactions are really complicated as well. The temperatures are ridiculous high, approaching  $T > 10^9$  K in order to burn some of the elements.

### 6.3.8 Binding energy per nucleon

$A$  is the number of nucleons. Less than Fe, energy is liberated via fusion. These reactions are exothermic and energy can be liberated with fusion. Elements heavier than Fe, energy is released with fission and these processes are exothermic.

Iron is most tightly bound and thus cannot fuse.

### 6.3.9 Evolution of a solar mass star

Eventually becomes a white dwarf which is supported by electron degeneracy pressure. White dwarfs are about the size of the Earth and about a solar mass.

### 6.3.10 Stellar remnants

Low-to-average mass ends in a white dwarf (up to 7 solar masses or so). Larger stars (between about 7 and 20 [roughly] solar masses) become neutron stars. They are a few solar masses and the size on Manhattan. They are supported by neutron degeneracy pressure. Lastly, the most massive stars become black holes.

## 7 September 15, 2021: Stellar Populations

### 7.1 Ingredients

- **Initial mass function:** How many stars of a certain mass  $M$  are born in a birth cloud  $N(M)$ ? See below for the initial mass function discussion. This gives  $N(m)$ .
- **Isochrones:** Gives the luminosity  $L$  and temperature  $T$  of a star as a function of mass  $M$ , age  $t$  and metallicity  $Z$  of a star. This gives  $L(M, t, Z)$  and  $T(M, t, Z)$ .
- **Spectral library:** Assigns a spectrum to each star using its luminosity  $L$ , temperature  $T$ , and metallicity  $Z$ . This gives  $f_\nu(L, T, Z) = f_\nu(M, t, Z)$ .

Simple stellar populations combine the IMF, isochrones, and stellar spectra to make  $f_{\nu,ssp}(t, Z)$ .

### 7.2 Initial Mass Function

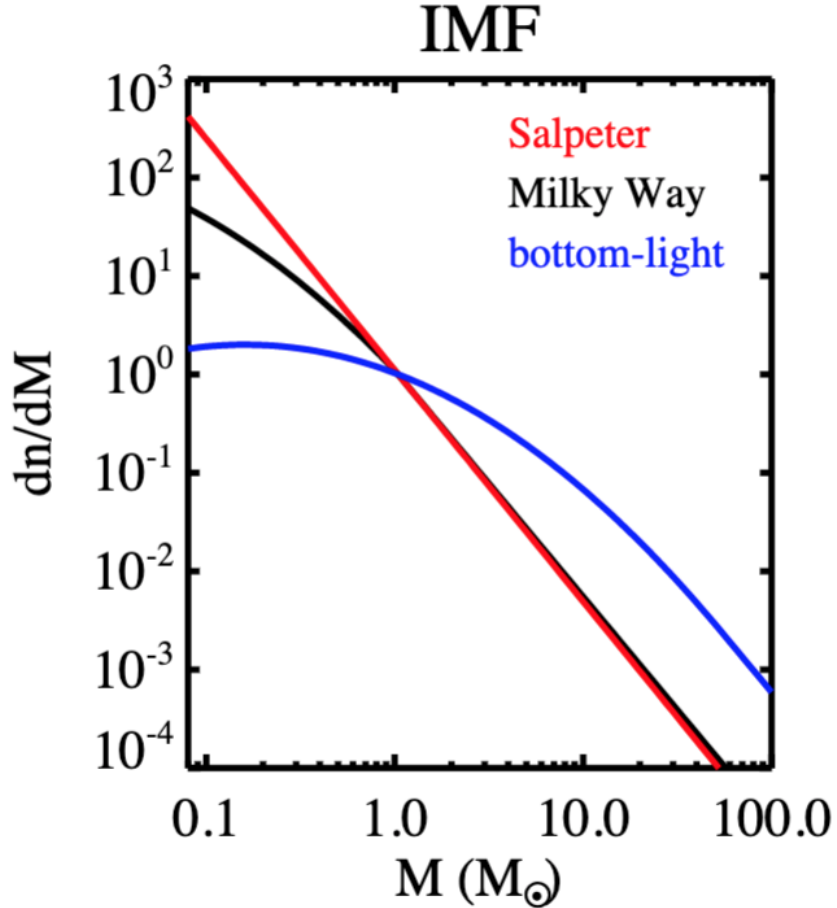


Figure 41: IMF

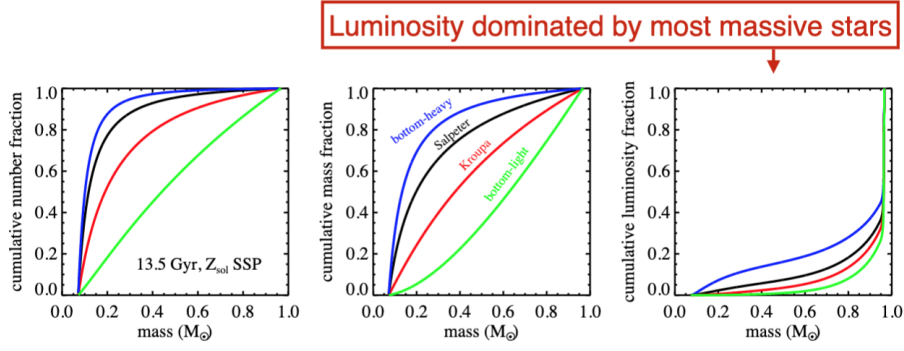


Figure 42: IMF cont.

This is the distribution of mass **at birth**, which makes it really difficult to measure. Qualitatively, the Salpeter IMF is a straight line in log-log space:

$$\xi(m) = \xi_0 M^{-\alpha}, \text{ where } \alpha = 2.35 \quad (30)$$

Sometimes we will see

$$\xi(m) = \xi_0 M^{-(1+\Gamma)}, \text{ where } \Gamma = 1.35 \quad (31)$$

The  $\xi_0$  is a normalization. One question we might have: how many stars exist between two masses?

$$N = \int_{m_1}^{m_2} \xi(m) dm \quad (32)$$

For the Salpeter, we have:

$$N = \frac{\xi_0}{1.35} \left[ \frac{1}{m_1^{1.35}} - \frac{1}{m_2^{1.35}} \right] \quad (33)$$

Sometimes you see:

$$\frac{dn}{dm} \propto m^{-2.35} \quad (34)$$

Note that we are assuming a universal IMF which we will take to be true. This is not necessarily the case.

### 7.3 Evolving a simple stellar population

A galaxy spectrum is dominated by the most massive stars still alive. The galaxy becomes redder and fainter over time, as massive stars die.

### 7.4 Evolution of Color and Mass-to-Light Ratio

Galaxies become redder in time, and the mass-to-light ratio increases in time.

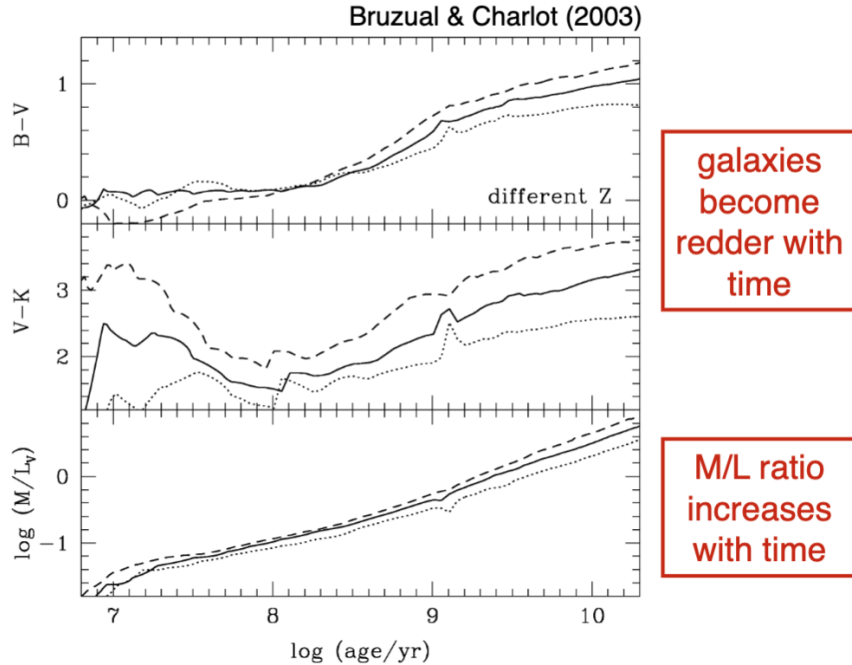


Figure 43: Evolution of color and M/L ratio.

## 7.5 Dust Attenuation Law

You typically see  $A(\lambda)/A(V)$ . This shows that the cross-section/optical depth at bluer wavelengths is larger than at redder wavelengths. In effect, you are losing blue light.

**Attenuation** is the net effect of the removal of light. There are many causes, however:

- Extinction (how much light is scattered out of the line of sight)
- Geometry (what's the geometry of a dust particle, what's the geometry of the galaxy relative to you)
- Radiative transfer

We typically describe attenuation with  $A_\lambda$ :

$$A_\lambda = \Delta m_\lambda = (m - m_0)_\lambda \quad (35)$$

This is really a magnitude difference (flux ratio) and can also be written as:

$$F_\lambda = F_{\lambda,0} 10^{-0.4A_\lambda} = F_{\lambda,0} e^{-\tau_\lambda} \rightarrow A_\lambda = 1.086 \tau_\lambda \quad (36)$$

It is also commonly to talk in terms of color excess  $E(B - V)$ :

$$E(B - V) = A_B - A_V \quad (37)$$

## 7.6 Dust Attenuation Curve

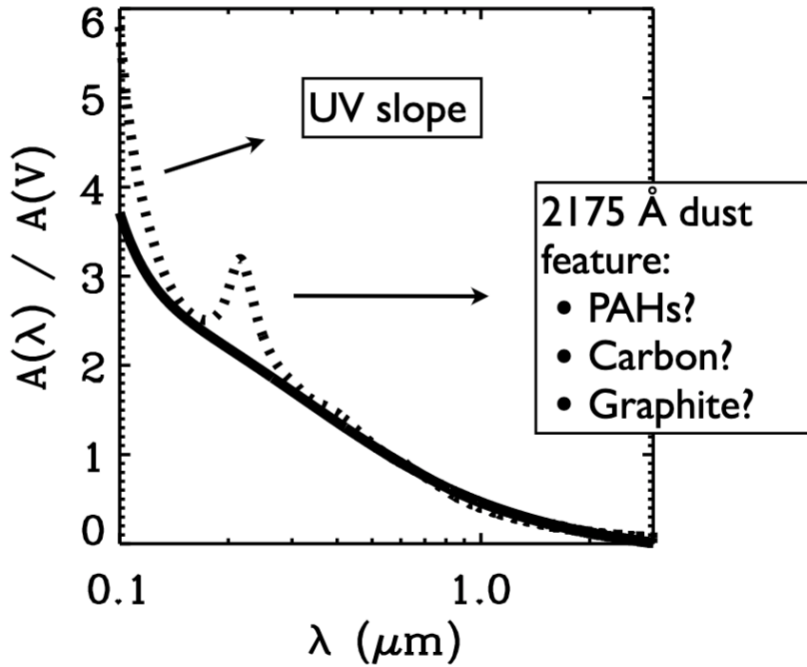


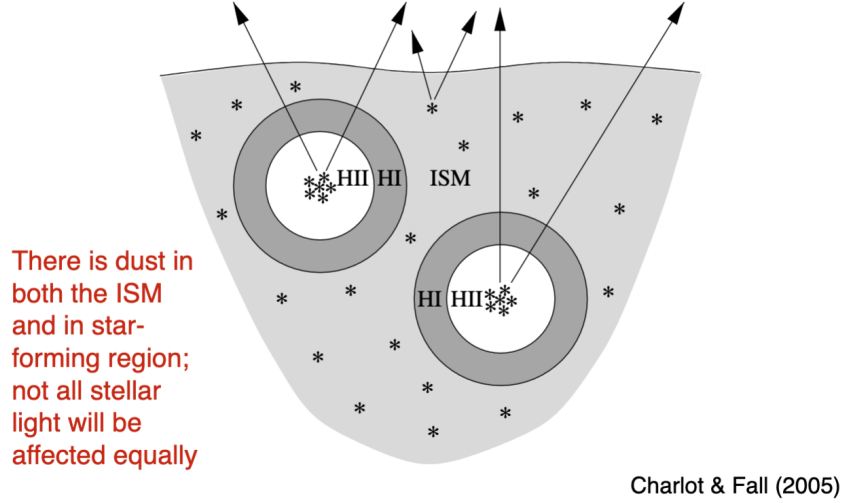
Figure 44: Dust attenuation law for starburst (solid) and MW.

You typically see  $A(\lambda)/A(V)$  where the center of  $V$  is  $5500\text{\AA}$ . We also have the “attenuation law” which is:

$$R_\lambda = \frac{A_\lambda}{E(B - \lambda)} \quad (38)$$

Here,  $R_\lambda$  is the slope of the attenuation curve. For the MW, this is  $R_V = 3.1$ . Note that often we assumed a grey atmosphere/slab of material.

## Dust geometry



27

Figure 45: Dust geometry implications.

### 7.7 Calzetti Law

Not all attenuation laws are the same. The Calzetti law is popular for starburst galaxies, where the maximum of the attenuation is 3.5 as opposed to 6 for the MW. Notice, too, that the MW has the  $2175\text{\AA}$  bump, which might be caused by:

- PAHs
- Graphite
- Carbon

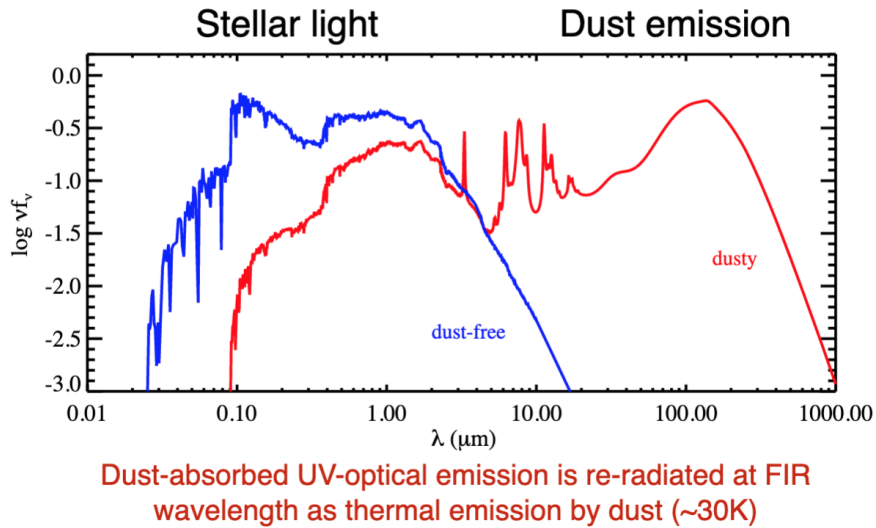


Figure 46: Sample Galaxy SED. Dust re-radiated at 30K which is warm dust.

## 8 September 17, 2021: Stellar Populations continued

### 8.1 An error from last time...

Last time, we had used a base  $e$  instead of a base 10 somewhere. Just correcting that.

$$A_\lambda = \Delta m_\lambda = (m - m_0)_\lambda = -2.5 \log_{10} \left( \frac{F_\lambda}{F_{\lambda,0}} \right) \quad (39)$$

## 8.2 Dust Emission Models (Draine and Li, 2007)

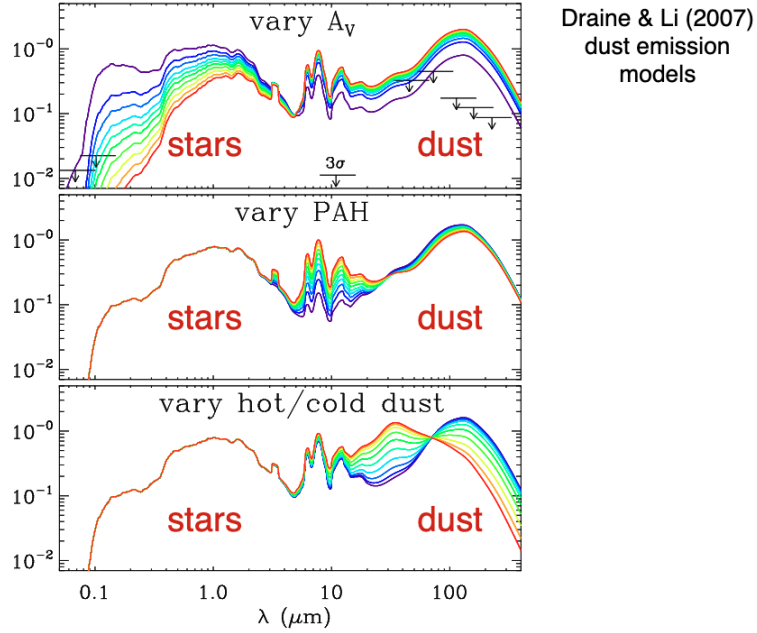


Figure 47: Varying  $A_V$  (increasing) dims starlight and increases dust light. Varying PAHs (increasing PAHs) peak near a few microns and cause many features there. Varying dust temperature (increasing temperature) peaks to smaller wavelengths. Note that varying PAH and temperature does not affect the stars that much.

## 8.3 Negative k-correction

For higher redshifts, the dust peak becomes fainter and shifts to longer wavelengths. However, the flux density at 1mm stays approximately constant and thus is independent of redshift. Because the spectrum won't fade/shift down, the  $k$  correction will be negative.

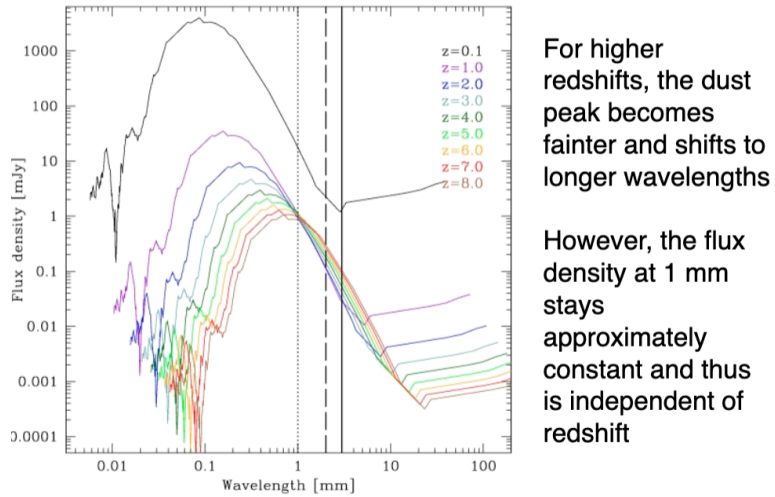


Figure 48: Negative K-correction

## 8.4 Simple Stellar Populations

For an SSP, we can write down the flux:

$$f_{SSP}(t, Z) = \underbrace{\int_{M=m_{lo}}^{M=m_{up}(t)} f_{\text{star}}[T_{eff}, \log g(M), t, Z] \Phi(M) dM}_{\text{integrate over masses}} \quad (40)$$

What are those integration limits? Well  $m_{lo}$  is the lowest mass star possible (about 0.08 solar masses). Higher mass stars die off and thus it is a function of time. Also notice that we are assuming the IMF is a function of mass alone. This is **controversial**.

## 8.5 Star formation history of a simulated galaxy

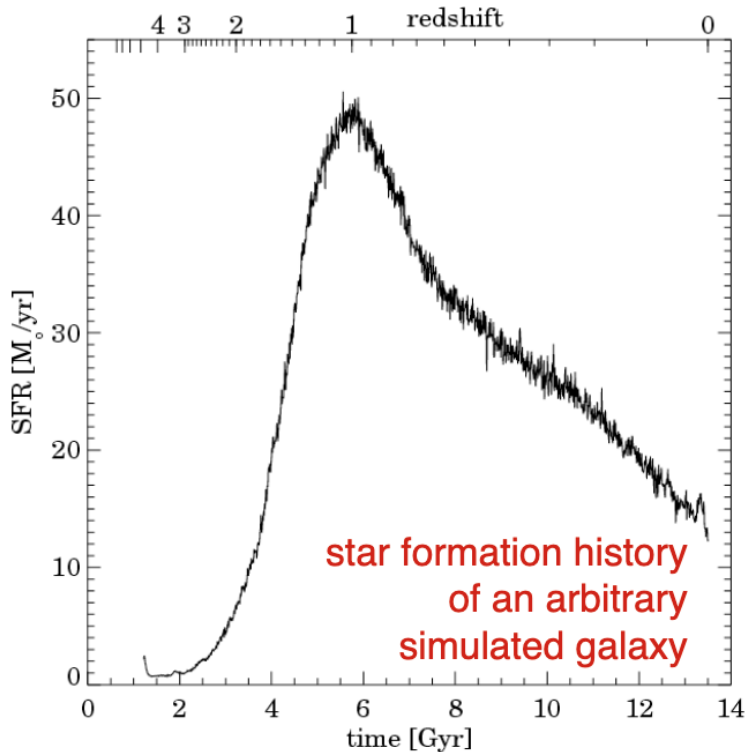


Figure 49: SFR of arbitrary galaxy.

Broadly, star formation rises rapidly, reaches a peak near  $z \sim 1$ , and then declines toward the present. There are wiggles over time, too, which might be bursty events.

Instead, we typically adopt a simplified “parametrized” star-formation rates (histories). It is usually parametrized by a smooth function. First, we have a **falling star formation history/exponential decay**:

$$SFR \propto e^{-t/0.1 \text{ Gyr}} \quad (41)$$

This is popular because it's a one-parameter model! This is also called a  $\tau$  model.  
Next, we have the **delayed exponential**:

$$SFR \propto te^{-t/\tau} \quad (42)$$

There is one other parametrization, called a **rising star formation history**:

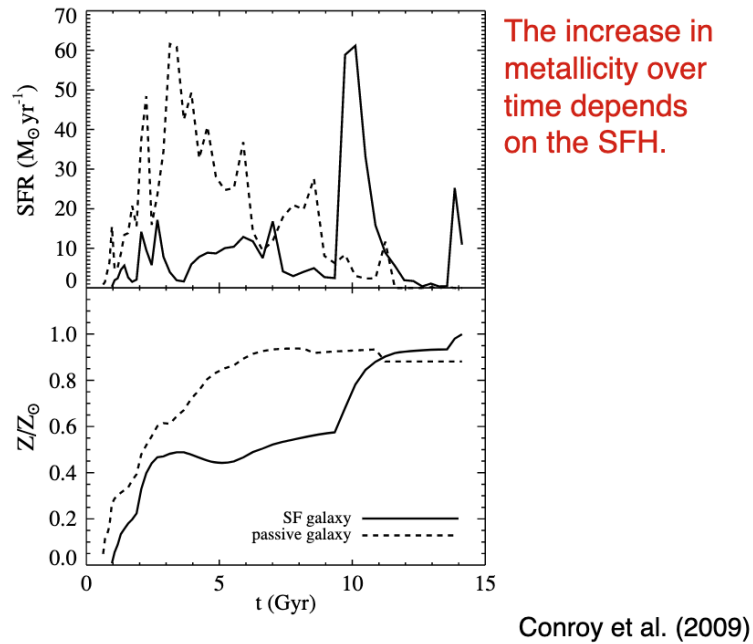
$$SFR \propto t \quad (43)$$

And a rising-tau model:

$$SFR \propto e^{t/\tau} \quad (44)$$

## 8.6 Star formation and enrichment history

The increase in metallicity over time depends on the star formation history.



Conroy et al. (2009)

Figure 50: Caption

## 8.7 Fractional contribution to the total flux

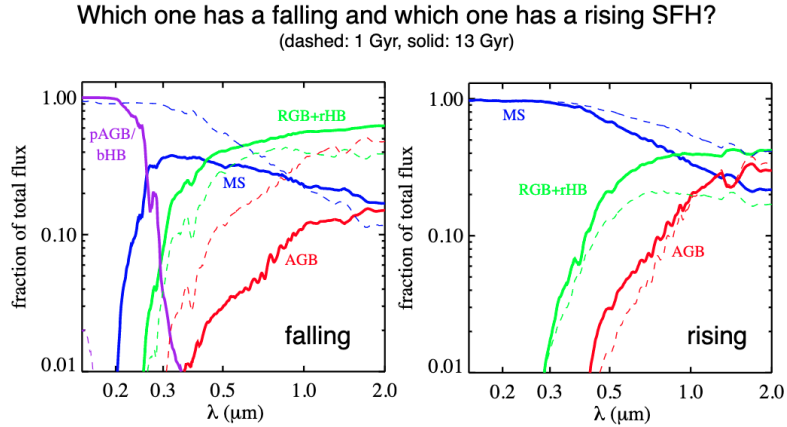


Figure 51: Fractional contribution to the total flux question.

Which one has a rising and a falling star formation history?

In a star forming galaxy, the main sequence always dominates. In a rising history, it's **always** dominated by young luminous stars. This makes the right side rising.

The left side shows that the other weird blue stars dominate instead of blue main sequence stars. This means that larger fractional contributions from post-MS evolution for a falling history.

**This plot is important!**

## 8.8 Fractional contribution to the total flux for a star forming galaxy

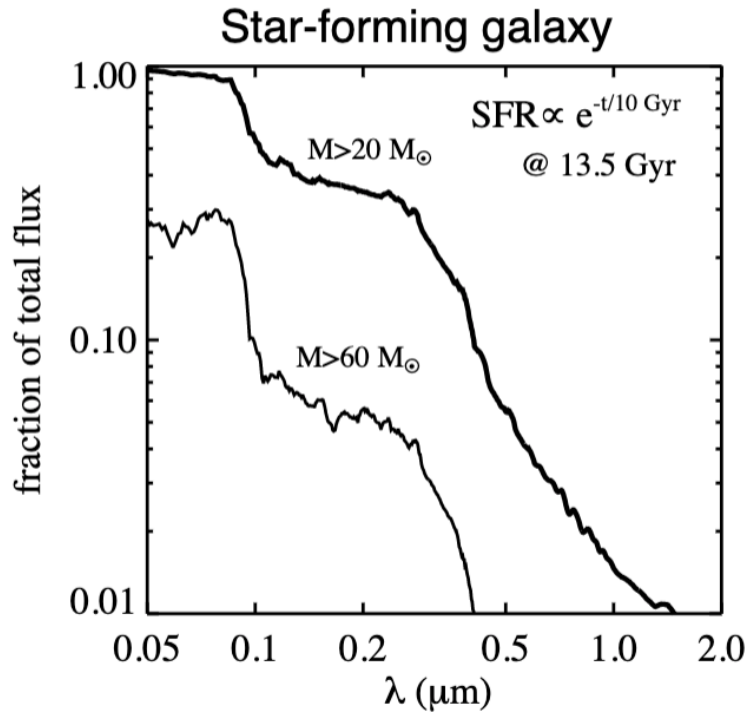


Figure 52: Fractional contribution 2.

Even though  $60M_{\odot}$  stars are luminous, they are RARE. Thus, star forming galaxies are really characterized by  $\sim 10 - 20M_{\odot}$  stars and not **super-massive** stars.

## 8.9 Light-weighted age as a function of wavelength

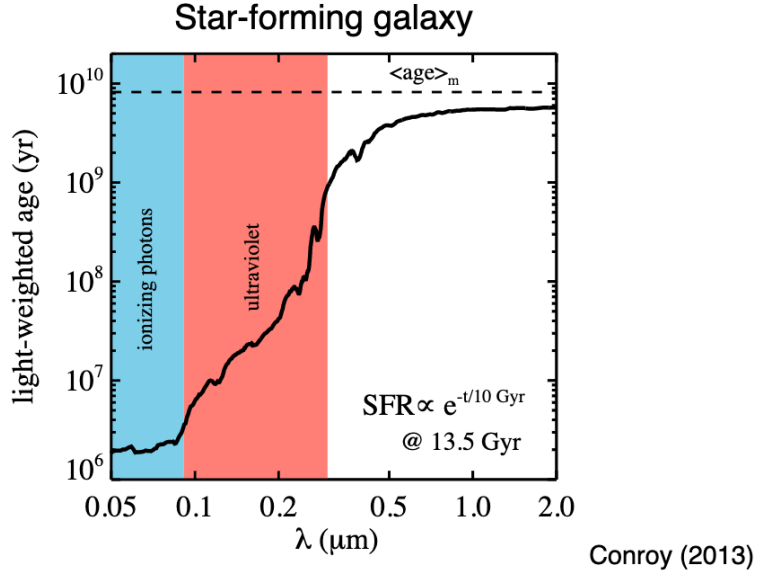


Figure 53: Light-weighted age as a function of wavelength.

The age that we measure is dependent on our wavelength, since everything is light-weighted. In the infrared, we are sensitive to older populations and thus get closer and closer to the real mass-weighted age. This **shows the importance of multi-wavelength observations**. It also shows how bad UV observations are at predicting galaxy ages. Also note that the light-weighted age only asymptotes to the mass-weighted age.

## 8.10 Nebular Emission

One thing we have totally neglected is the effect of nebular emission, which is one of the main ways that we see star-formation in young galaxies.

## 8.11 Complex Stellar Population

$$f_{csp}(t) = \int_{t'=0}^t \int_{Z=0}^{Z_{max}} \left[ SFR(t-t') P(Z, t-t') f_{ssp}(t', Z) e^{-\tau(t')} + A f_{dust}(t', Z) \right] dt' dZ \quad (45)$$

where  $t'$  is the age of the population,  $P$  is the metallicity distribution function,  $f_{ssp}$  is the integral we had before,  $e^{-\tau(t')}$  is an extinction term from dust, and the last term  $A f_{dust}$  represents dust emission (with  $A$  being a normalization to ensure energy conservation).

Computationally, this is a very annoying calculation to do.

## 8.12 Fitting broadband photometry

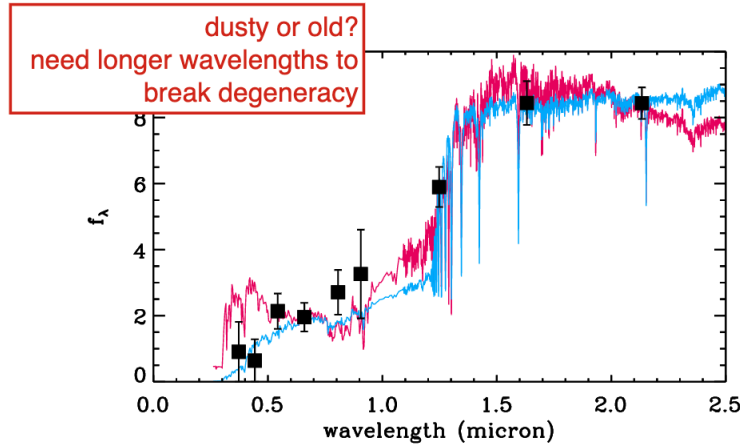


Figure 54: Need full SED to break degeneracies.

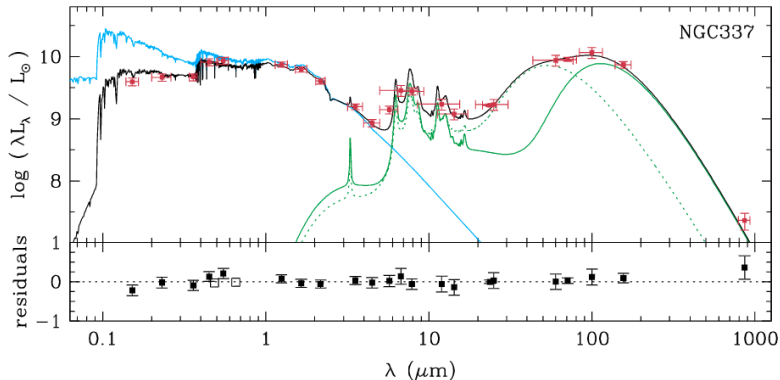


Figure 55: Full spectrum SED.

## 8.13 Fitting Spectra without parametrizing the SFH

## 8.14 Uncertainties in the stellar population modeling

## 8.15 Thermally pulsing AGB phase

These molecular features are imparted because of the AGB star. These are super bright and thus dominate the spectrum. The timescales over which they change their spectra can be short, too (days)!

## 8.16 Challenges of SPS Modeling

- Degeneracies between age and metallicity
- SPS models are not perfect; various stages of stellar evolution are poorly understood (AGB, HB, Wolf-Rayet stars, binary evolution, convection, rotation, etc)

- Dust law, initial mass function, and star formation history usually assumed
- Massive stars with low  $M/L$  will dominate the spectra
- Etc.

### **Challenges in stellar population synthesis (SPS) modeling**

---

- Degeneracies between age and metallicity
- SPS models are not perfect, various stages of stellar evolution that are poorly understood:
  - (TP-)AGB, horizontal branch, blue stragglers, post-AGB, wolf-rayet stars, convection, rotation, binary evolution, etc.
- Dust law, initial mass function, and star formation history usually assumed
- Massive stars with low M/L will dominate the spectrum
- etc.

Figure 56: Challenges.

## 9 September 22, 2021: Gas and Star Formation

### 9.1 IMF Completion

We had forgotten a few things. The total mass from an IMF is given by:

$$M_\star = \int_{m_1}^{m_2} m \xi(m) dm \quad (46)$$

An equivalent expression for luminosity:

$$L_\star = \int_{m_1}^{m_2} L(m) \xi(m) dm \quad (47)$$

One other thing, related to the stars...what about the lifetime on the main sequence?

$$\tau \propto \frac{M}{L} \rightarrow \tau = 10^{10} \frac{M}{L} \quad (48)$$

Let's explicitly state something about star formation rates, too. Mathematically, a star formation rate is defined as:

$$\text{SFR} = \frac{dM}{dt} = \dot{M} \quad (49)$$

For example, a  $\tau$  model is:

$$\frac{dM}{dt} = C e^{-t/\tau} \quad (50)$$

## 9.2 Star formation in the nearby Universe

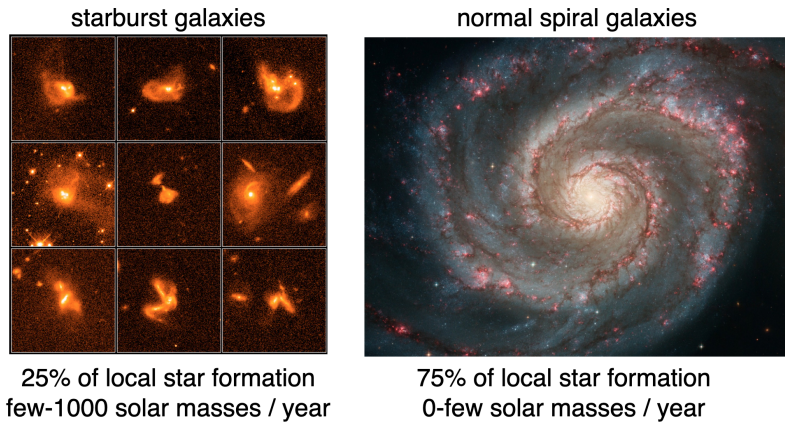


Figure 57: Starbursts vs. Normal Galaxy

At local  $z$ , roughly 3/4 of the star formation happen in normal spiral galaxies. The rates range from 0 to a few solar masses per year.

The other quarter of star formation is taking place in star burst galaxies. These have SFRs from a few to  $\sim 1000$  solar masses per year.

Stars form in giant molecular clouds (GMCs). They are roughly  $10^5$  to  $10^6$  solar masses. They extend over a few tens of parsecs, and they have temperatures near 10 Kelvin.

We eventually get cold enough that molecules form. Thus the outsides of clouds are less dense than the insides. Outside of the cloud, hot stars pound the surface with radiation (lots of **self-shielding** interior). There's molecular hydrogen, too, which protects from dissociation of molecules. Eventually gravity takes over, and you form a star!

### Giant Molecular Clouds (GMCs)



Figure 58: GMCs

### 9.3 Mass function of dense cores in GMCs (Alves+2007)

Star formation is very inefficient. For a couple of solar masses of stars, you need a TON of gas to make that happen.

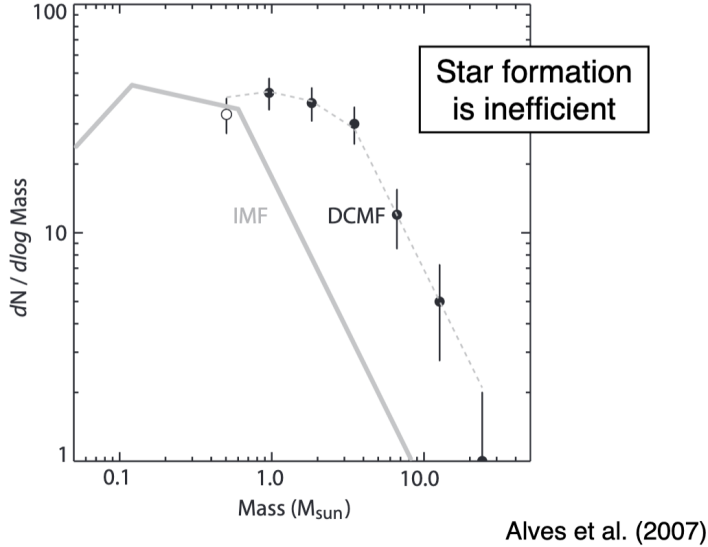


Figure 59: GMC mass function.

### 9.4 Jeans Mass and Cloud Fragmentation

If you balance gravity against the ideal gas law, you can get the Jeans mass!

The **Jeans mass**:

$$M_J \propto \frac{T^{3/2}}{\rho^{1/2}} \quad (51)$$

The cloud collapses if the mass of the cloud is greater than the Jeans mass:

$$M_{CLOUD} > M_J \rightarrow \text{COLLAPSE!} \quad (52)$$

In details:

$$\underbrace{\rho a}_{\text{accel.}} = \underbrace{-\frac{dP}{dr}}_{\text{pressure force per volume}} - \underbrace{\frac{GM_r}{r^2}\rho}_{\text{gravity per volume}} \quad (53)$$

There are two phases, roughly. This is summarized in the figure and lists. **In phase one...:**

- Photons can easily escape
- $T \sim \text{constant}$  (isothermal)
- Gravity force / volume  $\propto \frac{M^2}{R^5}$
- Pressure force / volume  $\propto \frac{MT}{R^4}$
- For constant  $T$ , gravity wins: keeps collapsing

### In phase two...:

- Clouds become too dense for photons to escape
- Adiabatic:  $T \propto \frac{M^{2/3}}{R^2}$
- Pressure force increases  $\propto \frac{M^{5/3}}{R^6}$
- Hydrostatic equilibrium
- Further collapse using Kelvin-Helmholtz contraction

Note that this is all pre main sequence, so KH contraction really is powering at this point. Then, fusion takes over.

Another useful thing to keep in mind is the **freefall timescale** which is generally shorter by a few orders of magnitude than the KH timescale:

$$t_{ff} \propto \frac{1}{\sqrt{G\rho}} \quad (54)$$

### Cloud collapse

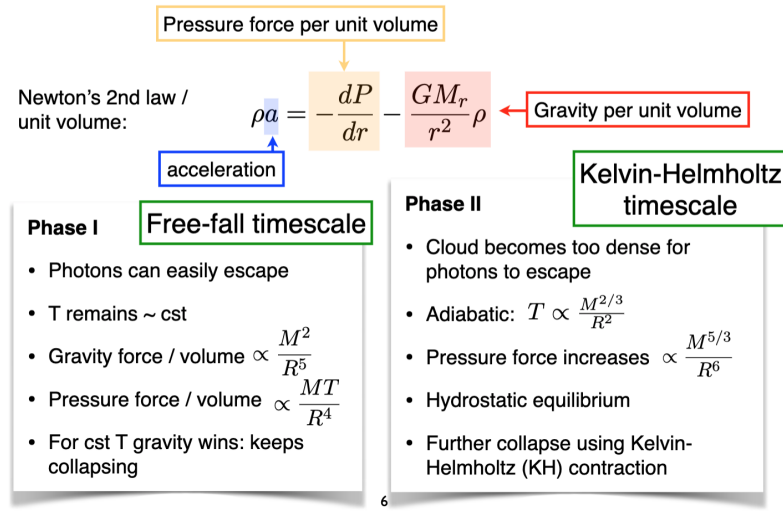
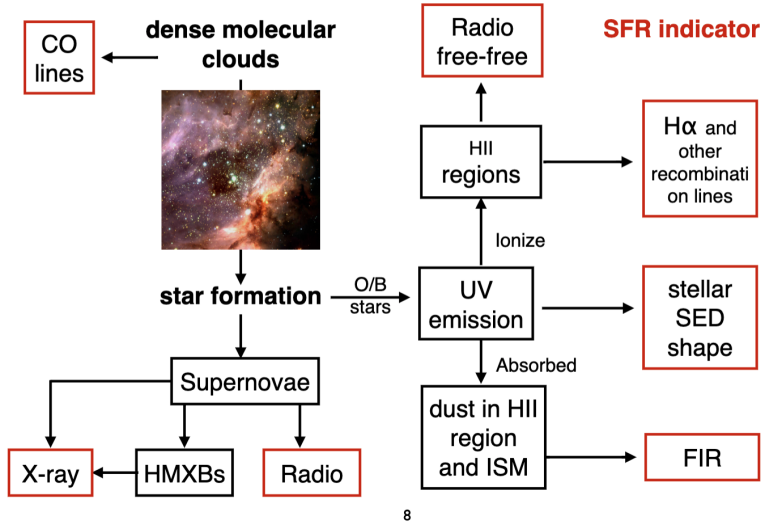


Figure 60: Cloud collapse.

## 9.5 Star formation rate indicators (recipes)

### Star formation rate (SFR) indicators



8

Figure 61: SFR Indicators.

**Fundamental question:** My galaxy has massive stars that we cannot necessarily observe. Can we find another indicator that there is recent or ongoing star formation?

Note that none of this works if we don't have O and B type stars since they have UV emission.

Let's step through SFR indicators.

## 9.6 UV Emission

The UV is really great to see **massive stars greater than  $3M_{\odot}$ , or so** (main sequence stars with  $T \gtrsim 10^4$  K with lifetimes of 10 – 200 million years. We can use this emission (corrected for dust with  $\beta$  slope) can be used to estimate the SFR of a galaxy.

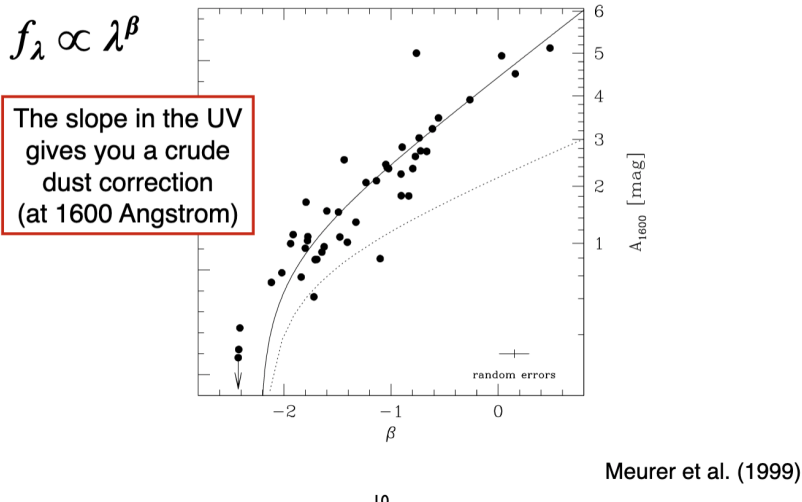


Figure 62: Correction with  $\beta$  slope.

Also note that  $A_{UV} \sim 8E(B - V)$  so dust can be really damaging. In practice, we use a **beta index** which is the slope between a far-UV and near-UV channel. The slope is  $\beta$ . You can assume that  $F_\lambda \propto \lambda^\beta$  to correct for the dust.

We are measuring the very high mass end of the IMF, and then extrapolating to lower and lower masses. This is part of the reason the IMF is so important.

#### Assumptions:

- Dust assumption for  $\beta$  correction.
- Need to assume an IMF.

If you take the SPS model, correct for dust, and assume an IMF, you get the **Kennicutt SFR (98)** relations:

$$SFR = 1.4 \times 10^{-28} L_\nu \frac{\text{ergs}}{\text{s} \cdot \text{Hz}} \quad (55)$$

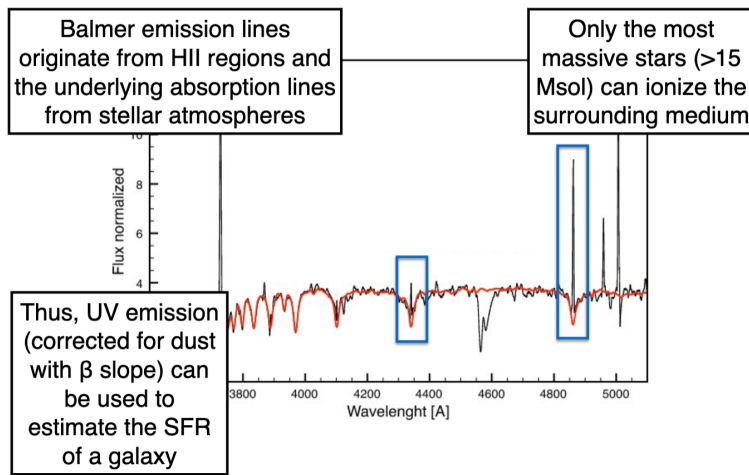
where  $L_\nu$  is typically over  $\lambda = [1500, 2800]\text{\AA}$ .

#### 9.6.1 Correction UV Emission using Beta Slope (Meurer+1999)

The slope in the UV gives you a crude dust correction (at 1600 Angstrom). This is all that is available at high  $z$ . Lower  $z$  has things like more SED points.

## 9.7 Recombination Lines

### II. Recombination lines



II

Figure 63: Recombination lines as SFR indicator.

Balmer emission lines (lower state  $n = 2$ ) originate from HII regions and the underlying absorption lines from stellar atmospheres. Only the most massive stars ( $\gtrsim 15 M_{\odot}$ ) can ionize the surrounding medium. Thus, UV emission (corrected for dust with  $\beta$  slope) can be used to estimate the SFR of the galaxy.

The continuum is set by all the stars, and the emission lines are due to the most massive stars ionizing the environment. Let's first look at  $H\alpha$ .

Let's focus on stars with  $M > 15 M_{\odot}$ ,  $T \gtrsim 3 \times 10^4$  K, and thus only O-type and B0-type stars.

If you can measure both  $H\alpha$  and  $H\beta$ , we know that  $H\alpha/H\beta = 2.8$ . If this is different, we need to correct for the dust changing this ratio.

There is an equivalent **Kennicutt Recipe (98)**:

$$\text{SFR} = \frac{L(H\alpha)}{1.26 \times 10^{41} \frac{\text{erg}}{\text{s}}} \quad (56)$$

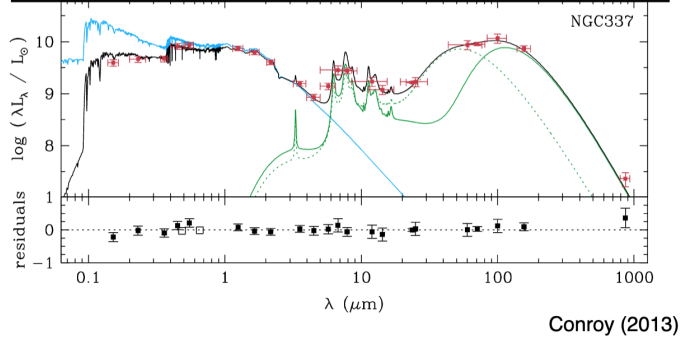
Note that this is only sensitive to the most massive stars and thus we are incredibly sensitive to the IMF. Here are some of the assumptions:

- Assume a metallicity.
- Dust correction.
- IMF is good since we are measuring only the most massive.
- Binary stars can effect this.
- Others.

## 9.8 FIR Emission

### Full spectral energy distribution of a star-forming galaxy

FIR emission mostly originates from attenuated UV light from massive stars, i.e., it serves as a SFR indicator. In order to catch both the unobscured and obscured star formation activity, we need to combine the UV and FIR SFRs



Conroy (2013)

13

Figure 64: FIR emission as SFR indicator.

FIR emission mostly originates from attenuated UV light from massive stars, i.e., it serves as an SFR indicator. In order to catch both the unobscured and obscured star formation acitivity, we need to combined UV and FIR SFRs.

There's a **Kennicutt relation**:

$$\text{SFR} = \frac{L_{FIR}}{2.2 \times 10^{43} \frac{\text{ergs}}{\text{s}}} \quad (57)$$

One strength of this is that we can probe regions of high extinction.

## 9.9 X-ray emission (Menou et al 2012)

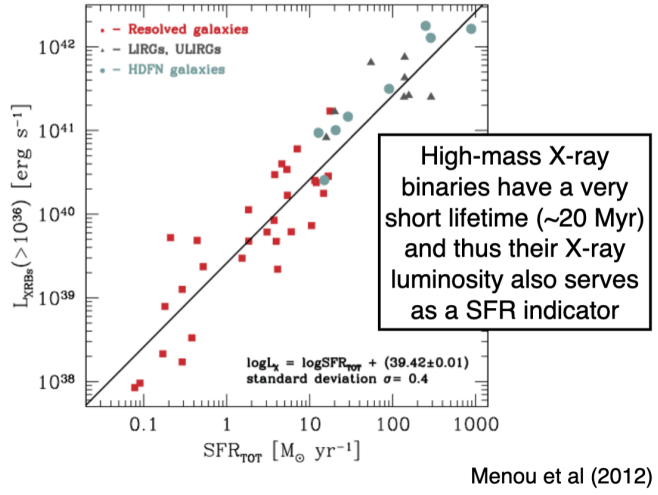


Figure 65: X-ray emission as SFR.

High-mass X-ray binaries have a very short lifetime ( $\sim 20$  Myr) and thus their X-ray luminosity also serves as a SFR indicator.

X-ray observations are hard to get, and thus this is not used that often.

## 9.10 Radio Emission

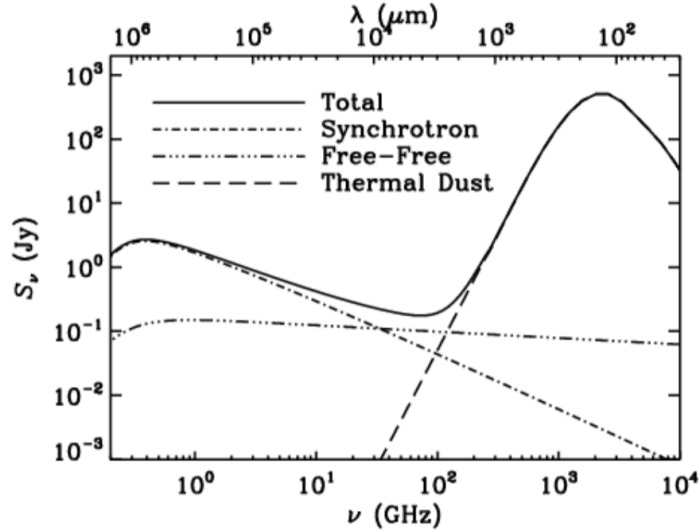


Figure 66: Free-free emission window where it is dominant.

Synchrotron, thermal free-free emission. There is a small, small window where free-free emission dominates. The wavelengths are really long and thus not affected by dust. There are very few radio telescopes measuring near 30 GHz, and thus this is hard.

If you could do it, this would be the gold standard since there's no dust and coming from HII regions.

## 9.11 Measuring gas surface densities

HI is diffuse cold case, CO traces stars forming.

We have two phases of gas – atomic hydrogen and molecular CO. The total gass surface density is thus  $\Sigma_{gas} = \Sigma_{HI} + \sigma_{H_2}$ .  $H_2$  is really hard to observe, so we end up measuring:

$$\Sigma_{gas} = \Sigma_{HI} + \alpha_{CO} I_{CO} \quad (58)$$

where  $\alpha_{CO}$  takes us from  $CO$  to  $H_2$ .

The total gas content of  $HI + CO$  turns out to be a good tracer of dust. Thus,  $\alpha$  is calibrated locally and extrapolated outward.

This is **metallicity dependent** since clouds are less-shielded.

## 9.12 Kennicutt-Schmidt Law (1998)

There is a really tight correlation between gas surface density and star formation rate. Often written as the **KS Relation**:

$$\Sigma_{SFR} \propto \Sigma_{gas}^n, \text{ where } n = 1.4 \quad (59)$$

## 10 September 24, 2021: Gas and star formation, chemical evolution

### 10.1 Group Exercise

#### **Challenges in stellar population synthesis (SPS) modeling**

---

- Degeneracies between age and metallicity
- SPS models are not perfect, various stages of stellar evolution that are poorly understood:
  - (TP-)AGB, horizontal branch, blue stragglers, post-AGB, wolf-rayet stars, convection, rotation, binary evolution, etc.
- Dust law, initial mass function, and star formation history usually assumed
- Massive stars with low M/L will dominate the spectrum
- etc.

Figure 67: Group exercise.

Imagine we take two measurements in the UV at  $1500\text{\AA}$  and  $2500\text{\AA}$  (far and near UV). The SFR is given by:

$$\dot{m} = C \times L_{UV} \quad (60)$$

Well, we first need **distance** to go from magnitude to a flux. We also need an estimate of the **dust correction**. This gives us  $L_{UV}$ .

The constant comes from theory. How do we get that? We need to assume an **IMF**, first of all. We also need a **metallicity** and assumed **star formation history**. We need a mass-luminosity relation to get an observable, which we can get from isochrones (more generally, stellar evolution model). One last really subtle thing (not as important for the UV), but it's the **escape fraction** (fraction of photons coming from star).

This comes down to basically assuming a Salpeter IMF, one metallicity (solar), a constant star formation history, picking a stellar evolution model, and then an escape fraction of 1.

If we saw this edge on, we need to trust our dust correction EVEN MORE!

If you could pick one more wavelength to observe, what would you pick and why? It might be best to get FIR measurements so that we can improve our measurement of  $\beta$  by seeing how much light is obscured.

We might also instead measure high mass X-ray binaries. Thus we have an independent handle (aside from O and B stars). Thus we have two different measurements of  $\dot{M}$ .

Another common SFR tracer is  $\text{H}\alpha$ . If we wanted to measure the  $\text{H}\alpha$  SFR of this galaxy, what do we do? We can go to a telescope and put a narrow band filter on our data and sum the entire image. The UV is produced from  $M > 3M_\odot$ , whereas  $\text{H}\alpha$  is dominated by  $M > 15M_\odot$  stars. **Do we expect that the SFRs agree between the X-ray and UV?** In an ideal world, yes they should be the same. However, if we plot the ratio SFR in  $\text{H}\alpha$  to SFR in UV, we find that the data is a function of stellar mass at low mass galaxies. This tells us that some assumption is being violated, and this is an active part of research. **Discrepancy in  $\text{H}\alpha$  and UV SFR tracers is huge!**

We can also take observations at the **free-free** part of the radio spectrum (where synchrotron is small and free-free dominates). This would be a dust-free measurement of the SFR.

## 10.2 Gas components of a galaxy

The easiest gas component of a galaxy to measure is HI from the 21 cm line. HI doesn't get dense enough on its own, so stars really form from  $H_2$  (molecule hydrogen). This can get colder and thus denser (because pressure decreases due to temperature).  $H_2$  only has a quadrupole moment because it's symmetric. This is **really weak**, and happens around  $\lambda \sim 30\mu m$ . Observing  $H_2$  directly is really, really difficult. Instead, we observe CO, which is easily observed. We observe CO near  $\lambda \sim 2.6$  mm. We want to know:

$$\Sigma_{gas} = \Sigma_{H_2} + \Sigma_{HI} \quad (61)$$

This is also written as:

$$\Sigma_{gas} = \alpha_{CO} I_{CO} + \Sigma_{HI} \quad (62)$$

Really, we can measure  $I_{CO}$  from the telescope and make assumptions on what  $\alpha_{CO}$  is. Often, you do not really get a clean measurement.

Instead, you infer the gas content from the dust content. The dust traces the gas, so sometimes this is written as:

$$\Sigma_{gas} = \underbrace{\delta_{GDR}}_{\text{gas-to-dust ratio}} \quad \Sigma_{dust} = \alpha_{CO} I_{CO} + \Sigma_{HI} \quad (63)$$

We can infer  $\delta_{GDR}$  to infer a value of  $\alpha_{CO} I_{CO}$ .

### **Challenges in stellar population synthesis (SPS) modeling**

---

- Degeneracies between age and metallicity
- SPS models are not perfect, various stages of stellar evolution that are poorly understood:
  - (TP-)AGB, horizontal branch, blue stragglers, post-AGB, wolf-rayet stars, convection, rotation, binary evolution, etc.
- Dust law, initial mass function, and star formation history usually assumed
- Massive stars with low M/L will dominate the spectrum
- etc.

Figure 68: Looking at HI only, we don't see strong correlation. If we have CO only, the same is true. However,  $HI + CO$  is very nicely correlated with gas surface density.

### 10.3 CO to H<sub>2</sub> Conversions

#### **Challenges in stellar population synthesis (SPS) modeling**

---

- Degeneracies between age and metallicity
- SPS models are not perfect, various stages of stellar evolution that are poorly understood:
  - (TP-)AGB, horizontal branch, blue stragglers, post-AGB, wolf-rayet stars, convection, rotation, binary evolution, etc.
- Dust law, initial mass function, and star formation history usually assumed
- Massive stars with low M/L will dominate the spectrum
- etc.

Figure 69: This has a metallicity dependence because at low metallicity, we expect less dust.

### 10.4 Kennicutt-Schmidt Law

$$\Sigma_{SFR} \propto (\Sigma_{gas})^n, \text{ where } n = 1.4 \quad (64)$$

#### **Challenges in stellar population synthesis (SPS) modeling**

---

- Degeneracies between age and metallicity
- SPS models are not perfect, various stages of stellar evolution that are poorly understood:
  - (TP-)AGB, horizontal branch, blue stragglers, post-AGB, wolf-rayet stars, convection, rotation, binary evolution, etc.
- Dust law, initial mass function, and star formation history usually assumed
- Massive stars with low M/L will dominate the spectrum
- etc.

Figure 70: Kennicutt-Schmidt relation. Extremely famous. Relates star formation rate to gas density. What is going on in nature to tell us this correlation?

### 10.5 KS Law Explanations

One of the things we discussed was the gas consumption timescale (efficiency factor between gas conversion to stars). It turns out efficiency varies galaxy-to-galaxy. There are three theories.

- Efficiency should be constant (wrong).
- **Theory 1: Free Fall Collapse:** Star formation rate is proportional to gas density and free-fall time:  $SFR \propto \frac{\rho}{t_{ff}} \propto \rho\sqrt{G\rho} \propto \rho^{3/2} \propto n^{1.5}$ . This is close to Kennicutt-Schmidt! This was first posited in 92 by Larsen.
- **Theory 2: Orbital Argument:** Maybe the star formation rate scales with the dynamical (orbital time) of a galaxy. The result is  $\Sigma_{SFR} = 0.017\Sigma_g\Omega_g$ . Paper is 1997 from Elmegreen and Silk.
- **Theory 3: Molecular Gas Formation is Tough:** Maybe what varies is the ability to **make** gas. Maybe really  $\Sigma_{SFR} \propto \Sigma_{H_2}$ , and then we need to figure out how a galaxy can produce  $\Sigma_{H_2}$  and with what efficiency. Paper by Krumholz (with review in 2014). The corollary of this is that really low metallicity galaxies don't have CO, but they have stars! **At low metallicity, CO formation is not good and thus our story falls apart! Everyone has molecular hydrogen.  $\Sigma_{H_2}$  is probably just varying a lot!** Lots of theories for why.

### **Challenges in stellar population synthesis (SPS) modeling**

---

- Degeneracies between age and metallicity
- SPS models are not perfect, various stages of stellar evolution that are poorly understood:
  - (TP-)AGB, horizontal branch, blue stragglers, post-AGB, wolf-rayet stars, convection, rotation, binary evolution, etc.
- Dust law, initial mass function, and star formation history usually assumed
- Massive stars with low M/L will dominate the spectrum
- etc.

Figure 71: Efficiency is more complicated. There is no one efficiency in galaxies.

## **10.6 The star formation law in atomic and molecular gas**

THINGS team finds:

$$\Sigma_{SFR} = 10^{-2.1}\Sigma_{H_2}1.0 \quad (65)$$

### **Challenges in stellar population synthesis (SPS) modeling**

---

- Degeneracies between age and metallicity
- SPS models are not perfect, various stages of stellar evolution that are poorly understood:
  - (TP-)AGB, horizontal branch, blue stragglers, post-AGB, wolf-rayet stars, convection, rotation, binary evolution, etc.
- Dust law, initial mass function, and star formation history usually assumed
- Massive stars with low M/L will dominate the spectrum
- etc.

Figure 72: Data from THINGS team. We get the Kennicutt-Schmidt relation really well!

### **Challenges in stellar population synthesis (SPS) modeling**

---

- Degeneracies between age and metallicity
- SPS models are not perfect, various stages of stellar evolution that are poorly understood:
  - (TP-)AGB, horizontal branch, blue stragglers, post-AGB, wolf-rayet stars, convection, rotation, binary evolution, etc.
- Dust law, initial mass function, and star formation history usually assumed
- Massive stars with low M/L will dominate the spectrum
- etc.

Figure 73: More dta

## **10.7 Molecular Fraction vs. Gas Surface Density**

Really low surface densities have almost **NO**  $H_2$ . Less molecular gas is less star formation. Very tips of spiral arms is not as strong and thus less star formation. Same in dwarf galaxies (cannot pull gas in!).

### **Challenges in stellar population synthesis (SPS) modeling**

---

- Degeneracies between age and metallicity
- SPS models are not perfect, various stages of stellar evolution that are poorly understood:
  - (TP-)AGB, horizontal branch, blue stragglers, post-AGB, wolf-rayet stars, convection, rotation, binary evolution, etc.
- Dust law, initial mass function, and star formation history usually assumed
- Massive stars with low M/L will dominate the spectrum
- etc.

Figure 74: Molecular gas fraction and surface density of gas.

## **10.8 Summary of Today**

### **Challenges in stellar population synthesis (SPS) modeling**

---

- Degeneracies between age and metallicity
- SPS models are not perfect, various stages of stellar evolution that are poorly understood:
  - (TP-)AGB, horizontal branch, blue stragglers, post-AGB, wolf-rayet stars, convection, rotation, binary evolution, etc.
- Dust law, initial mass function, and star formation history usually assumed
- Massive stars with low M/L will dominate the spectrum
- etc.

Figure 75: SUMMARY of today.

## **11 September 29, 2021: The Circumgalactic Medium**

This probably won't be on the final, nor will there be homework on this!

The first paper; 1956, ApJ, 124, 20S. Lyman Spitzer speculates “the possibility of a galactic corona.” The idea was that there must be a medium that supports the gas cloud showing absorption lines far out in the Galaxy! This corona should be really hot, near  $10^4 - 10^6$  K. See reviews by **Putman, Peek, Joung (2012)** and **Tumlinson, Peeples, Werk, 2017**.

If a galaxy is the size of a dime, the CGM is the size of the DM halo (about the size of a basketball).

Metals in stars can get recycled to the ISM (and observed with gas phase metallicity), or with inflows and outflows to the CGM, with recycling. This mixes everything together in the galaxy!

## 11.1 History of CGM

- 1950s to 1960s: Concept of a galactic corona, discovery of NaI and CaII lines in hot star spectra.
- 1980s - 2000s: Emerging effort to study the CGM and IGM with QSO absorption lines out to  $z \sim 3$ . The CGM/IGM gives rise to strong Ly $\alpha$ , metal absorption lines and x-rays.
- 2010s: The installation of Cosmic Origins Spectrograph on HST.

## 11.2 The Missing Baryons & Where Are They

See: Persic and Salucci (1992), Fukugita (1998), Fukugita and Peebles (2004), Shull 2003, Bregman 2007, and Behroozi 2010.

$$f_b = \frac{M(\text{stars, gas, dust})}{M_b} \quad (66)$$

$$M_b = \frac{\Omega_b}{\Omega_m} M_{DM} \quad (67)$$

$$\Omega_b = 0.0486, \text{ and } \Omega_m = 0.308 \text{ (from Planck 2015)} \quad (68)$$

It turns out, we are missing a lot of baryons that we expect from  $\Lambda$ CDM. Turns out we are missing a lot of metals, too! The CGM can help explain this, maybe?

## 11.3 General GCM Properties

The CGM is incredibly diffuse, having number densities around  $n \in [6 \times 10^{-7}, 0.6] \text{ cm}^{-3}$ . We can plot this as a function of temperature in a **phase diagram**.

## 11.4 Top 10 Observationally Derived Properties of the CGM (Jessica Werk)

- Large covering fraction of multi-phase ions (We can relate the column density to equivalent width through the curve-of-growth.)
- Observations strongly hint that CGM gas is bound to the galaxy halo.
- The CGM gas contains a substantial fraction of baryons and metals, and its content is somehow modified by whatever process shuts down and fuels star formation in galaxies. The CGM phase structure and dominant physical processes are far from being solved, yet data support a complex shocking and mixing of gas within a galaxy virial radius and dominant processes that vary as a function of halo mass.

## 11.5 Curve of Growth

Relates column density to equivalent width, which have three parts.

- Linear regime with  $\tau < 1$
- Flat regime where width is insensitive, near  $10 < \tau < \tau_{damp}$
- Very steep regime where  $N \propto W^2$  for larger than  $\tau_{damp}$

## 12 October 6, 2021: Chemical Evolution

### 12.1 Chemical Evolution Outline

- Metallicity definition
- Sources of heavy elements
- Measuring metals
- Chemical evolution models

### 12.2 Terminology and Things

In most work, we see something like  $[X/H]$ . This means “the number of atoms in X relative to the number of atoms in hydrogen, with the brackets mean relative to the sun. The most common example is  $[Fe/H]$ . This is:

$$[Fe/H] = \log_{10} \left( \frac{N(Fe)}{N(H)} \right)_* - \log_{10} \left( \frac{N(Fe)}{N(H)} \right)_\odot \quad (69)$$

There are quantities called mass fractions,  $X$ ,  $Y$ , and  $Z$ .  $X$  is the mass fraction of hydrogen,  $Y$  is the mass fraction of helium, and  $Z$  is the mass fraction of metals. What this really means is:

$$X = \frac{m_{hydrogen}}{m_{total}} = \frac{\rho_{hydrogen}}{\rho_{total}} \quad (70)$$

By construction,  $X + Y + Z = 1$ .

Another example:

$$[M/H] = \log_{10} \left( \frac{N(\text{metals})}{N(H)} \right)_* - \log_{10} \left( \frac{N(Fe)}{N(H)} \right)_\odot \quad (71)$$

We can re-write this:

$$[M/H] = \log_{10} \left( \frac{n_m}{n_H}_* / \frac{n_m}{n_H}_\odot \right) = \log_{10} \left( \frac{(Z/X)_*}{(Z/X)_\odot} \right) \quad (72)$$

In the Sun, we have:

- $X_\odot = 0.734$
- $Y_\odot = 0.25$
- $Z_\odot = 0.016$  (controversial – helioseismology tension!)

## 12.3 Solar Abundance Pattern

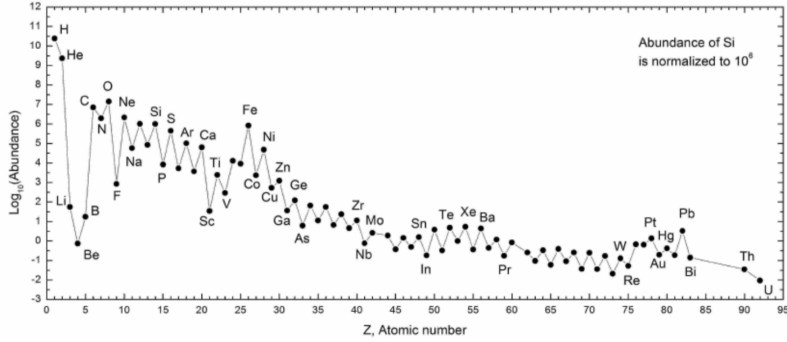


Figure 76: Solar abundance pattern. This is what you should think about when you talk about abundance patterns, but this is not constant for stars!

## 12.4 Sources of Heavy Elements

Hydrogen, helium, and lithium are BBN elements.

Stars return substantial fractions of their initial masses to the ISM at the end of their lifetimes through stellar winds and supernovae.

- **Low mass stars ( $M < 8M_{\odot}$ )**: He, C, N, O ejected during AGB phase
- **Massive stars ( $M > 8M_{\odot}$ )**: Produce more O and Mg compared to Fe. Enrich ISM via stellar winds and final explosions as core collapse (Type II) supernovae
- Type Ia supernova: C/O white dwarf accretes material from a close companion and explodes once it reaches the Chandrasekhar limiting mass. Produces mostly Fe and little O.

Side note: Hydrogen burning stops, contracts, and inert helium core. Then you have hydrogen shell burning as it ascends RGB. Then helium flash stars the horizontal branch, burning helium in the core burning to C, O. Around the core, you have H burning shells. Then you run out of helium, the core is contracting but not burning. This is the AGB. Everytime its stable, you have same luminosity. Unstable is increasing luminosity. Temperature gradients are really steep and thus you have convection. Dredges up carbon and oxygen into the atmosphere, with winds kicking it off. It then becomes a white dwarf.

## 12.5 Neutron Capture Elements

Most heavy nuclei ( $A > 56$ ) are formed by neutron addition onto Fe-peak elements, followed by beta decay. Beta is an electron or a positron. The neutron capture regime is  $n > 10^{20}$  neutrons per centimeter cubed. Low density regime is  $n < 10^8$ . Anything between depends on other factors. Rapid process takes place in SN explosions, colliding neutron stars, BH/neutron star mergers, etc. S process mostly occurs in AGB stars and in massive stars in the He burning core and convective C-burning shell, just prior to SN explosion.

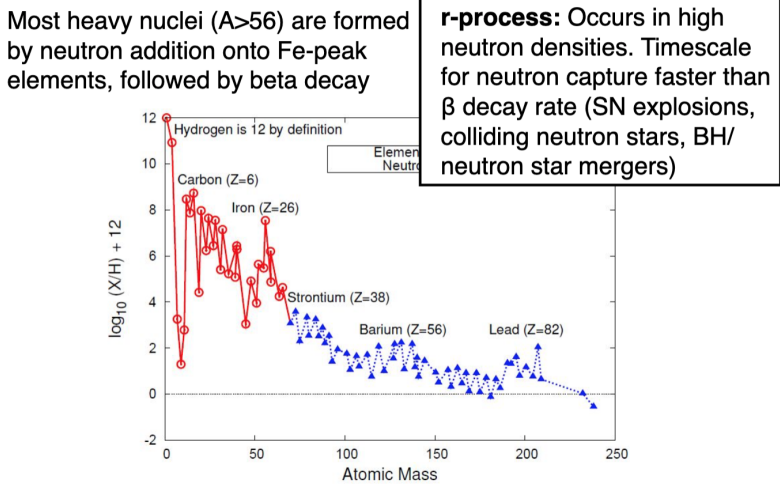


Figure 77: R and S process. Rapid process takes place in SN explosions, colliding neutron stars, BH/neutron star mergers, etc. S process mostly occurs in AGB stars and in massive stars in the He burning core and convective C-burning shell, just prior to SN explosion. S process is responsible for about half of elements larger than iron. Decay timescale is about 15 minutes.

## 12.6 R vs. S Process Elements

### R vs. S process elements

**R-process elements:** timescale for neutron capture faster than  $\beta$  decay rate (SN explosions, colliding neutron stars, BH/neutron star mergers)

**S-process elements:**  $\beta$ -decay happens before the next neutron capture; elements fall along stable nuclei track

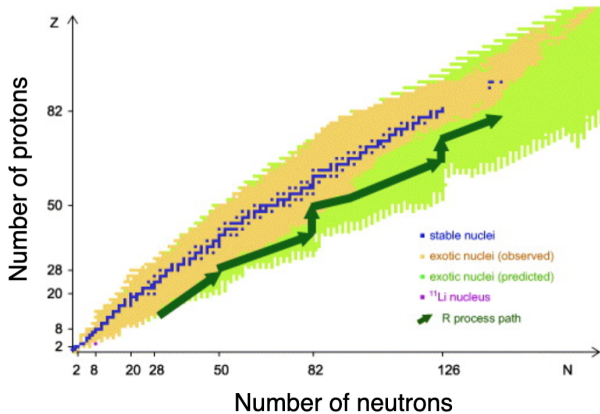


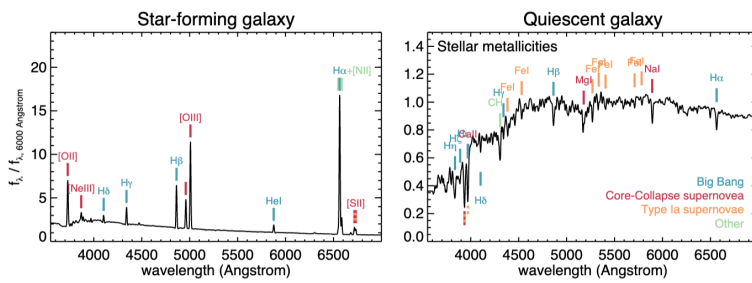
Figure 78

## 12.7 Metallicities of galaxies

You need high resolution spectra to resolve individual lines. Can also measure the temperature, gravity, and metallicity all at the same time. Can you do the same thing for an integrated population of stars? You can get a value, sure, but it will be luminosity weighted and thus dominated by the brightest stars.

Also, doppler broadening in galaxies makes individual measurements impossible.

## Metallicities of galaxies



### Gas-phase metallicity

- Oxygen abundance
- Measured from emission lines originating in star-forming regions
- Primarily measured for star-forming galaxies
- Instantaneous metallicity in star-forming regions

### Stellar metallicity

- General combined Mg and Fe abundance
- Measured from metal absorption lines originating in stellar atmospheres
- Primarily measured for quiescent galaxies
- Reflects ISM metallicities at times the stars were formed

9

Figure 79: For a star forming galaxy, you measure metallicity from an HII region (equivalent width of emission lines, mostly)! This is a tracer of current metallicity. For quiescent galaxies, we have to measure **stellar metallicities**, not **gas-phase metallicities**. Generally measure Mg and Fe abundance. **Reflects ISM metallicities at times the stars were formed.**

## 12.8 Gas-phase metallicities, direct T method

You have an optically-thin plasma in a high temperature HII region. The takeaway of the below figure, is: In HII regions, the OIII and NII lines are banged on by other elements. This collisionally excites the plasma, which is great because that's temperature! Thus measuring the temperature gives us the oxygen atoms, and then we can get the metallicity.

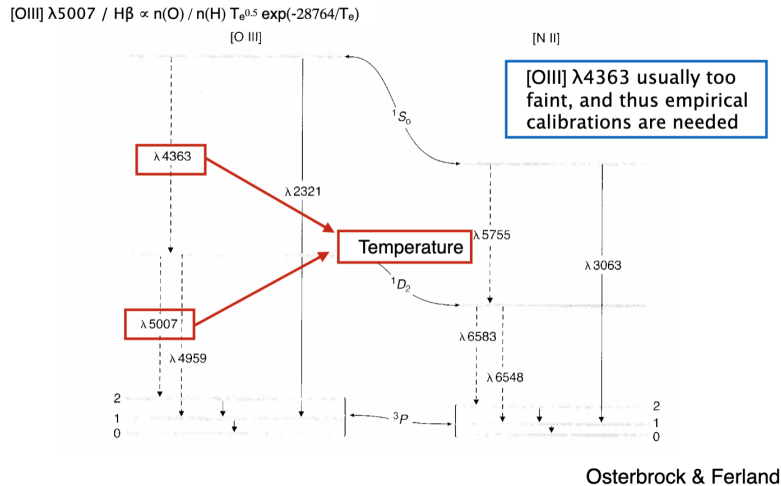
How do we get temperature? For OIII specifically, if we can measure ratios of transitions (aka Boltzmann distribution measurements) at specific places, there are places sensitive only to temperature. In practice, many of these lines are weak and hard to measure (like the 4360 line compared to the 5007 line).

Instead, you measure the 5007 line, and then something else like H $\beta$ , giving:

$$OIII/H\beta \propto n(O)/n(H) \times T^{0.5} \exp\{(-28764/T_e)\} \quad (73)$$

which is unfortunately dependent on density, which we must assume! This figure shows this phenomenon:

## Gas-phase metallicities, direct T method



Osterbrock & Ferland

14

Figure 80: See above.

We get around this with the strong line method:

## Gas-phase metallicities, strong-line method

$$12 + \log (\text{O/H}) = 9.185 - 0.313x - 0.264x^2 - 0.321x^3$$

$$x \equiv \log R_{23}$$

$$R_{23} = ([\text{O II}] + [\text{O III}]) / \text{H}\beta$$

Combination of strong lines correlated with the oxygen abundance and thus can be used as indirect (strong-line) metallicity measurements

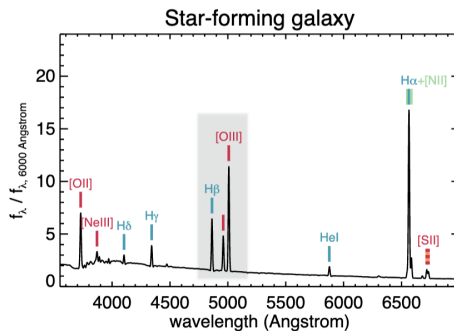
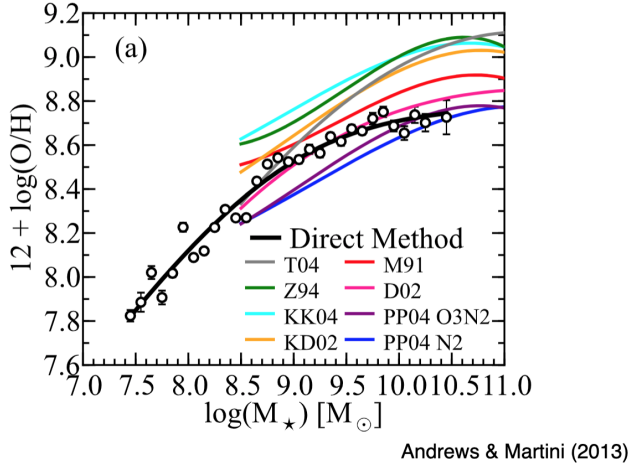


Figure 81: Combination of strong lines correlated with oxygen abundance and can be used. Really dangerous though because calibration has lots of scatter.

## Direct vs. indirect (strong-line) metallicity method

There are several indirect methods, though none is perfect.



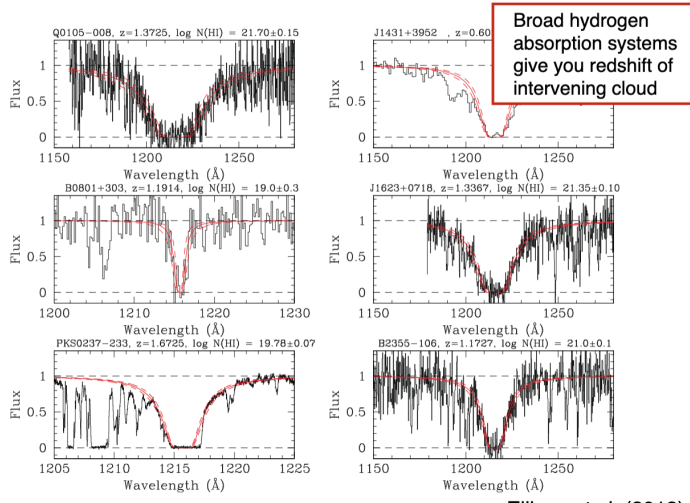
16

Figure 82: Direct and indirect method comparison.

## 12.9 Quasar Absorption Line Studies

Light travels through the medium at many different redshifts, and thus we can measure metallicities of gas patches. This is what Lyman-alpha systems (damped) are:

### Damped Lyman alpha systems, detection

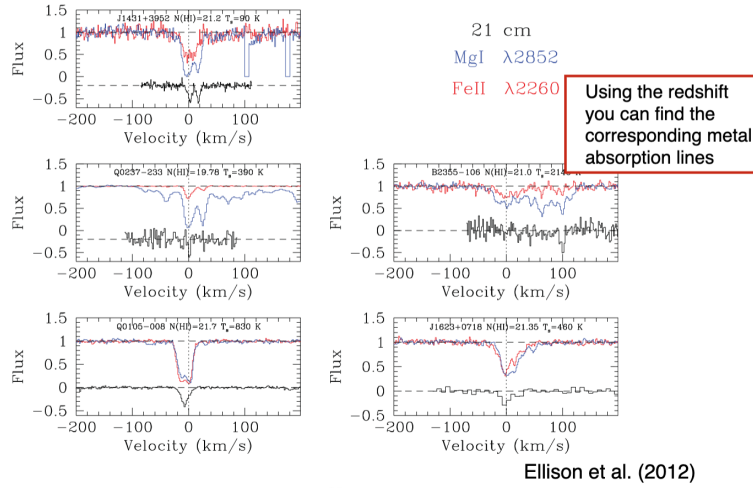


19

Figure 83: QSO damped lyman-alpha system. The amount of damping is due to the metal in the gas. Then do photo-ionization modeling.

We can also get metals, too:

## Damped Lyman alpha systems, metals



20

Figure 84: We can model other lines which are much weaker, but we know redshift from lyman-alpha.

## 13 October 8, 2021: Chemical Evolution Continued

### 13.1 Damped Lyman Alpha Systems

It might be called this because of radiation damping OR because of the shape of the wings.

### 13.2 Chemical Evolution Models, ingredients

- Initial conditions
  - Pre-enriched or primordial
  - Closed box or open system
- Birthrate function  $B(M, t) = \psi(t)\xi(M)$ 
  - Star formation rate history:  $\psi(t) \propto \sigma^n$  (KS relation)
  - Stellar initial mass function  $\xi(m)$
- Stellar yields
  - Core collapse SN yields depend on stellar mass and metallicity

### 13.3 Closed Box Model Chemical Evolution

Let's first define some variables. We have:

- $\psi(t)$ : SFR in solar masses per year
- $M_g(t)$  : gas mass at time  $t$
- $M_s(t)$ : Stellar mass at time  $t$
- $M_t(t) = M_g(t) + M_s(t)$ : Total mass at time  $t$  which is constant

- $Z(t)$ : fraction of metals in the gas

Now, let's discuss initial conditions:

- At  $t = 0$ ,  $M_t(0) = M_g(0)$  and  $Z(0) = 0$ .

We have a few other assumptions:

- No gas flow in or out of the system:  $\frac{dM_t}{dt} = 0$ .
- Instantaneous recycling approximation – no delay time between enrichment and recycling to gas reservoir.
- We basically have an IMF with two mass bins: low mass stars keep stellar mass locked up, high mass stars return the mass to the system. (Recycling of material comes **only** from high mass stars. Low mass stars retain the mass).

We can calculate the stellar mass at time  $t$ :

$$M_s(t) = \int_0^t \alpha\psi(t') dt' \quad (74)$$

where  $\alpha$  defines the fraction of mass in long-lived stars. Another way to write this same equation:

$$\frac{dM_t}{dt} = \alpha\psi \quad (75)$$

We can write down:

$$\frac{d(M_g Z)}{dt} = \underbrace{-Z\psi}_{\text{removal of metals from system}} + \underbrace{(1-\alpha)Z\psi}_{\text{contribution to metals from high mass stars (enrichment)}} + \underbrace{q\psi}_{\text{ }} \quad (76)$$

where  $q \equiv \frac{\text{metals returned}}{\text{total mass}}$  ratio of mass in metals returned to that of the total mass at a given time. In other words, at some time  $t$  massive stars are returning metals to the system, which has some total mass at time  $t$ .

We can re-write the left hand side of the equation above:

$$\frac{d(M_g Z)}{dt} = q\psi - \alpha Z\psi = \psi(q - \alpha Z) \quad (77)$$

Now, we are going to use a little black magic to expand this...

Let's start with **Equation 1**:

$$\frac{d(M_g Z)}{dM_s} = \frac{d(M_g Z)}{dt} \frac{dt}{dM_s} = \psi(q - \alpha Z) \frac{1}{\alpha\psi} = \frac{q}{\alpha} - Z = y - Z \quad (78)$$

Here, we define  $y \equiv \frac{q}{\alpha}$ . We can now define **Equation 2**, noting that  $dM_g = -dM_s$ :

$$\frac{d(M_g Z)}{dM_s} = M_g \frac{dZ}{dM_s} + Z \frac{dM_g}{dM_s} = -M_g \frac{dZ}{dM_g} - Z = -\frac{dZ}{d \ln M_g} - Z \quad (79)$$

Let's equate **Equation 1** and **Equation 2**:

$$y - Z = -\frac{dZ}{d \ln M_g} - Z \quad (80)$$

Let's simplify:

$$y = -\frac{dZ}{d \ln M_g} \quad (81)$$

Integrate:

$$\int_0^t dZ = -y \int_0^t d \ln M_g \quad (82)$$

$$Z(t) - Z(0) = -y (\ln M_g(t) - \ln M_g(0)) \quad (83)$$

$$Z(t) = -y \ln \frac{M_g(t)}{M_t} = -y \ln F_g(t) \quad (84)$$

where  $F_g$  is the gas fraction at time  $t$ .

We end up wanting to observe the metallicity distribution  $\frac{dN}{dZ}$ .

### 13.4 The G-Dwarf Problem: THIS IS PRE-LIM PRIME

See Dauphas+2005. G-dwarf dominates the solar neighborhood (because they are easy to observe, by number it's actually the M-dwarfs). The crux of the problem is the low metallicity tail that is totally unfit! So, what's the solution to the closed box model?

The main issue is that we are not in a closed box! The big reason it fails is that we have multiple yields, we have recycling (not instantaneous), and inflow/outflow more broadly speaking and not immediately recycling back into the disk. **The closed box model needs inflows and outflows, as well as non-instantaneous timescales.**

#### The G-dwarf problem

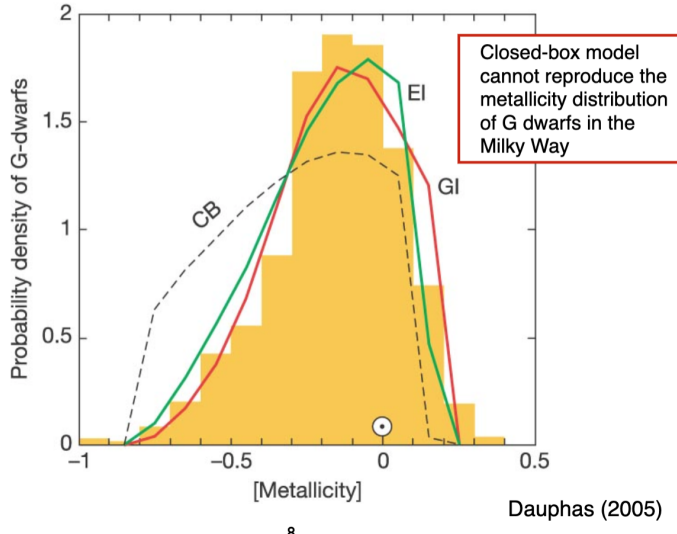


Figure 85: CB model does not reproduce what is observed!

### 13.5 Mass-metallicity relation

We can also look at the mass-metallicity relation. The closed box model fails at reproducing the observed trend. The trend is because, as we change galaxy mass, outflow and inflow are different as a function of mass.

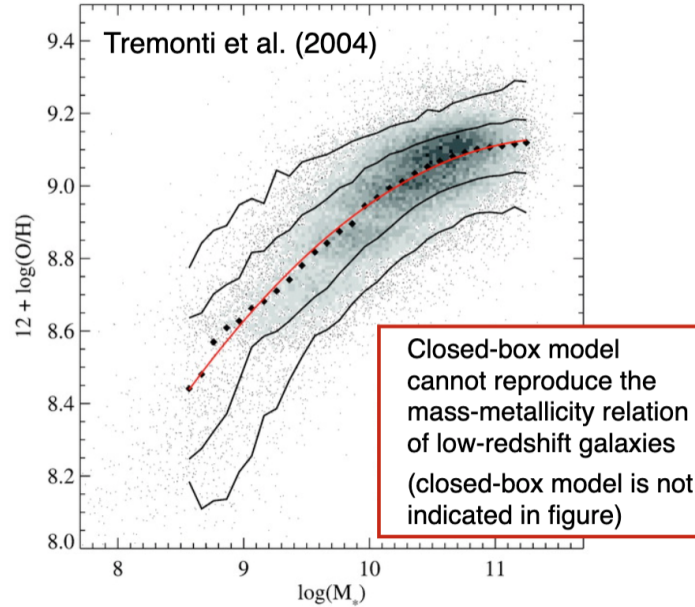
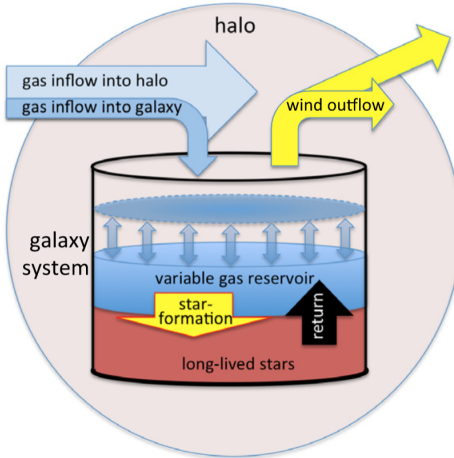


Figure 86: CB model does not reproduce what is observed for mass-metallicity relation as well!

### 13.6 Leaky Box model

Modifying the instantaneous recycling approximation, as well as adding in inflows and outflows, and we better fit the data.

## A “leaky” box model better describes the data



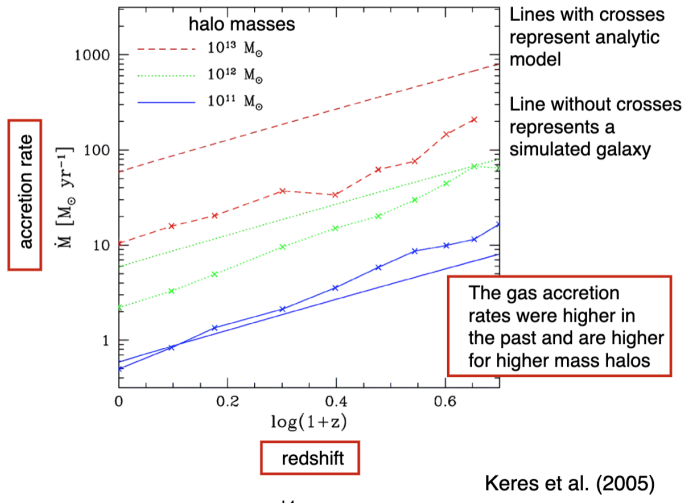
Lilly et al. (2013)

II

Figure 87: Leaky box better fits the data!

## 13.7 Gas Accretion over Time

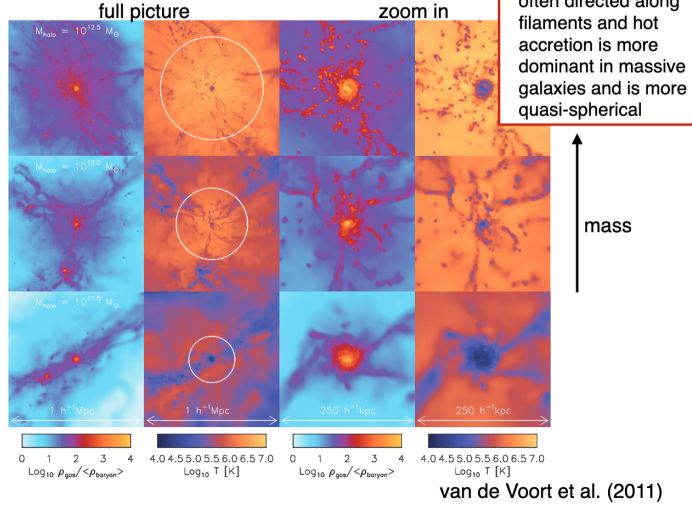
### Average gas accretion rates



14

Figure 88: Gas accretion slows in the nearby Universe.

## Hot and cold accretion in simulations



15

Figure 89: Cold mode accretion.

## Hot vs. cold accretion

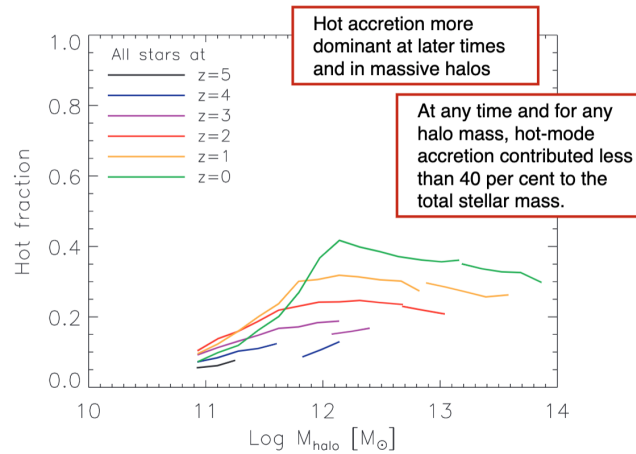
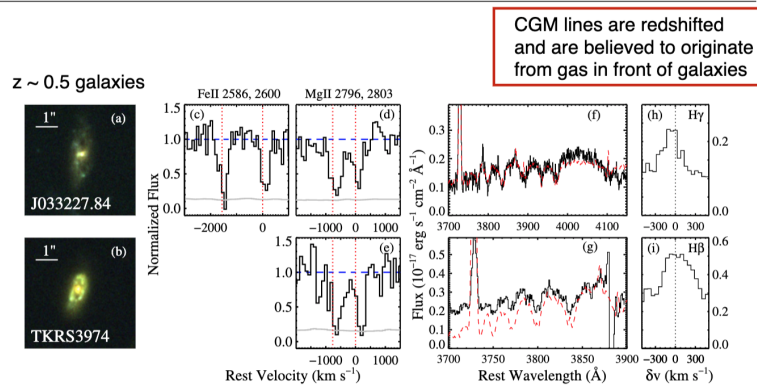


Figure 90: Hot mode accretion goes down with low halo masses.

## 13.8 Observational Constraints on Infall

### Observational constraints on infall?



Rubin et al. (2012)

17

Figure 91: Densities are low, temperatures are low, and thus we have a hard time observing inflows.

## 13.9 Lyman Alpha Blobs

### Observational constraints on infall?

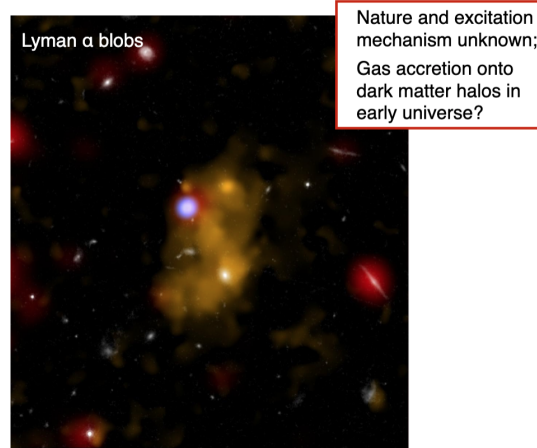


Figure 92: La blobs. Best evidence for inflow.

### 13.10 Milky Way Clouds?

#### Observational constraints on infall?

High velocity clouds around the Milky Way

9000 K neutral gas clouds at 2-15 kpc

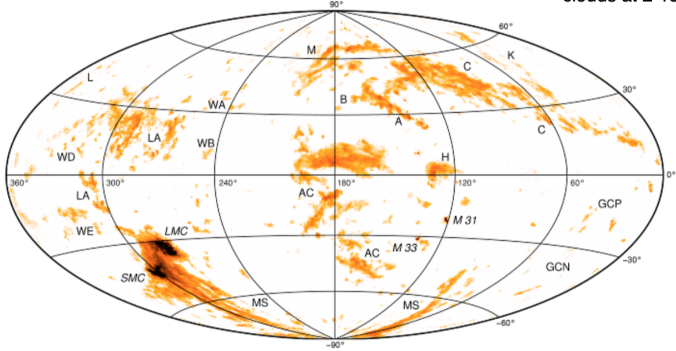


Figure 93: What the heck are these high velocity clouds?

## 14 October 13, 2021: Chemical Evolution and DM Halos

### 14.1 CC SN Stellar Yields Depend on the Stellar Mass

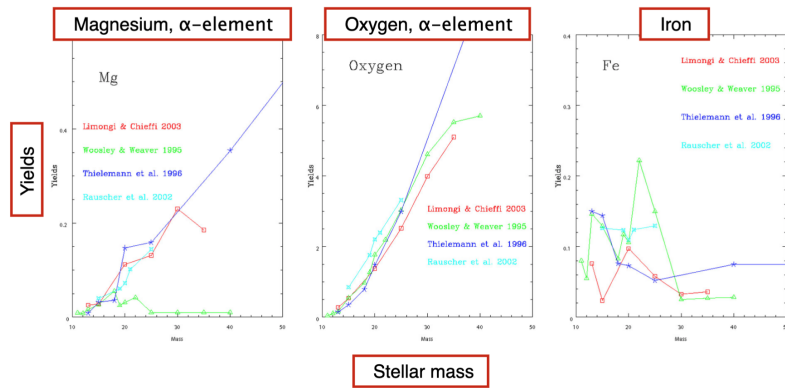
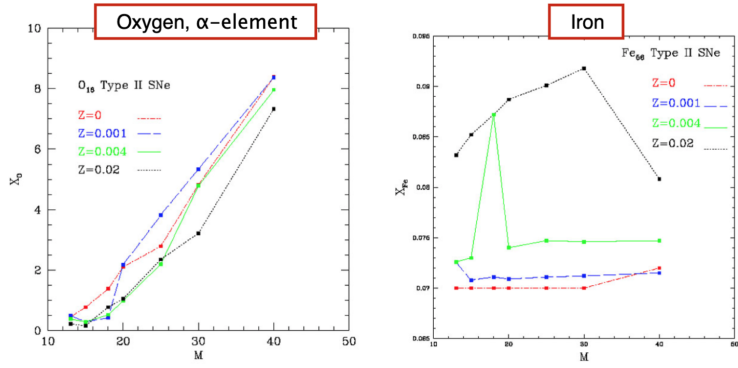


Figure 94: CC SN.

## 14.2 CC SN Stellar Yields Depend on the Stellar Metallicity

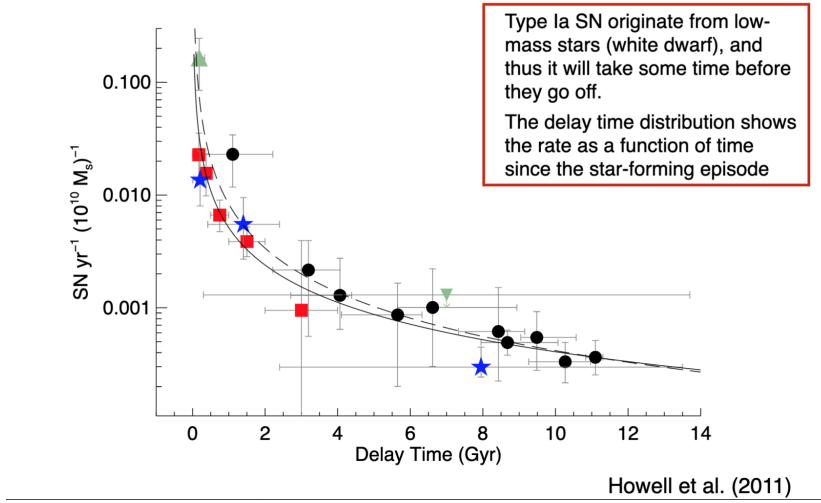


Nomoto et al. (2006)

Figure 95: Nomoto models are common.

## 14.3 Type Ia Supernovae Delay Time Distribution

How many go off as a function of when the star formation episode happened.



Howell et al. (2011)

Figure 96: Delay time distributions.

## 14.4 R-process Elements

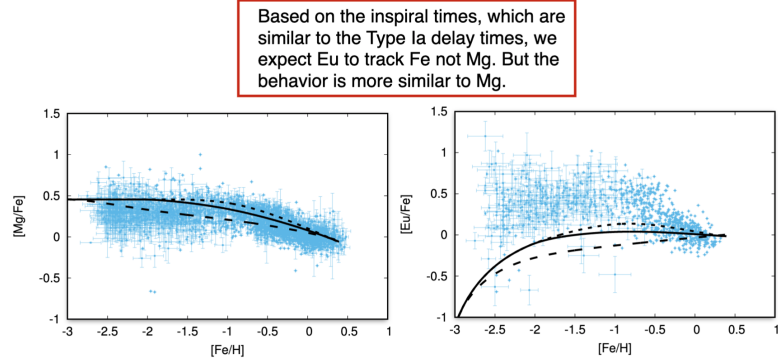


Figure 97: These were thought to track Ia SN. Eu tracks more closely with Mg, which we did not predict. **We don't know the delay time distribution of neutron star mergers at all which give uncertainty.**

## 14.5 PRELIMMABLE: Core-Collapse vs. Type Ia Supernovae Enrichment

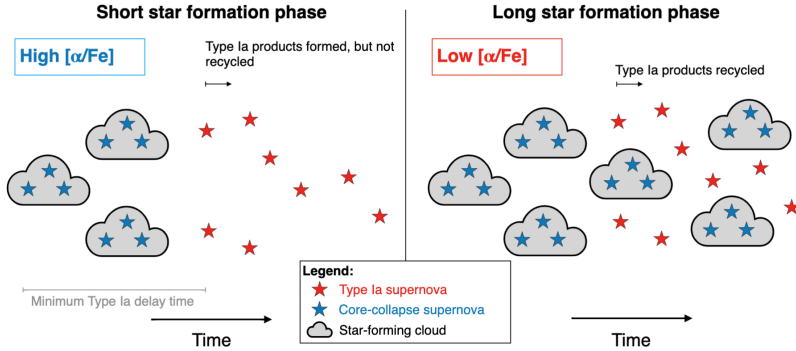


Figure 98: Type II SN go off and produce alpha elements (Mg, Oxygen, Carbon, etc) and not Fe. If you look at a star formation episode shortly after it happens, you find a high alpha sequence (enrichment relative to iron). This is because the Ia's have not happened yet and thus have not produced iron. The first Ia goes off a few hundred million years later, and we enrich the ISM with iron. Effectively, this brings down the alpha-to-iron ratio.

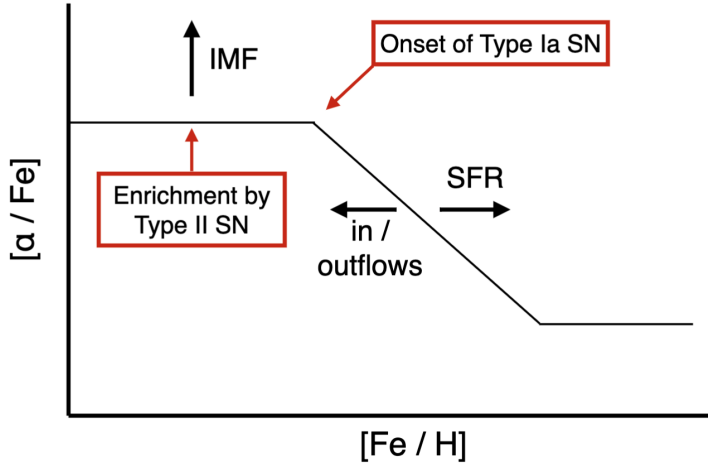


Figure 99: Initial plateau: “high-alpha sequence.” Turnover: “knee.” Secondary plateau. This is a diagram that basically traces the various enrichments for Type Ia vs. Type II SN. To get high alpha sequence, we need CCSN. This creates a high alpha population into the ISM. At some time, ISM gets enriched with iron and we have a drop-off in the ratio. Then, we settle in equilibrium. Various aspects of this diagram are sensitive to various SPS parameters. More high mass stars means more CC SN and thus high plateau. The exact shape and slope, location, etc., are set by the balance of star formation rate and inflow/outflow.

#### 14.6 Examples - Effect of IMF on Alpha-Fe and Fe-H Diagram

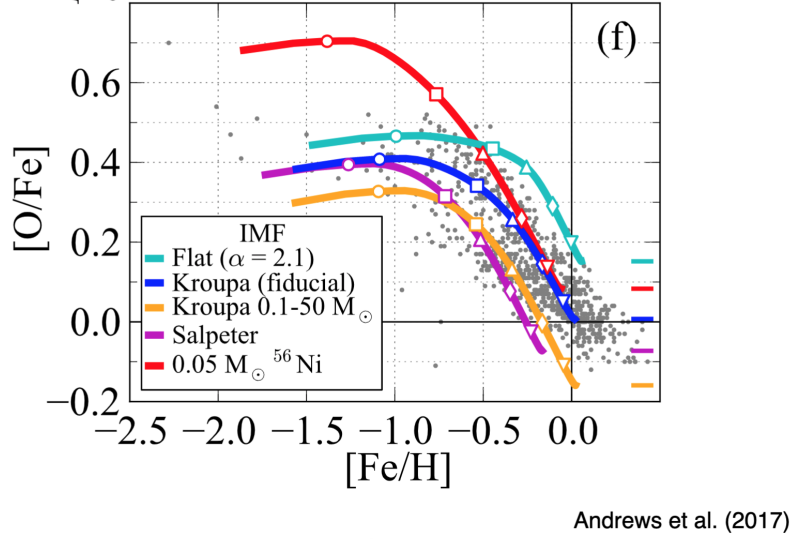
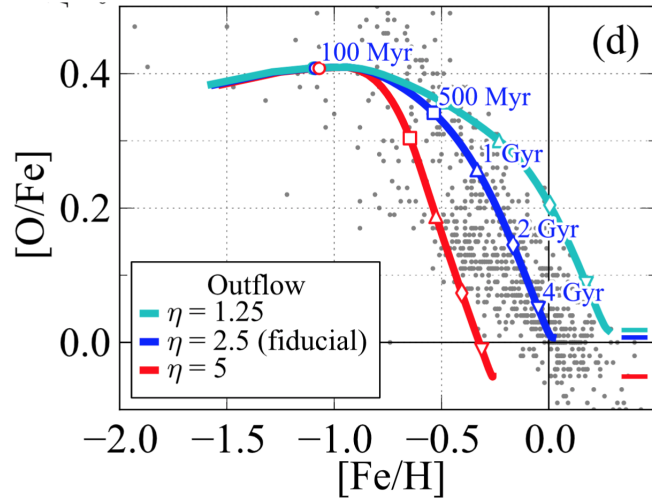


Figure 100: Cyan is more supernova because more high-mass stars.

## 14.7 Examples - Effect of Star Formation on Alpha-Fe and Fe-H Diagram



Andrews et al. (2017)

Figure 101: Outflows create spread at the down-turn.

## 14.8 Examples - Effect of Inflow and Outflow on Alpha-Fe and Fe-H Diagram

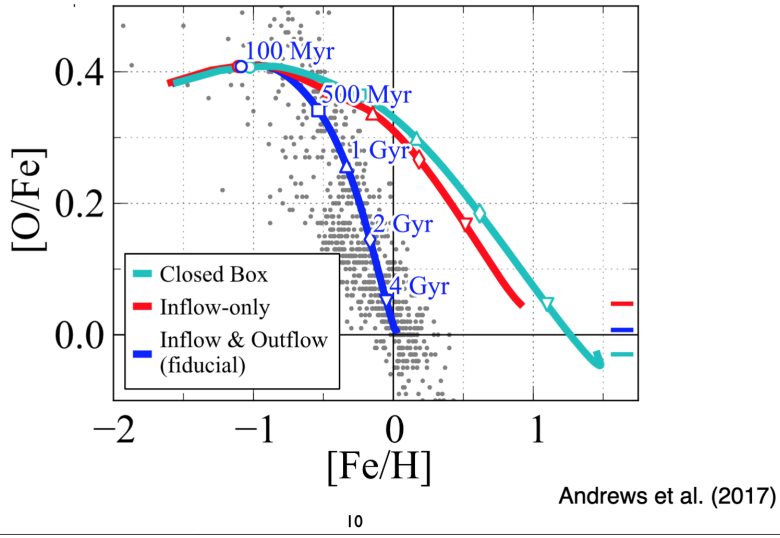


Figure 102: Effects of inflows and outflows.

## 14.9 The Dark Matter Rap

## 14.10 Cold, Warm DM Power Spectrum

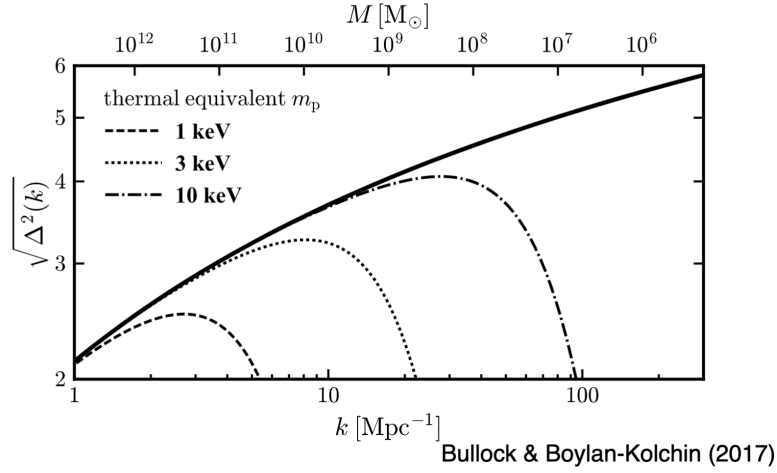
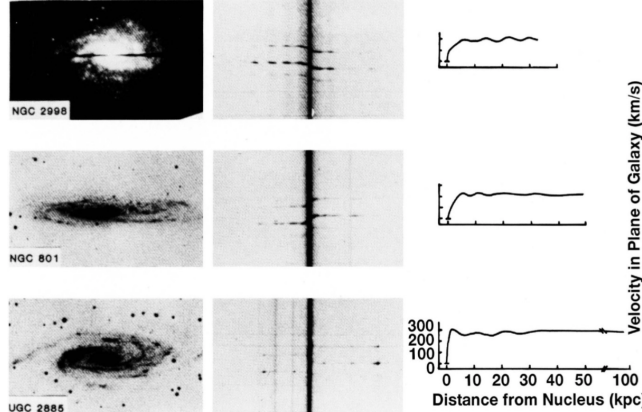


Figure 103: Characteristic distance scale (x) vs power (y) on sky. Solid line is power spectrum for cold dark matter. We mean by “cold”: no thermal component. It is just a gravitationally interacting point mass, more or less. The energies corresponding to intrinsic kinetic energy. Warm dark matter has a turnover in the power structure, and you lose small scale structure.

## 14.11 Rotation Curves



Rubin et al. (1980)

Figure 104: Vera Rubin!

## 14.12 Probes for Dark Matter Halos and Halo Shapes

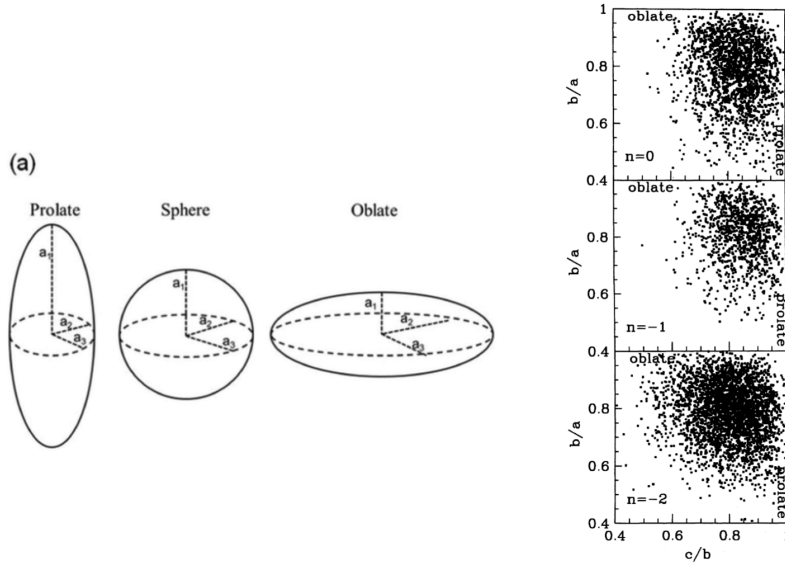


Figure 105: Prolate and oblate haloes. Things tend to be a bit more prolate, by the way. Typical shape:  $a : b : c = 1 : 0.8 : 0.65$

## 14.13 Dark Matter Halo: A universal density profile

The NFW Profile is given by:

$$\rho(r) = \frac{\rho_s}{\frac{r}{r_s} \left(1 + \frac{r}{r_s}\right)^2} \quad (85)$$

where  $r_s$  is the scale radius of the halo and  $\rho_s$  is the density at  $r_s$ .

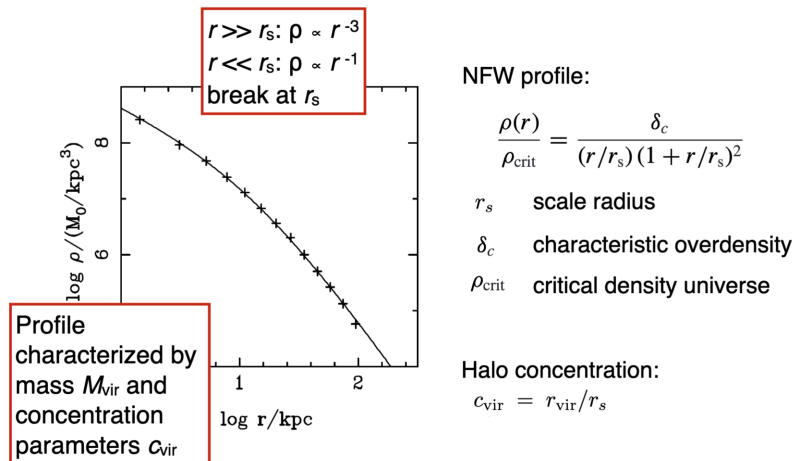


Figure 106: NFW Profile.

In practice, however, most people talk about the virial radius. This is the effective radius if the halo were a sphere. If we define  $r_{vir}$  and  $c_{vir} = \frac{r_{vir}}{r_s}$  is the concentration parameter:

$$\rho_s = \rho_c \delta_c, \text{ where } \rho_c = \frac{3H^2(z)}{8\pi G} \quad (86)$$

and where  $\delta_c$  is the characteristic overdensity. Typically we pick something like 200 or 500 times the overdensity.

#### 14.14 Halos which form earlier are more concentrated

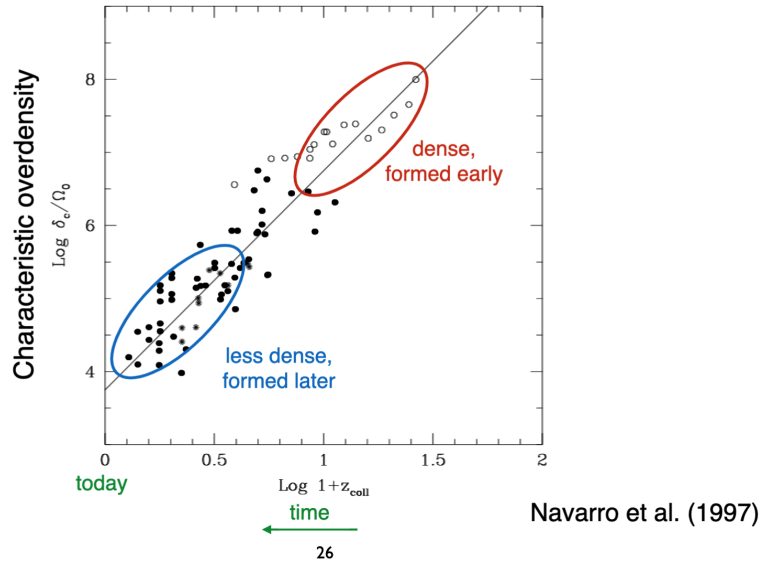


Figure 107: Late halos are less dense, as a result of looking at simulations. The characteristic overdensity scales well with the formation epoch. The more concentrated ones tend to be less massive. More massive galaxies have lower dark matter concentration parameters.

## 14.15 Mergers of Dark Matter Halos

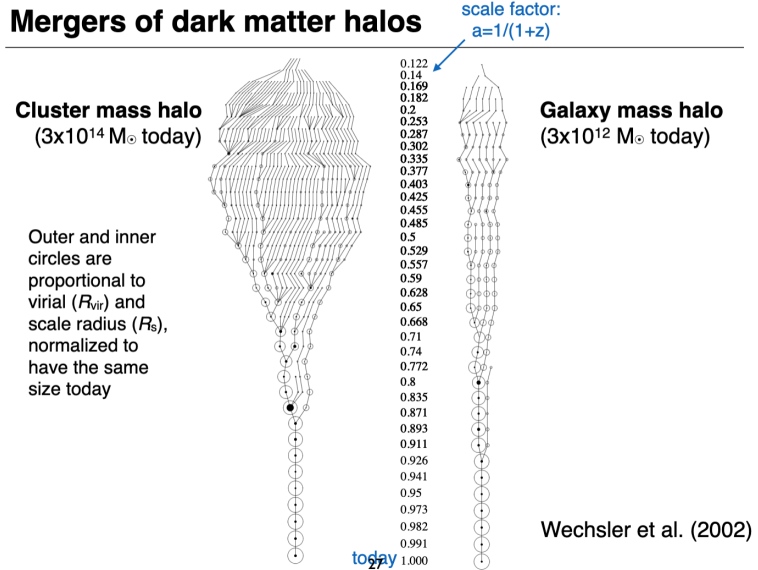


Figure 108: Merger trees. Read from bottom to top moving backward in time.

## 14.16 Halo growth; mass accretion histories

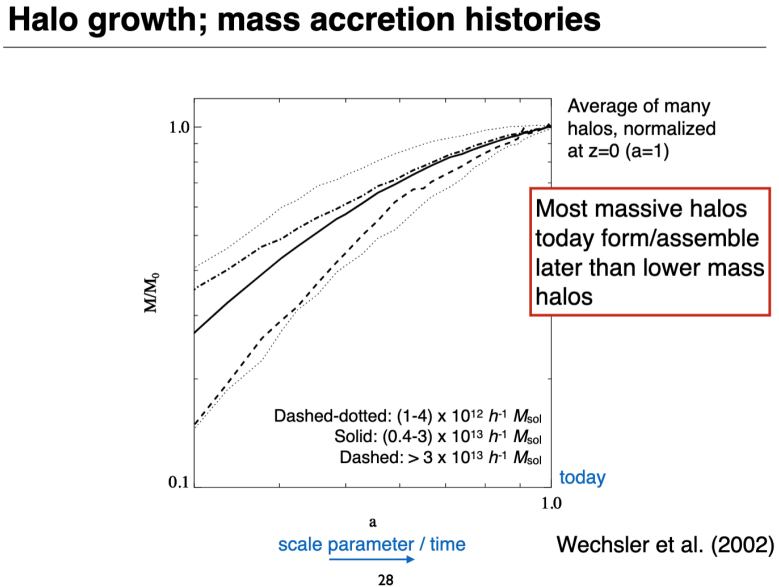


Figure 109: Assembling more DM over time. More massive haloes form later than low mass halos.

## 14.17 Halo growth; concentration parameter histories

### Evolution of the concentration of dark matter halos

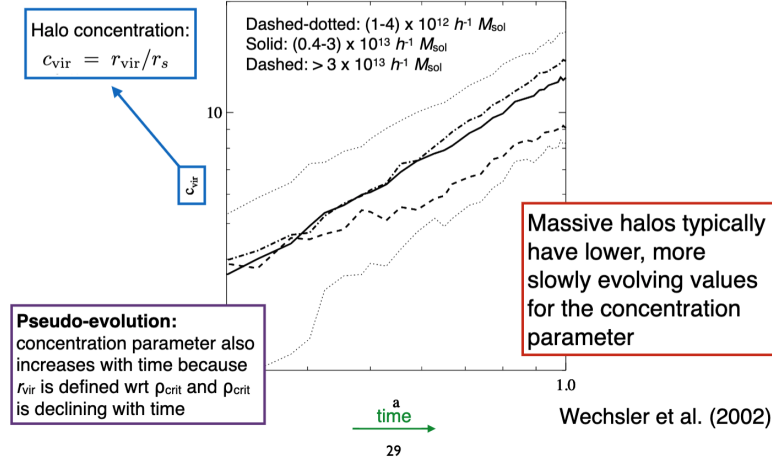


Figure 110: Same thing can be said for concentration index. This has to do with the fact that they accrete more stuff. Low mass are more simple and thus have simple merging histories.

## 14.18 Dark Matter Halo Mergers: A Universal Fitting Form

### Dark matter halo mergers: a universal fitting form

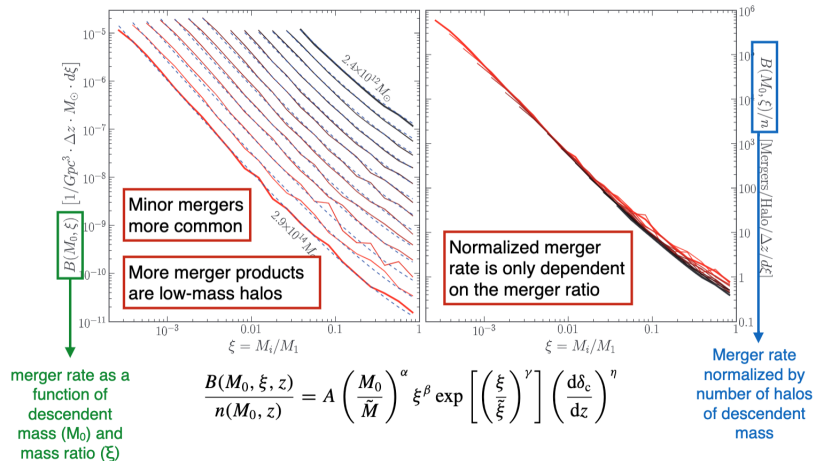


Figure 111: Immensely important.

## Evolution of the dark matter halo mergers rate

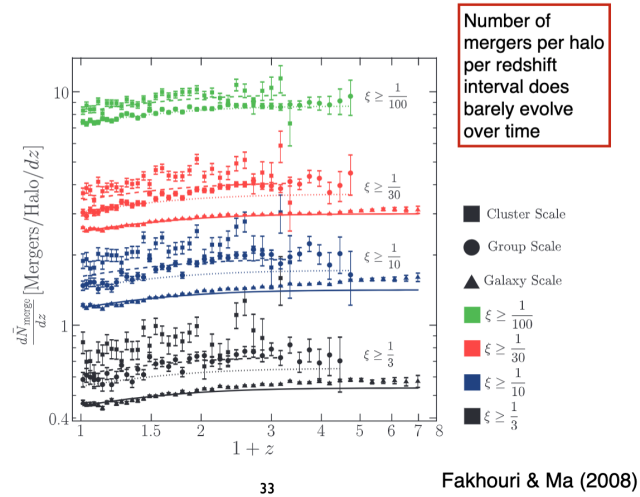


Figure 112: Immensely important. More!

## Evolution of the dark matter halo mergers rate

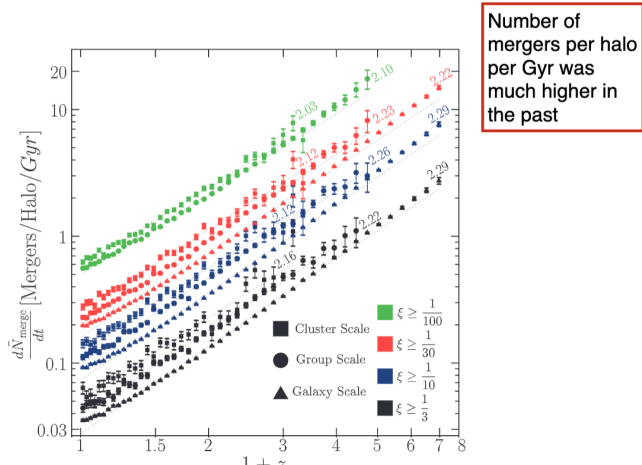
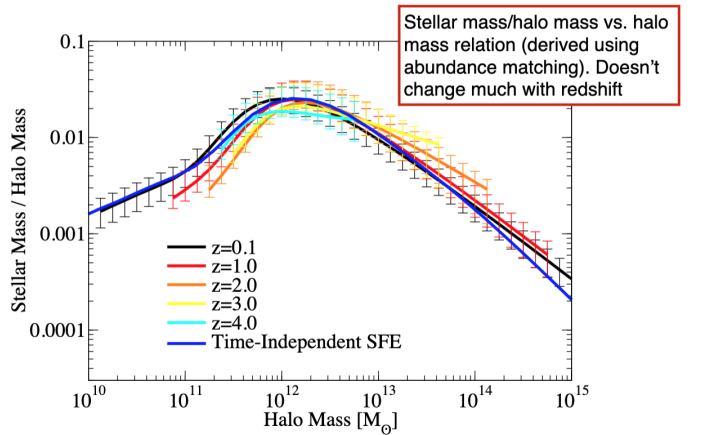


Figure 113: Immensely important. More!

## Stellar to dark matter halo masses



Behroozi et al. (2012b)

Figure 114: Barley changes.

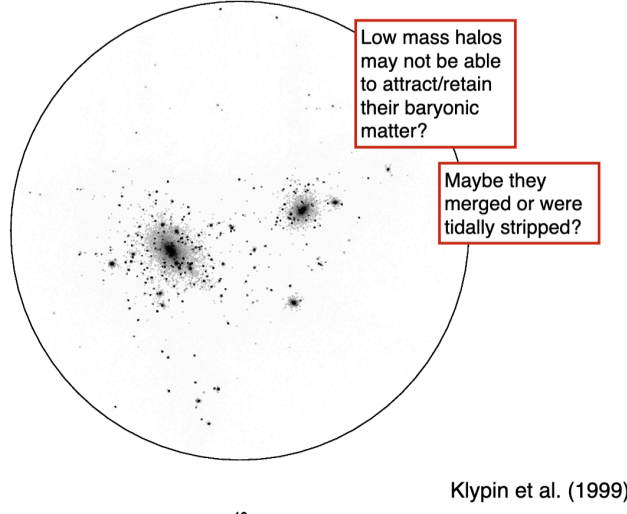
### 14.19 Problems with Cold Dark Matter

- The missing satellite problem
- Cusp-core problem
- Halos are triaxial, why don't we see evidence for that?
- Why are there so many pure disk galaxies?
- Too few galaxies in voids?

### 14.20 Missing Satellites Problem

There are tons of tiny little halos that are predicted. Where are they?

Distribution of particles for a small group of DMHs, similar in mass to local group



40

Figure 115: Where the hell are the satellites?

Maybe dark matter isn't cold?

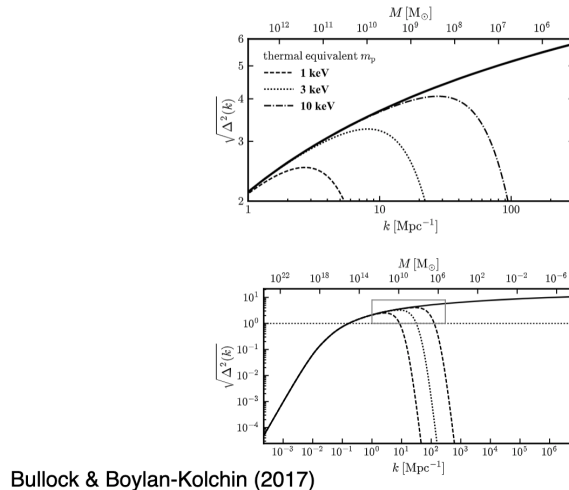


Figure 116: Maybe the turnover is due to a warm dark matter turn over? Warm models predict different small DM halos. Probably least likely solution.

## 14.21 Core vs. Cusp Problem

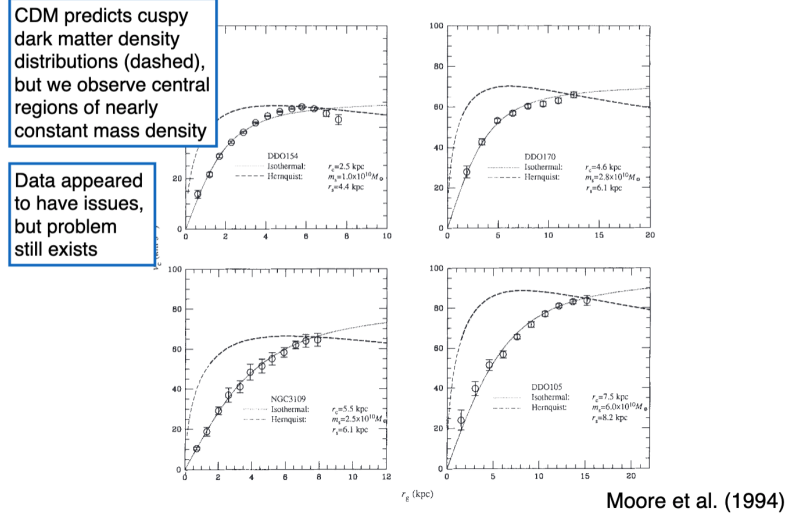


Figure 117: NFW is universal, but we observe central regions of nearly constant mass density. This has been used against universal mass profiles. Data appeared to have issues, but problem still exists.

## Core vs. cusp problem

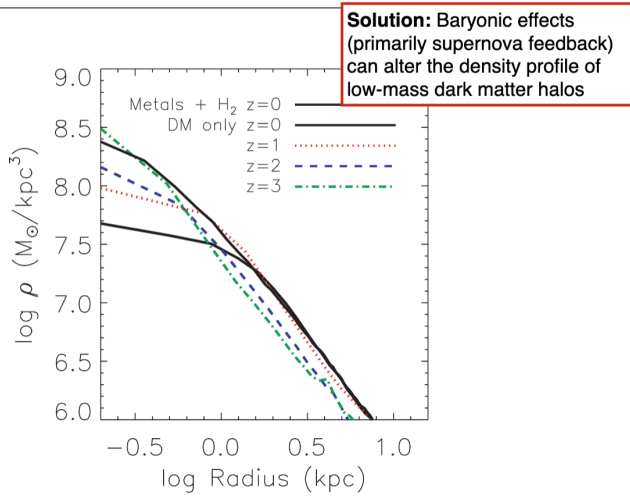


Figure 118: Proposed solution: baryonic effects (primarily SN feedback) can alter the density profile of low-mass dark matter halos. This is called “unbinding.” Probably the best explanation right now.

## 14.22 Summary of DM Halos

### Summary dark matter halo evolution

---

- DMHs that collapse first are more concentrated
- More massive DMHs assemble later
- The concentration in more massive DMHs evolves slower as more late-time mergers lead to lower concentration parameters
- The dark matter halo merger rate can be described by a universal function
  - ▶ The normalized merger rate per redshift interval is primarily a function of the merger ratio
- CDM still has some problems, but none are problematic enough to change our paradigm

Figure 119: Summary of DM Halos!